PHENOTYPIC AND GENOTYPIC ALTERATIONS OF MATURE CELLS DISPERSED IN INJECTABLE ZONAL HYDROGELS MIMICKING THE CARTILAGE MATRIX COMPOSITION

By

KENNETH JAMES WALKER

Bachelor of Science in Chemical Engineering
Oklahoma State University
Stillwater, Oklahoma
2010

Master of Science in Chemical Engineering
Oklahoma State University
Stillwater, Oklahoma
2011

Submitted to the Faculty of the
Graduate College of the
Oklahoma State University
in partial fulfillment of
the requirements for
the Degree of
DOCTOR OF PHILOSOPHY
May, 2015

PHENOTYPIC AND GENOTYPIC ALTERATIONS OF MATURE CELLS DISPERSED IN INJECTABLE ZONAL HYDROGELS MIMICKING THE CARTILAGE MATRIX COMPOSITION

Dissertation Approved:

Dr. Sundararajan Madihally

Dissertation Adviser

Dr. Gary Foutch

Dr. James Smay

Dr. Donald Ruhl

.

ACKNOWLEDGEMENTS

During my tenure at Oklahoma State University, I have received a great deal of care, support, and guidance from many people in different capacities. I have learned through my experiences that a person cannot succeed through a doctoral program without help of this nature. I will begin by expressing my deepest gratitude and appreciation to my family for their continuous love and support at all times, including Kayly Combs, who continued to love, care for, encourage, and comfort me no matter my temperament. I want to thank Dr. Khaled Gasem for recommending that I pursue my Doctorate following my Master's; without his suggestion, I may not have written this dissertation. I also want to give a tremendous amount of appreciation and thanks to my adviser and mentor, Dr. Sundar Madihally, for his insight, guidance, support, and recognition. Since the beginning of my graduate career, Dr. Madihally has continuously encouraged my research goals, and his passion for research continues to inspire me daily. I would like to extend my gratitude to my colleagues Lukasz Witek, Dr. Jagdeep Podichetty, Christian Tormos, Kumar Singarapu, Kevin Roehm, Abdu Khalf, Carrie German, Swapneel Deshpande, and Leigh Krause for their contributions in my doctoral tenure. I would like to extend my utmost thanks to my committee members, Dr. Gary Foutch, Dr. Donald Ruhl, and Dr. Jim Smay, for their continuous guidance, suggestions, and use of equipment. I would also like to thank Curtis Andrew for his endless efforts in preparing and performing histological samples for me, Lobat Tayebi and her group for their

Acknowledgements reflect the views of the author and are not endorsed by committee members or Oklahoma State University.

collaborative efforts, and Dr. Todd Jackson and Carl Gedon for their help and training in animal care and use at the LAR.

I am very grateful to Dr. Rob Whiteley and the Chemical Engineering faculty for their continuous support and guidance to all graduate students. I am also very appreciative of the contributions made by the Chemical Engineering staff, Shelley Potter, Paula Kendrick, Shelley Taylor, Eileen Nelson, and Carolyn Sanders. I am honored and fortunate for Dr. Marty High and again Dr. Foutch in choosing me to join them in delivering unique educational experiences with the development of Online Thermodynamics and study abroad with Southwest Jiaotong University's Mao Yisheng Honors College, respectively. I also want to thank the Chemical Engineering Graduate Student Association (ChEGSA) past and future committees for continually building on the platform the founding committee and I established. I also want to acknowledge Oklahoma Center for Advancement of Science and Technology (HR12-023), Edward Joullian Endowment, Cherokee Nation Foundation, Robberson Summer Dissertation Fellowship, Hunter Stone Endowed Scholarship, Distinguished Graduate Fellowship, GPSGA Travel Grants, Graduate College, and CEAT for providing my research funding, and support that financed my continued education. Finally, I would like to thank the City of Stillwater and Oklahoma State University for providing me with a great home, a rich experience, and a wealth of knowledge.

GO POKES!!!

Name: KENNETH JAMES WALKER

Date of Degree: MAY, 2015

Title of Study: PHENOTYPIC AND GENOTYPIC ALTERATIONS OF MATURE CELLS DISPERSED IN INJECTABLE ZONAL HYDROGELS MIMICKING THE CARTILAGE MATRIX COMPOSITION

Major Field: CHEMICAL ENGINEERING

Abstract: Cartilage is a soft multilayered tissue found in the articular capsule of joint areas. Physical activity and osteoarthritis (OA) can damage and deteriorate the avascular, metabolically low tissue. Because of this, chondrocytes are incapable of regenerating cartilage tissue when a defect occurs. Therefore, regenerative therapies incorporating the fundamental concepts of tissue engineering are required to repair the damaged cartilage. Previous efforts employed the use of highly invasive surgical procedures and 3D isotropic scaffolds, many of which lacked similarity to native cartilage composition. This research focused on two main areas i) the importance of cartilage composition for designing scaffolds, ii) the involvement of physical and chemical factors on promoting growth, differentiation, and biological function of cells. Chitosan-based zonal hydrogel scaffolds were designed for three out of the four layers of cartilage ranging from the superficial zone (chondrocytes) to the calcified zone (osteoblasts with the biochemical composition of cartilage in mind. Mechanical, physical, rheological properties of the hydrogels were assessed. Additionally, the hydrogels were subcutaneously injected into the dorsal area of mice to observe the immune responses and gelation characteristics of the hydrogels in an *in vivo* environment. Since chondrocytes are not a viable source due to low metabolism and stem cell sources come with an array of problems as well. Therefore, this research explored the use of human foreskin fibroblasts in chondrogensis and osteogenesis. The zonal hydrogels were used with chemical stimulus from differentiation medium to induce chondrogenesis and osteogenesis on the fibroblasts. The cultures analyzed using genotypic and phenotypic analyses to fully assess the quality of the tissue produced and the transformation of the fibroblasts into the chondrogenic and osteogenic lineages. Anisotropy was achieved through sequential layering of the hydrogels. Further the absent cartilage zone was created during the layering process. Hydrogel gelation was observed upon injection, and the hydrogels were also observed to be stable in the *in vivo* mouse models and retain shape throughout the duration of the study. The genotypic and phenotypic analyses of the induction cultured were suggestive of fibroblast transformation into the chondrogenic and osteogenic lineages.

TABLE OF CONTENTS

Chapter Page

Chapter Page

LIST OF TABLES

Table Page

LIST OF FIGURES

Figure Page

Figure Page

CHAPTER I

INTRODUCTION

Arthritis is the most cause of disability in the United States with osteoarthritis (OA) being the most prevalent type. An estimated one out of two people will be diagnosed with this potentially life-altering joint disease in their lifetime (Prevention, 2007). In 2005, OA was estimated to be affecting the quality of life for 27 million people in the U.S. with the number of patients diagnosed with some type of arthritis projected to increase to over 67 million by 2030 (Hootman & Helmick, 2006; Murphy & Helmick, 2012). Additionally, OA alone has raised the current economic impact to healthcare by $186 billion per year (Spine-health). This is a dramatic increase from the estimate of $128 billion in 2003 for all arthritis and rheumatic diseases (Prevention, 2007). OA can be caused by various factors such as age progression and tissue deterioration, physical activity, or obesity. This disease is also known to partially of permanently disable the person limiting mobility by deteriorating cartilage and bone until the tissues' functionality is rendered useless. The damaged cartilage must be replaced due to its limited healing capacity. OA can also be the result of obesity, which is a precursor for cardiovascular disease (CVD) (Center, 2012; Federation; Foundation). Interestingly, when U.S. maps of the geographical areas of OA, obesity, and CVD are displayed together (**Figure 1.1**), a pattern emerges from the southern U.S. linking the three diseases suggesting one disease could lead to the others. There is data linking obesity to CVD but not OA to CVD, however one can speculate that OA could be a precursor for CVD, the No.1 killer in the U.S. since 1918 according

to the American Heart Association(Association, 2013). This link makes OA a prime target for research involving strategies repair the defective cartilage tissue.

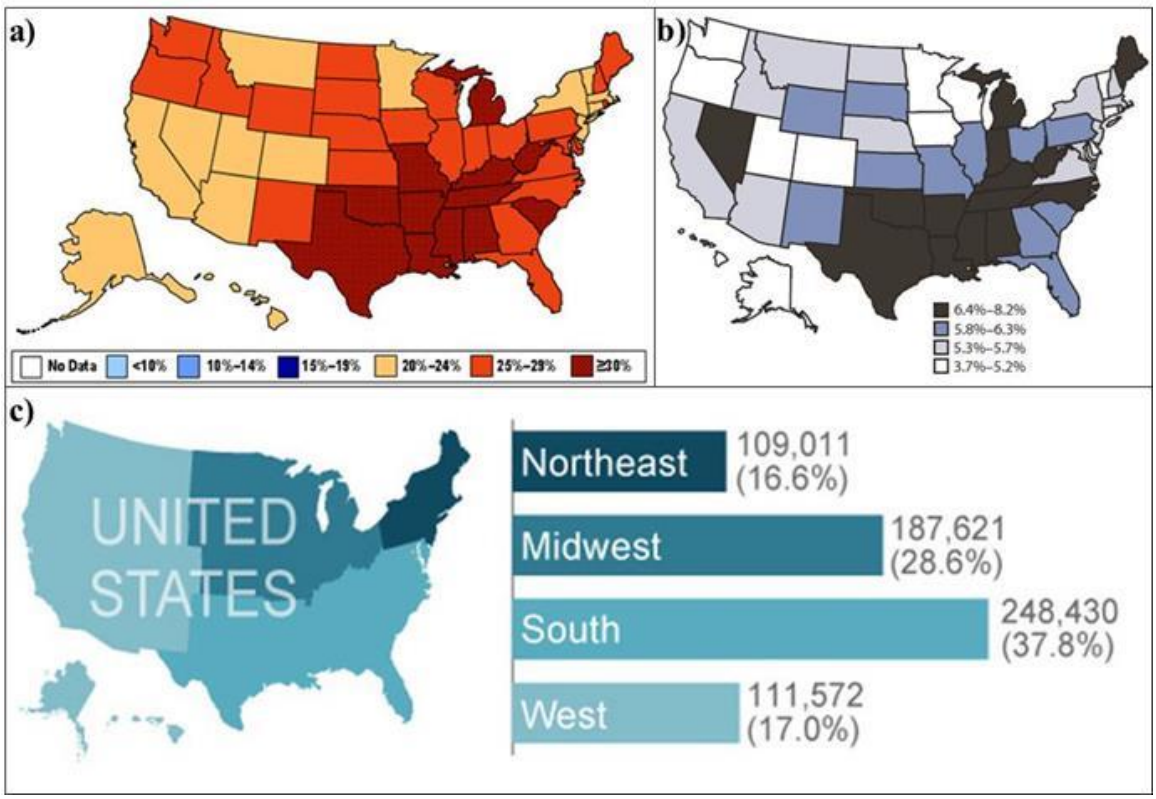

Figure 1.1. Geographical areas affected by (a) obesity (Health, 2012), (b) CVD (Prevention, 2011), and (c) OA (Healthline, 2012c).

Current treatment modalities include autografting (patient), allografting (donor), xenografting (animal), and commercially available artificial medical devices. However, several issues are incorporated with autografts, allografts, and xenografts. Autograft issues include lack of availability of a sufficient tissue source for multiple implantations due to the patient's pathological state. The issue with allografting and xenografting are immunological rejection and increased risk of disease transmission. Medical devices are commercially available for use in partial or total knee replacements. This has become a popular strategy to counteract OA with currently more than 600,000 knee replacements performed each year (Surgeons, 2013) and

projected to surpass 3.5 million by 2030 (Prevention, 2007). However like the tissue grafts, knee replacements come with many problems such as potential for weight gain (Daily, 2013), reduced mobility, increased risks due to infection, metal allergy, and anesthesia complication (Healthline, 2012e), multiple surgeries (Surgeons, 2010), cost averaging up to $65,000 dollars (Healthline, 2012g), and the potential to affect the state of mind (Healthline, 2012a). While these modalities possess potential to improve health, novel alternative approaches seeking an improved outcome need to be developed.

Tissue engineering has become an emerging field over the past twenty years combining the use of cells and scaffolds with the goal of repairing or regenerating native tissue. The fundamental strategy is to design a scaffold capable of promoting cellular function, proliferation, differentiation, growth, and extracellular matrix (ECM) production to ultimately facilitate tissue function *in vitro* to be used later in *in vivo* models. These approaches differ from convention therapies because the engineered tissue becomes an integral part of the body replacing damaged tissue with the functional regenerated tissue potentially permanently curing the disease. The precursor to *in vitro* tissue engineering is to embed functionally elicited cells within fully functional scaffolds to promote expression of the desired phenotypic and genotypic cues of the targeted tissue. In the case of cartilage and bone tissues, the engineered tissue must produce a matrix mimicking the biochemical, biomechanical, and architectural properties native to the osteochondral interface. Although engineered cartilage and bone constructs are commercially available, many of the efforts over the past fifteen to twenty years have failed to produce functional cartilage and bone tissues sufficient for clinical and nonclinical applications. Additionally, multiple cell types, differentiation factors, scaffolds, and culture environments have been studied for tissue regeneration; however, development of an effective, reliable *in vitro* strategy capable of producing similar properties to cartilage and bone has yet to be seen. The most popular scaffold used of regeneration of the tissues at the osteochondral interface has been

hydrogels. Hydrogels have been a desirable scaffold because of the bi-phasic nature, easy incorporation of cells, and alternative to invasive surgeries. In order to ensure growth of a tissue mimicking cartilage, the specific biological responses activated by scaffold properties must be known. Some of the scaffold and environmental properties studied to regulate differentiation through cell adhesion, morphology, migration, and the cytoskeletal network are the chemical, physical, mechanical, and environmental stimuli (Mahmoudifar & Doran, 2012). However, the signals produced by cartilage cells (chondrocytes) and bone cells (osteoblasts) between the physical environment, intracellular network, and cell phenotype have not been fully elucidated.

Cell type and availability also play an important role in tissue engineering. Since chondrocytes have low metabolic activity, the cells are typically not utilized in regenerating engineering tissues. Therefore, alternative sources for use in chondrogenesis and osteogenesis are desired. Physiologically, human mesenchymal stem cells (hMSCs) are the progenitor cells differentiating into chondrocytes and osteoblasts through the process of endochondral ossification. Although, hMSCs have been the popular cell source utilized for differentiation into both cells lines, significant issues such as poor quality tissue production and generation of an unstable phenotype remain (Mahmoudifar & Doran, 2012). Other cell sources such fibroblasts have been incorporated through genetic reprograming, transforming the cell into a pluripotent stem cell known as induced pluripotent stem (iPS) cells (Yamanaka, 2008, 2009). However, iPS cells have not been fully tested for clinical purposes (Apostolou & Hochedlinger, 2011) and currently remain a unreliable cell source. Alternatively, fibroblasts and osteoblasts exhibit phenotypic and genotypic similarities, and fibroblasts embedded in a hydrogel scaffold has shown phenotypic similarities to chondrocytes.

This research focused on how scaffold properties, architecture, and composition combined with biochemical influences affect the genotypic and phenotypic cues in cells (**Figure 1.2.**). Chitosan was used as the base material in all of the hydrogels representing each of the cartilage zones.

Additionally, four different cell types presenting different cellular characteristics were used to understand the influence the hydrogels and media had on chondrogenesis and osteogenesis.

1) Human foreskin fibroblasts (hFF-1s) are dermal cells isolated from the foreskin of males and the most common cell type in connective tissues. hFF-1s are known assist in wound healing and produce collagen to form the structural framework for tissues.

2) Human mesenchymal stem cells (hMSCs) are present in bone marrow and are the primary progenitor cell for osteochondral differentiation into the osteoblastic and chondrogenic lineages.

3) Normal human osteoblasts (NHOsts) are mature bone cells that provide a positive control to the osteogenic differentiation.

4) Hepatocellular carcinomas (HepG2s) present an outside cell control to check for phenotypic and genotypic alterations of osteogenic differentiation.

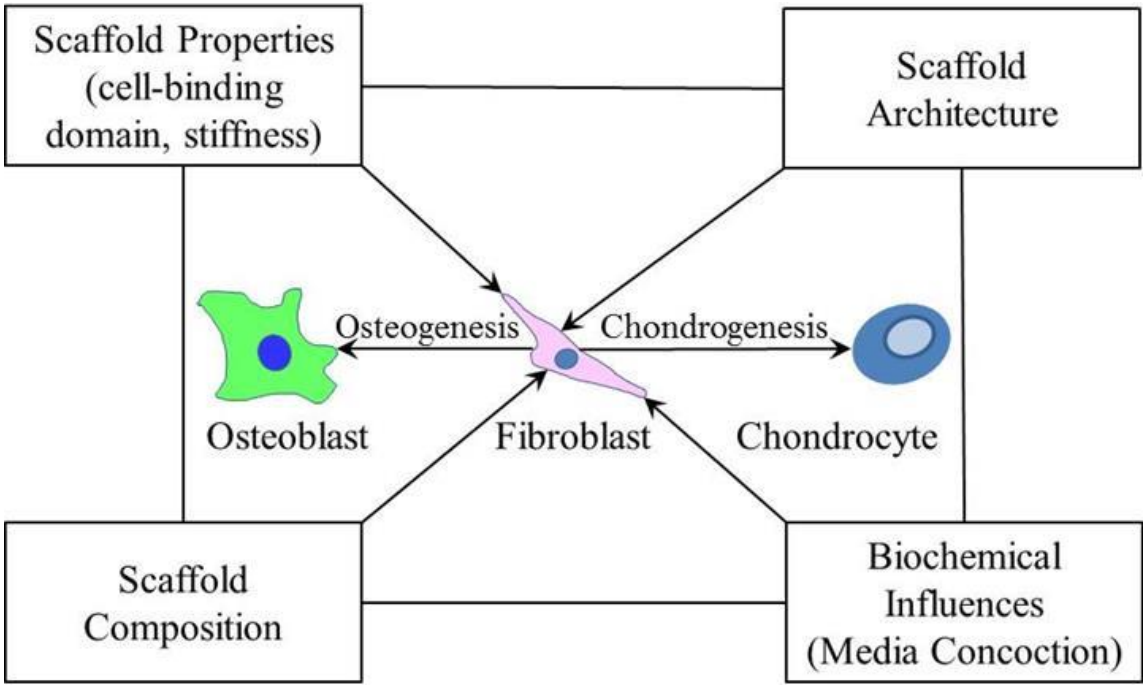

Figure 1.2. Scheme showing important factors influencing chondrogenesis and osteogenesis.

The underlying hypothesis of this research is ***"biologically inspired scaffolds mimicking the in vivo environment will serve as a permissive substrate for fibroblast growth, differentiation, and biological function"***. The schemes illustrating the research used to test this hypothesis are compiled in **Figures 1.3.**, **1.4.**, and **1.5.**

Specific Aim I: Forming anisotropic injectable hydrogels with properties mimicking cartilage.

Isotropic hydrogels were formulated using chitosan, gelatin, hyaluronic acid (HA), and/or beta tri-calcium phosphate (β-TCP) representing the superficial, radial, and calcified zones. Mechanical (compressive and cyclical), rheological, and structural properties were examined for each layer. Thermal gelation properties of the hydrogels were assessed for the gelation temperature and rate of gelation.

Specific Aim II: Test the plasticity of fibroblasts into chondrogenic lineage in the zonal hydrogels.

hFF-1 and hMSC cells were cultured in hydrogel systems for four weeks. Supernatants and cell-hydrogel composites were analyzed for specific protein secretion, matrix metalloproteinase (MMP) activity, immunohistochemistry (IHC), and histology. The hallmark of chondrocyte differentiation is the production and assembly of collagen type II and aggrecan instead of collagen type I expressed by fibroblasts. Aggrecan was measured via ELISA. Glycosaminoglycan (GAG) content was assessed using alcian blue (pH 1.0) staining of the tissues and aggrecan, collagen type II, and collagen type I content in the tissue was tested using immunohistochemistry. Changes in the degradation enzymes MMP-2/MM-9 and MMP-13 were analyzed using a fluorogenic substrate specific for each MMP.

Specific Aim III: Test the plasticity of mature cells into osteogenic lineage in calcified zone hydrogel.

The hallmark of osteoblast differentiation is the production of calcium deposits and alkaline phosphatase (ALP). Hence, hFF-1s, hMSCs, NHOsts, and HepG2s culture supernatants were assayed and alkaline phosphatase to suggest successful differentiation. Histology analyses via haematoxylin and eosin (H/E) and von Kossa were performed to analyze cell and matrix distributions and calcium phosphate deposition. Quantitative polymerase chain reactions (qPCR) were used to identify genes for proteins such as collagen type I, Runx2, osteocalcin, osteopontin, osteonectin, osterix, Sox-9, bone sialoprotein, ALP, and β-Actin.

This research showed significant potential of anisotropic hydrogel formation and the hFF-1s ability to differentiate into the chondrogenic and osteoblastic lineages (described in Chapters 3, 4, and 5). The conclusions and recommendations are summarized in Chapter 6.

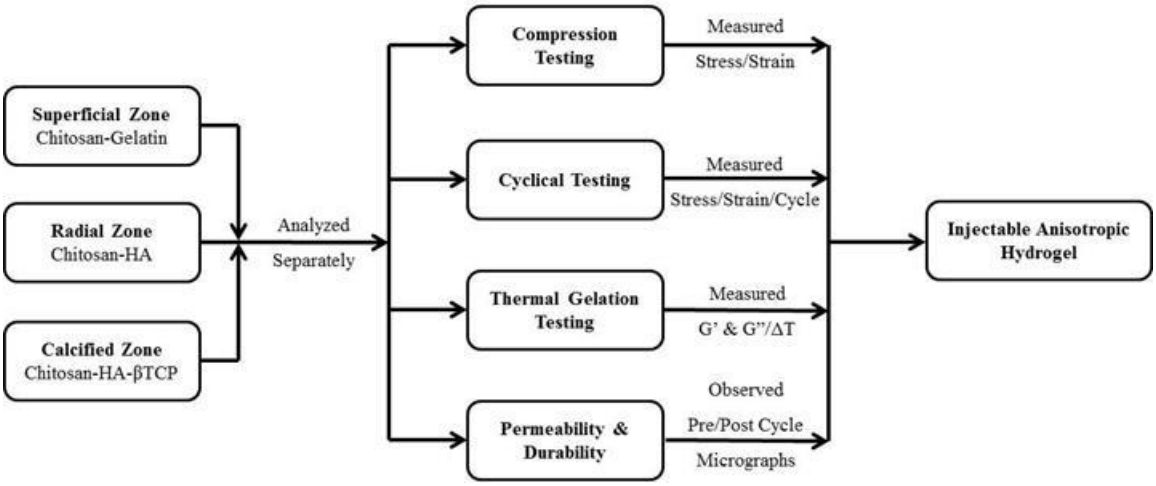

Figure 1.3. Research scheme for Aim I

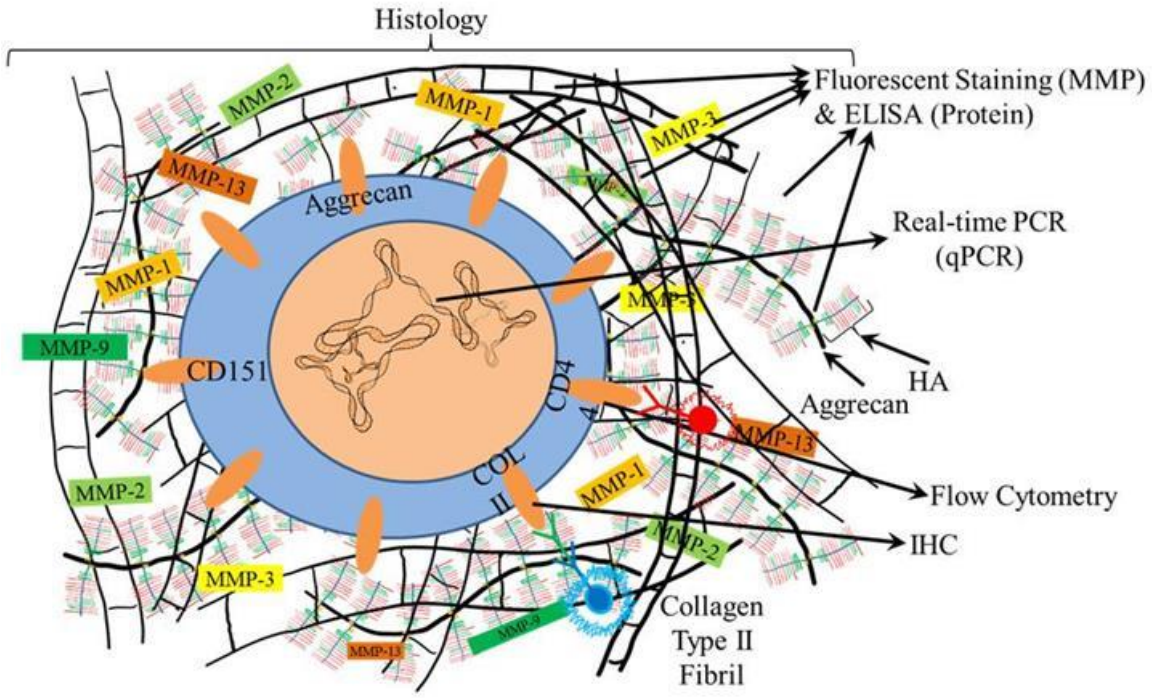

Figure 1.4. Research scheme for Aim II

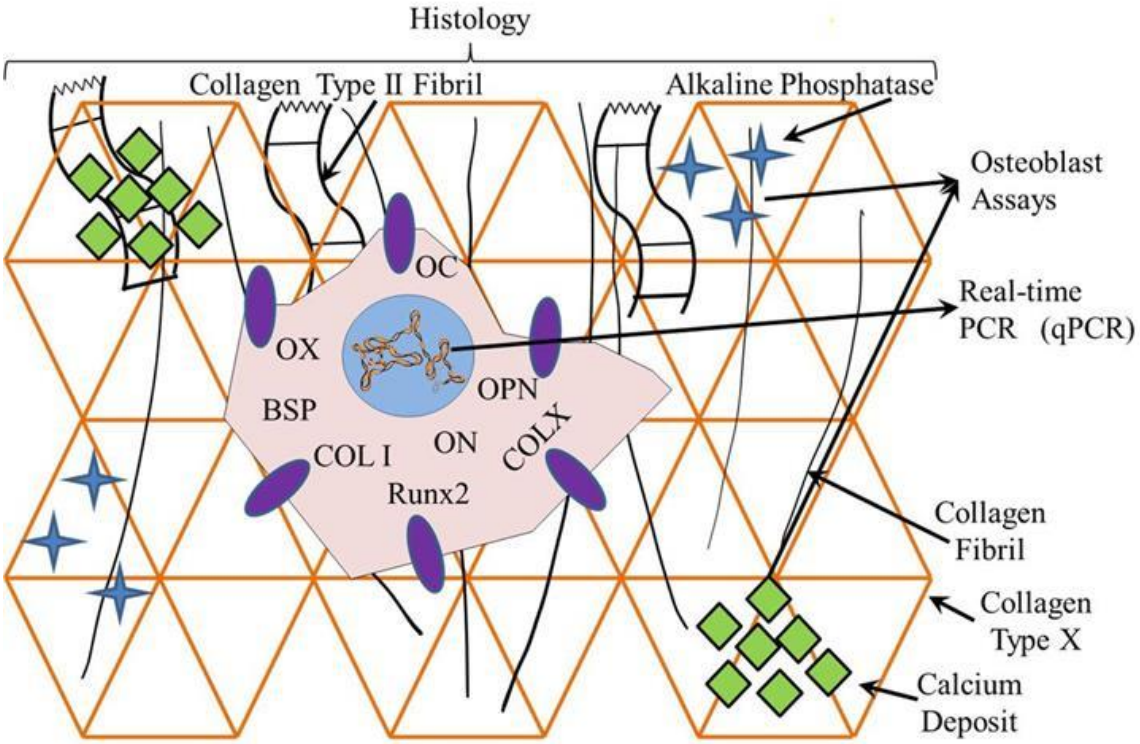

Figure 1.5. Research scheme for Aim III

CHAPTER II

REVIEW OF LITERATURE

2.1. Tissue Engineering: A method for regenerating cartilage

Articular cartilage is a soft anisotropic tissue found in articulating joints that covers the ends of bones in vertebrates. Cartilage acts as a lubricant and force distributor in the contact area between bones. Without articular cartilage, stress concentration and friction would occur to the degree that the joint would not permit ease of motion. Articular cartilage houses cells known as chondrocytes ranging in phenotype and occupying approximately 2 to 3% of the total volume. Nearly 80% of the total weight is water and the remaining weight is extensive extracellular matrix (ECM) primarily composed of collagen type II and proteoglycans. Smaller weight percentages of cartilage ECM are composed of lipids, phospholipids, noncollagenous proteins, and glycoproteins (Fox, Bedi, & Rodeo, 2009). However, cartilage lacks a vascular system reducing chondrogenic proliferation potential leaving the chondrocytes with low metabolism. Therefore, damage or deterioration from defects or osteoarthritis can be detrimental to the tissue requiring repair assistance from an alternative source. Defects due to injury may develop into osteoarthritis (OA) if not treated early.

Traditional treatments for osteoarthritis were partial or total knee replacements (arthroplasty) where the cartilage, ligaments, and patella are replaced with femoral, tibial, and patellar components (Surgeons, 2011). Unfortunately, this method requires highly invasive surgeries and opens the possibility of infection, increased pain, and reduced mobility. Current conventional

treatment modalities for damaged cartilage include the removal and/or surgical repair of the damaged cartilage. Osteochondral allografting and autografting are tissues that have previously demonstrated some potential to regenerate hyaline cartilage. Allografts are transplantable tissues from a donor with a different genotype. Autografts, referred to as the "gold standard", are tissues from the patient's body explanted from one area to be implanted in another (Stuart, 2009). Despite the continuous developments in surgical procedures, cartilage regeneration from transplanted/implanted permanent artificial materials is still insufficient due to multiple factors such as immunosuppressive therapy, mobility and pain reduction, and mechanical mismatch. These deficiencies and early approaches have given rise to new advancements through orthopedic tissue engineering.

A strategy mimicking natural cartilage is the key to successfully reducing the cost and care of cartilage issues (Bobick, Chen, Le, & Tuan, 2009; Diekman, Estes, & Guilak, 2010; Guochun Gong, Deborah Ferrari, Caroline N. Dealy, & Robert A. Kosher, 2010; Tew, Murdoch, Rauchenberg, & Hardingham, 2008). Traditional tissue engineering strategies offers new possibilities for the regeneration of damaged or diseased tissue. Tissue engineering meshes biological and engineering principles to develop functional alternatives for damaged and diseased tissues (Langer & Vacanti, 1993). The concept of tissue engineering is to embed isolated cells from the patient or a donor into a biocompatible and biodegradable scaffold. The cell-encapsulated scaffold is surgically implanted into the patient to promote regeneration of the damaged tissue. Improved tissue engineering techniques have led to tissues more closely relating to native cartilage. These tissues are known as hydrogels and are attractive for cartilage repair due to the biphasic nature (liquid and solid compartments). Some hydrogels offer an alternative strategy for implantation through injection creating a similar but modified tissue engineering approach (**Figure 2.1.**).

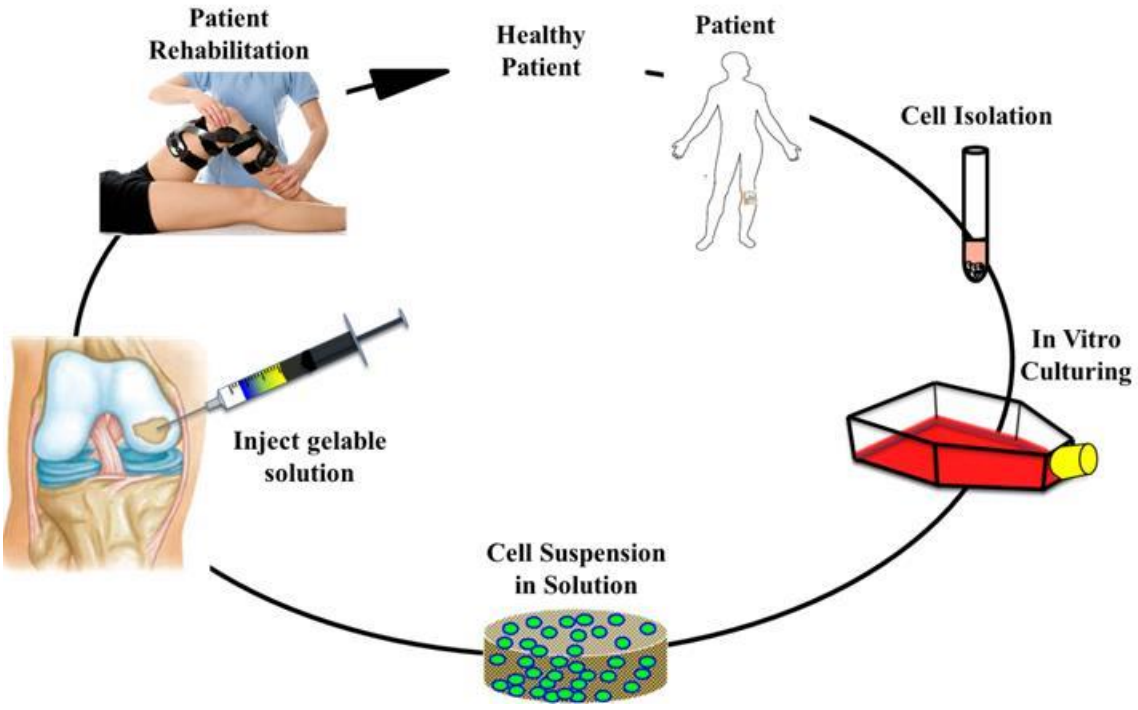

Figure 2.1. Tissue engineering approach for regenerating tissue

2.2. Scaffold based Tissue Engineering

It is imperative to understand cartilage composition and architecture as this knowledge could dictate the success of a scaffold used for regeneration. Since cartilage does not have a continuous nutrient supplementation, the tissue relies on the cellular dormancy and responsiveness to the surrounding ECM. The ECM controls the tissue structure by holding the cells together and regulating the cell phenotype (Stevens & George, 2005) and should be considered as a resourceful platform for designing regenerative tissues. ECM elements are produced by the resident chondrocytes and take up a variety of forms in different tissues. Water, collagen, GAG/proteoglycan, and noncollagenous proteins are the principle ECM constituents of cartilage. These proteins interact with one another to form a highly organized and specialized connective tissue matrix (Gentili & Cancedda, 2009). There are two major elements of the ECM forming the cartilage framework: collagen type II fibrils and the proteoglycan (PG), aggrecan. On a dry

weight basis, the most abundant is collagen type II, which makes up approximately 60% while the rest of the ECM is composed of 25-35% PGs, and 15-20% other lipids, phospholipids, noncollagenous proteins, and glycoproteins (Fox et al., 2009; Mow, Wang, & Hung, 1999). Structurally, there are four zones, superficial, transitional, radial, and calcified, (**Figure 2.2.**) in articular cartilage that can be microscopically observed, which differ in collagen fibril orientation (Eyre, 2002), ECM composition, and cellular phenotype (Mow et al., 1999). Further, each of the individual zones possesses different biomechanical, biochemical, and biophysical cues distinguishing one from the other.

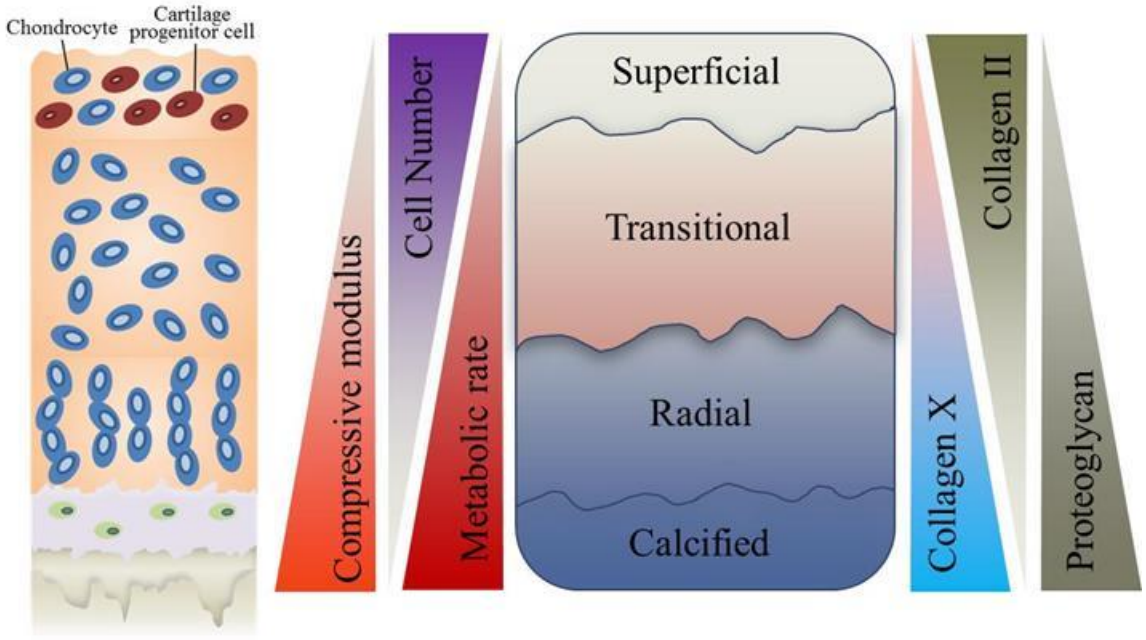

Figure 2.2. Cartilage architecture, and biochemical and mechanical characteristics.

The superficial zone makes up the top 10%-20% of cartilage and is mostly composed of collagen type II fibrils, which are arranged parallel to the articular surface. The transitional zone is anatomical bridge between the superficial and radial zones. This zone makes up approximately 40%-60% and made mostly of a randomly organized composition of collagen and aggrecan. The radial zone is mostly composed aggrecan with collagen fibrils perpendicularly oriented to the

articular surface and accounts for approximately 30% of the volume. Following the radial zone begins the calcified cartilage zone. The tide mark distinguishes the calcified cartilage from the subsequent zones and begins the cartilage transformation into bone. This zone is rich in collagen types I and X, promotes vascularization, and begins bone mineralization. Additionally, the superficial zone is in contact with synovial and provides mechanical resistance imposed by articulation whereas the deeper zones provide mechanical resistance to compressive forces with the radial zone providing the greatest resistance (Fox et al., 2009; Gentili & Cancedda, 2009; Wilson, Whitelock, & Bateman, 2009). Homeostasis of the ECM within these zones is upheld by complex mechanisms involving turnover and remodeling of the resident cells and macromolecules. However, the zones can be subjected to deterioration due to osteoarthritis, rheumatoid arthritis, or cartilage injury causing severe discomfort and reduced lifestyle. In the occurrence of local trauma, mechanical overload, or joint surface injury, local factors of the resident cell, cytokines, inflammatory mediators, and MMPs, could promote excessive ECM degradation. Disease can be the unfortunate result if all of the factors are not harmonious in their reparations (Eyre, 2002; Gentili & Cancedda, 2009; Mow et al., 1999). Thus, each of these aspects must be assessed when developing a functional scaffold system for cartilage regeneration.

In lieu of total knee replacements and cartilage grafting surgeries, several methods have been explored for regenerating cartilage with synthetic and natural polymers. The scaffold must be biodegradable implying the ability of the material to degrade into non-toxic byproducts leaving as waste with healthy tissue as the result. The scaffolds must also be biocompatible, which combines the use of materials promoting biochemical and biomechanical cues as well as cell attachment without provoking unwanted immune responses. Additionally, scaffold stiffness of the substrate has been found to be influence cellular growth and function (Discher, Janmey, & Wang, 2005; Wells, 2008; Yeung et al., 2005). However, the main challenges of tissue engineering cartilage is providing the essential cells and signals to synthesize ECM and

reestablish the molecular organization to form the basis of the essential mechanical properties of the tissue. Most of the current modalities require invasive surgeries to employ cartilage regeneration. For example, Anika Therapeutics (Bedford, MA) uses an isomorphic benzylic ester of HA, HYAFF, based scaffold cultured with autologous chondrocytes to produce autographs for invasive surgical cartilage regeneration, which are currently in clinical trials outside of the United States (Therapeutics, 2012). Alternatively, cartilage regeneration in the form of biphasic hydrogels has been examined. Piramal Healthcare Ltd. (Armand-Frappier Laval, Quebec, Canada) has combined the use of a polymer hydrogel (BST CarGel®) and microfracture surgery as another regenerative method (Piramal Healthcare Ltd). However, polymer based hydrogels have been explored more recently as a regenerative therapy for cartilage lesions and disease and to counteract the invasive surgery requirements. Some groups have developed hydrogels that require the absorption of photons to undergo degradation, cellular encapsulation, and polymerization (J. Elisseeff et al., 2000; Kloxin, Kasko, Salinas, & Anseth, 2009; Mow et al., 1999; Werkmeister et al., 2010). Yet, there has been no previous study introducing an injectable anisotropic scaffold to mimic the multi-layered morphology of natural cartilage.

2.3. Hydrogel Fabrication Materials

Hydrogels are hydrophilic synthetic or natural polymers consisting predominantly of water without dissolution. Hydrogel scaffolds are desired for cartilage regeneration because the gel offers a comparable environment to native cartilage. The water content generates both mechanical and osmotic pressures which play a significant role in nutrient supplementation and waste removal. These pressures affect fluid flow across the superficial zone/synovial fluid interface and within the cartilage zones. Articular cartilage is an avascular tissue and hence waste is eliminated when fluid is extruded through the permeable articular capsule during compressive loading. Alternatively, nourishment comes when synovial fluid is reabsorbed through the capsule into the cartilage during rest section of the compression cycle. The driving force for the

reinfusion is the osmotic pressure differences between the articular cartilage and the synovial fluid (Mow et al., 1999). Thermo-sensitive hydrogels main advantage is the injectable availability provided by the ability to be liquid at room temperature and gel at body temperature. Injectable hydrogels have been widely explored because they offer ease of incorporation of cells and biologically active agents and a minimally invasive alternative to orthopedic surgeries (Jason A. Burdick, Peterson, & Anseth, 2001; Kuo & Ma, 2001; Mann, Gobin, Tsai, Schmedlen, & West, 2001). Furthermore, injectable hydrogels have multiple fabrication methods composed of materials including synthetic and natural based biomaterials.

2.3.1. Synthetic Biomaterials

Synthetic polymers provide alternative scaffold materials to natural polymers for use in hydrogel fabrication and come in numerous material compositions including, but not limited to, poly(ethylene oxide) (PEO), polyurethane, polyethylene glycol (PEG) and poly(vinyl alcohol) (PVA). Synthetic polymers offer reproducibility and control of the mechanical and physical properties, however, many of these materials lack cell binding sites and interactions, direct biocompatibility, and biodegradability (K. Y. Lee & Mooney, 2001; Sakiyama, 2008). Few recent studies have attempted to mimic the spatial organization of articular cartilage (Ng, Ateshian, & Hung, 2009). Photopolymerization techniques have been used to form gels in a fast and controllable manner (J. Elisseeff et al., 2000; J. H. Elisseeff). Other groups have also used photons as a mechanism for polymerizing and degrading hydrogels. These methods are not practical for *in vivo* cartilage regeneration due to the lack of photon emission intensity in the body. Some have utilized UV cross-linking in situ (Sharma et al., 2007). However, this approach has inherent safety concerns at the clinical settings (Nguyen, Kudva, Saxena, & Roy, 2011). Thus, natural polymers are also explored for cartilage regeneration purposes.

2.3.2. Natural Biomaterials

Natural biomaterials from ECM components are used because their role in diverse molecular mechanisms has been extensively explored. A natural polymer such as HA has been used as the platform material for hydrogels. The HA hydrogel was utilized in human embryonic stem cells (hESCs) differentiation to synthesize ECM-enriched cartilaginous constructs and investigate long-term reparative ability of hydrogels (Wei Seong Toh et al., 2010). Alginate hydrogels containing embedded hMSCs have been studied to observe hMSC chondrogenic differentiation in a gel system to better understand the temporal aspects of relevant gene expression and phenotypic changes (Xu et al., 2008). Collagen is a commonly used protein due to its commonality between multiple mammalian tissue ECMs such as skin, bone, cartilage, tendon and ligament. However, collagen hydrogels have limited mechanical properties, potential immunogenicity, and can be economically undesirable (K. Y. Lee & Mooney, 2001). Alternatively, gelatin, partially denatured derivative of collagen, has been explored as a hydrogel scaffold in place of collagen due to its biocompatibility, biodegradability, and ease of gelation. Like collagen, gelatin has weak mechanical characteristics and is not a viable standalone hydrogel scaffold. Another commonly used natural polymer is chitosan, which is derived from the deacetylation of chitin. Chitosan is a polysaccharide consisting of glucosamine units with structural similarities to HA. Previously, chitosan has been used as the base material for preparing the thermo-sensitive hydrogels using β-glycerophosphate (GP) chemistry. Additionally, chitosan-GP gels demonstrated the formation of cartilage after three weeks when used for *in vivo* purposes (Ahmadi & de Bruijn, 2008). The chitosan-GP based chemical combination is ideal for drug delivery, cell encapsulation, and injectable tissue engineering applications because the solution maintains physiological pH in the liquid state and gels when approaching body temperature (**Figure 2.3.**). Furthermore, integration of chitosan with other materials such as calcium phosphate (CP) (Zhang & Zhang, 2001) and hydroxyapatite (Kawakami et al., 1992) have been

used to create bioactive composites demonstrating osteoconductivity and enhanced mineralization (Di Martino, Sittinger, & Risbud, 2005). However, injectable hydrogels have not met the compressive capabilities of natural cartilage. Therefore, to be used clinically as an alternative for cartilage regeneration, similar post-operative procedures to invasive surgeries, i.e. braces or casts, must be used for additional support.

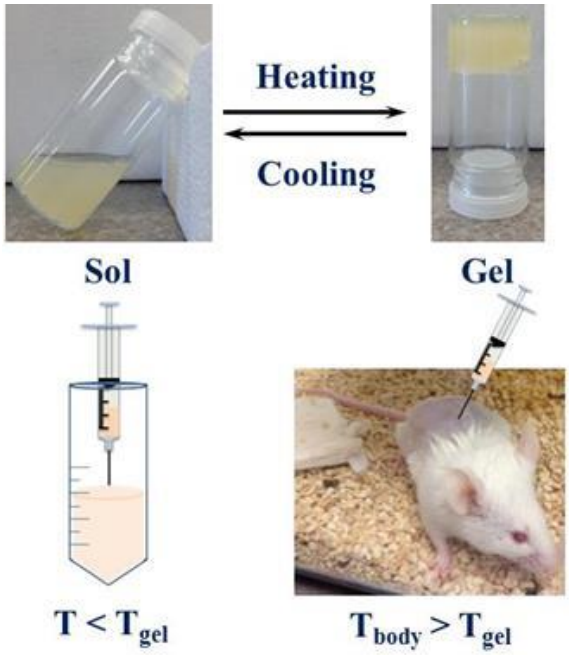

Figure 2.3. Illustration of thermo-sensitive hydrogel phase change.

2.4. Chitosan-based Hydrogel's Thermo-sensitive Gelation Mechanism

In 2000, Chenite et al. developed a new thermo-sensitive hydrogel system by neutralizing an acidic chitosan solution with GP and increasing temperature (A Chenite, Buschmann, Wang, Chaput, & Kandani, 2001). Thermo-sensitive hydrogels using chitosan employ a gelling agent such as GP to not only assist in the pH neutralization but gelation as well. The neutralization is necessary because chitosan solubility requires acidic conditions with a pH lower than the pKa of 6.2, which is too low for most biological systems. Chitosan becomes protonated at lower pH inducing electrostatic repulsion between polymers in turn causing solvation. When the pH is

neutralized the chitosan chains begin forming gel-like precipitates without phase separation or gelation (Li, Rodrigues, & Tomas, 2012). However, gelation was not observed until the temperature was increased suggesting multiple mechanisms behind the gelation.

Many groups have studied the mechanistic effects of gelation at the molecular level. These groups concluded that at the molecular level, the sol/gel transition could be attributed to the competition between several intermolecular interactions. These interactions included attractive interactions from hydrophobicity and hydrogen bonding between the chitosan molecules, electrostatic repulsions between positively charged chitosan molecules, and inducing a screening effect on this repulsion caused by the negatively charged β-GP (Cho, Heuzey, Begin, & Carreau, 2005; Lavertu, Filion, & Buschmann, 2008; Qiu et al., 2011). Earlier studies have focused on these phenomena with the assumption that a protective hydration layer around the chitosan chains was created from the glycerol part, therefore hindering self-interactions and aggregation at low temperatures and neutral pH (A Chenite et al., 2001; Ruel-Gariepy, Chenite A Fau - Chaput, Chaput C Fau - Guirguis, Guirguis S Fau - Leroux, & Leroux, 2000; Wu, Su Zg Fau - Ma, & Ma, 2006). Alternatively, inorganic phosphate salts alone without polyol moieties as well as phosphate-free polyols, with the pH controlled from 6.5−6.8 by sodium hydroxide, yielded temperature sensitive sol/gel transition (Patois et al., 2009; Schuetz, Gurny R Fau - Jordan, & Jordan, 2007). However, these studies did not fully elucidate the role temperature and polyol moiety plays in the sol/gel transition.

In 2013, Supper et al. combined efforts from the previous studies to establish a mechanism for gelation. The observations suggested that the polyol moiety of the gelling agents was responsible for the temperature sensitivity of the chitosan solution. Additionally, the polyol chemical size and structure performed a significant role in controlling the gelation process. When the gelling agent was added to the acidic chitosan solution, a hydration protective layer around the chitosan chains was created by the polyols, which was largely built through weak intermolecular

interactions, such as hydrogen bonding. Disruption of the polyol layer was caused by temperature increases allowing the polymers to interact through stronger hydrophobic bonding. This induced gelation resulting in the sol/gel transition to the hydrogel state. Further, the polyol size was observed to have an impact on stability of the hydration layer, and therefore an impact on the transition temperature and kinetics of the sol/gel formation (Supper et al., 2013).

2.5. Sources for Cells

2.5.1. Chondrocytes

Articular cartilage is composed of a sparse amount of cells called chondrocytes, which are embedded in an anisotropic mixture of ECM elements. Chondrocytes are generally round in morphology and have varying arrangements depending on the cartilage zone. The superficial, transitional, radial, and calcified zones contain flattened chondrocytes and chondroprogenitor cells, randomly organized spherical chondrocytes, columnar organized round chondrocytes, and terminally differentiated chondrocytes undergoing apoptosis (**Figure 2.2.**). Due to the limited supply, proliferation, and phenotypic changes of chondrocytes, alternative cell sources have been explored for regenerating cartilage (Bobick et al., 2009; Diekman et al., 2010; Guochun Gong et al., 2010; Tew et al., 2008). Chondrogenic differentiation from allogeneic human bone marrow derived mesenchymal stem cells has been the standard for these drawbacks. However, there are limitations incorporated with hMSCs such as the lack of autologous sources and high risk procedures for the donors and patients. Alternatively, skin fibroblasts have been explored for plasticity by reprogramming adult cells into induced pluripotent stem (iPS) cells using genetic recombinant techniques (Lowry et al., 2008; Meissner, Wernig, & Jaenisch, 2007; Keisuke Okita, Tomoko Ichisaka, & Shinya Yamanaka, 2007; Takahashi et al., 2007; Yamanaka, 2008). Similar to hMSCs, iPS cells have shortcomings hindering their applicability in differentiation and clinical applications: *in vitro* reprogramming has displayed low efficiency thus far and patient safety

considerations must be addressed. Fibroblast differentiation has not been explored in a synthetic environment, but efforts have been made on comparing phenotypic differences between fibroblasts and adult hMSCs (Blasi et al., 2011).

2.5.2. Osteoblasts

Osteoblasts are the cells responsible for cellular bone formation and are the result of differentiated bone marrow derived osteoprogenitors such as hSMCs. The osteoprogenitors are lie at the growth plate section where calcified cartilage and newly formed bone meet. Osteoblasts can be obtained from bone via enzymatic digestion or from outgrowth of bone explants (Czekanska, Stoddart, Richards, & Hayes, 2012; Declercq et al., 2004). Studies have been performed to associate *in vitro* performance with isolation technique. Additionally, cells obtained through enzymatic degradation tend to proliferate faster than cells from outgrowth explants. Alternative sources have been investigated due to the disadvantages incorporated with human isolated osteoblasts such as, heterogeneous phenotype, long isolation procedure, limited accessibility, and sensitive cellular phenotype to donor related factors (Czekanska et al., 2012). Similar to chondrocytes, stem cells, specifically hMSCs, have become the common source for obtaining the osteoblastic cell line. However, as previously mentioned stem cells have many disadvantages incorporated with all stages for use. Using fibroblast differentiation for chondrocyte and osteoblast regeneration would be advantageous due to the less invasive surgical procedures required to harvest a small autologous skin biopsy and *in vitro* cell expansion in a serum free environment reduces safety concerns related to xenogeneic products (Meissner et al., 2007). Commonly observed advantages and disadvantages for the potential cell sources are listed in **Table 2.1.**

Table 2.1. Advantages and disadvantages of potential cell sources.

Cell Line	Cell Source	Advantages	Disadvantages
Chondrocytes	Autologous/allogeneic (Cartilage tissue)	• Immunogenicity (Autologous)	• Loss of phenotype (Allogeneic) • Painful procedure • Lack of cells
hMSCs	Autologous/allogeneic (Adipose, amniotic fluid and bone marrow)	• Multiple sources • High viability to chondrogenesis/ osteogenesis • Easily to expand *in vitro* • Immunogenic(Autologous)	• Progeny tendency • Risk to donor (extraction) • Risk to allogeneic patient (transmission)
iPS cells	Autologous (Adult human dermal tissue)	• Ability to differentiate cells from an abundant source • Economic • Less painful cell isolation procedure	• Low efficiency of reprogramming • Significant safety considerations to address • Require immune suppressive therapies
Fibroblasts	Autologous (Adult human dermal tissue)	• Immunogenicity (Autologous) • Easy to obtain • Reprogrammable (iPS) • High metabolism and proliferation • High efficiency	• Not well explored for differentiation

Sources: (Fritz, Pelaez, & Cheung, 2009; Meissner et al., 2007; Keisuke Okita et al., 2007; Simion, Botez, Murphy, Eloae, & Barry, 2010; Takahashi et al., 2007; Tıglı et al., 2009; Yamanaka, 2008).

2.6. Cellular Signaling Pathways

2.6.1. Chondrogenesis

Chondrogenesis is the process during endochondral ossification in which a chondroprogenitor cell is transformed into mature chondrocyte. The differentiation process is initiated with the condensation of bone marrow derived hMSCs, which is caused by Sox-9 (*SOX9*) pathway, a cartilage-specific transcription factor (de Crombrugghe, Lefebvre, & Nakashima, 2001). *SOX9*

has been reported to inhibit chondrocyte maturation and regulate the chondrogenic genes for proteins such as collagens type II, IX, and XI, and aggrecan (M. B. Goldring, 2012; Nishimura et al., 2012). Additionally, N-cadherin, N-cam, and tenascin are expressed during the early stages of chondrogenesis. As chondrogenesis continues, the chondroprogenitors transform into proliferating chondrocytes, which produce an ECM rich in collagen type II and aggrecan. Further, the chondrocytes begin developing specific phenotypic cues following the differentiation stage and zonal location within cartilage. The proliferating cells are also expressing low levels of fibroblast growth factor receptor 3 (*FGFr3*), a target of the Indian hedgehog (*Ihh*) signaling pathway (Gentili & Cancedda, 2009). In the radial zone, high expression levels of *FGFr3* and *Ptc1* as well as low expression levels of *RUNX2* and osterix (*SP7*). In the calcified zone, chondrocyte maturation begins the process of hypertrophic differentiation where the chondrocytes enlarge and terminally differentiate and are sequentially mineralize and become apoptotic. During this process, chondrocyte maturation is regulated by Ihh, parathyroid hormone-related protein receptor (*PTHrP-R*), and alkaline phosphatase (Gentili & Cancedda, 2009; Nishimura et al., 2012). Unable to inhibit chondrocyte maturation any longer, *SOX9* expression is arrested, and *RUNX2* expression is elevated, activating expression of collagen type X alpha 1 (*COL10A1*), matrix metalloproteinases (MMPs) 9, 13, and 14, and various growth factors including vascular endothelial growth factor (*VEGFα*) (Gentili & Cancedda, 2009; M. B. Goldring, 2012). The chondrogenic differentiation is a precursor to the differentiation of osteoprogenitor cells into osteoblasts.

2.6.2. Osteogenesis

Toward the end of the endorchondral ossification process, the calcified cartilage tissue has begun mineralization and vascularization at the osteochondral interface. At this point, the osteoprogenitor cells (bone marrow derived hMSCs) express bone matrix protein genes such as collagen type I alpha 1 (*COLIA1*), osteopontin (*SPP1*), bone sialoprotein (*IBSP*), and osteocalcin

(*BGLAP*), and alkaline phosphatase (*ALPL*). These genes are activated and regulated by *RUNX2*, which is highly expressed early in osteogensis, through binging to the specific enhancer regions (Bae et al., 2007; Kaveh, 2011; Komori, 2010). *RUNX2* can be stimulated from various pathways such as *MAPK/ERK* or protein kinase A (*PKA*). These pathways are activated by growth factors, ECM, hormones, and mechanical stimulus (Franceschi & Xiao, 2003). Following the osteoprogenitor stage, *ALPL* expression levels decrease while the cells mature and synthesize new bone. Another transcription factor essential for osteogenesis and matrix vesicle formation is *SP7*, which is a downstream gene of *RUNX2* and expressed during the bone formation phase (Kaveh, 2011; Nishimura et al., 2012). *SP7* is also present during calcified cartilage matrix degradation via MMPs and osteoclast (bone resorbing cells) activity (Gentili & Cancedda, 2009). *SP7* is activated by *Smad* signaling and regulated by *RUNX2* pathways via bone morphogenic protein 2 (BMP-2) and insulin growth factor-1 (*IGF-1*) signaling (Hong, Lu, Nanes, & Mitchell, 2009; Matsubara et al., 2008) and inhibited by the *Wnt*-signaling pathway and parathyroid hormone (*PTH*) *cAMP* signaling. SP7 is known to target MMP-13, which must be up-regulated for *RUNX2* and *SP7* physical functional interactions to exist. Additionally, several osteoblastic genes (*BGLAP*, *COLIA1*, collagen type XI alpha 2 (*COLXIA2*), and *SPP1*) are induced by *SP7* under forced expression conditions (Hong et al., 2009). The phase of osteogenesis following is the formation of vascularized hardened bone surrounding a soft cellular tissue known as bone marrow.

2.7. Induction Strategies for Stem Cells

The chondrogenic and osteogenic lineages can be produced from the *in vitro* induction of hMSCs through various chemical, physical, mechanical, and environmental stimuli such as growth factors, scaffolds, loading, and hypoxia. Each stimulus yields a different cellular response signaling a genetic pathway, ultimately leading to a variety of cell fates. Typically combinations of the stimuli have been used as differentiation strategies for both chondrogenic and osteogenic

processes. Some *in vitro* induction strategies and the resultant genotypic and phenotypic cellular responses chondrogenesis and osteogenesis are described below.

2.7.1. Chondrogenesis

The chondrogenic and osteogenic potential, easy isolation and vigorous proliferation make hMSC the attractive candidate cell for cartilage tissue engineering. hMSCs have been extensively investigated to regenerate chondrocytes as well as osteoblasts. Inducing hMSCs for chondrogenesis can be accomplished by various soluble factors. Specifically, transforming growth factors (TGF-β1, TGF-β2, or TGF-β3) and bone morphogenetic proteins (BMP-6) are most commonly utilized for differentiation of hMSCs into chondrocytes (Danisovic, Varga, & Polak, 2012; Tıglı et al., 2009). Some of the genes expressed in early stages of chondrogenesis include *SOX4*, *SOX9*, BMP-2, and collagen types I and XI whereas in progressed stages (eighteen days or later) aggrecan, collagen types II, IX, and X, *BGLAP*, and *ALPL* (Barry, Boynton, Liu, & Murphy, 2001; Guochun Gong et al., 2010; H. J. Lee et al., 2008; Xu et al., 2008). Further, analysis of chondrogenesis can be assessed through cell surface molecules. Cells with greater chondrogenic capacity expressed higher levels of a number of surface molecules, all known to play a key role in mesenchymal condensation (Mary B. Goldring, Tsuchimochi, & Ijiri, 2006). These include the hyaluronan (CD44), tetraspanin (CD151), and α3 integrin (CD49c) receptors (Grogan et al., 2007). Other common markers for assessing chondrogenic differentiation include to collagen type II and aggrecan (L. Wang et al., 2001).

Previously, micromasses were believed to provide a suitable environment for chondrogenic differentiation due to the similarity to hMSC condensation in physiological chondrogenesis. However, this method does not provide the cells the essential physical and mechanical cues, and lacks functionality clinically. Alternatively, three dimensional (3D) culture systems have become more popular recently and have had a positive influence on chondrogenic differentiation.

Physical stimulus from the scaffold materials combined with chemical stimulus is a widely utilized differentiation strategy. Additionally, cell-cell and cell-matrix interactions during differentiation are regulated by scaffold properties of the scaffolds such as stiffness, elasticity, architecture, and hydrophobicity (Mahmoudifar & Doran, 2012; Wells, 2008). For example, a silk-gelatin hydrogel with TGF-β (Das et al., 2013) and chondroitin sulfate-collagen with (Du et al., 2014) have shown potential in chondrogenic differentiation.

Mechanical stimulus from compression, tension, or hydrostatic forces is also known to have an influence on differentiation in physiologic cartilage; therefore, inclusion of this stimulus may also play a role in regulating differentiation *in vitro* (Mow et al., 1999). This is also a useful method for assessing physiologic cellular responses to scaffolds *in vitro*. Since cartilage is avascular it does not receive steady supplementation of nutrients and oxygen (Zhou, Cui, & Urban, 2004). Therefore cartilage primarily produces energy through glycolysis. However, chondrocytes exhibit the Crabtree effect, where in a reduced glucose environment the energy can be maintained via oxidative phosphorylation (Heywood, Knight, & Lee, 2010). Reducing glucose levels and monitoring for the Crabtree effect is another method for achieving chondrogenic differentiation. Alternatively, another common method used for chondrogenic induction is mimicking the native cartilage environment and stimulating through hypoxia. Pellet cultures experiencing hypoxic environments underwent chondrogenesis, however, the same cultures were observed to resist apoptosis blocking the pathway necessary to fulfill the endochondral ossification process (H. H. Lee et al., 2013).

2.7.2. Osteogenesis

Similar to chondrogenesis, osteogenesis can be achieved by inducing hMSCs with soluble factors. Typical medium concoctions for osteogenesis contain dexamethasone, ascorbic acid, and β-glycerophosphate (β-GP). Dexamethasone is a synthetic corticosteroid that imitates cortisol,

estradiol, testosterone, vitamin D3, thyroxine, and retinoic acid. Dexamethasone binds special regulatory proteins in the cell and subsequently activates transcription of osteoblastic genes. *In vitro* cellular responses to dexamethasone are observed by the increase in ALP activity. Ascorbic acid stabilizes osteoblasts *in vitro* and facilitates in p0roliferation and maintaining osteoblast phenotype through increasing total protein synthesis and ALP activity. β-GP plays an important role in osteogenesis by activating mineralization by providing the chemical potential for promoting bone mineral deposition *in vitro* (Czekanska et al., 2012; Kaveh, 2011). Osteogenic differentiation can be accomplished using glucocorticoids, osteogenin, BMPs, and basic fibroblast growth factors (bFGFs) (Kaveh, 2011). Additionally, strontium has shown potential for inducing hMSCs for differentiating into the osteogenic lineage (Sila-Asna, Bunyaratvej, Maeda, Kitaguchi, & Bunyaratavej, 2007). Scaffolds have also been used for osteo-induction purposes. Osteoprogenitors were induced using a 3D, partially demineralized bone scaffold, mechanical stimulation via four-point bending, and induction medium (Mauney et al., 2004). Pulsed electromagnetic fields (PEMFs) with induction medium have also been shown to promote osteogensis in hMSCs (Tsai, Li, Tuan, & Chang, 2009). Osteoblast differentiation can be monitored using transcription factors (*RUNX2* and *SP7*, and canonical *Wnt*) and osteoblastic markers (*SPP1*, *BGLAP*, *ALPL*, calcium deposits, *COL1A1*, *COL10A1*, *Vegf*, and *Ihh*) (Gentili & Cancedda, 2009; Komori, 2006, 2010). *RUNX2* expression is found in the stages prior to osteoblast formation as well as the immature and intermediate stages. *SPP1* and *BGLAP* are expressed in immature and mature osteoblasts, respectively (Komori, 2010). Another method for tracking osteogenesis is staining cells for ALP and calcium deposits. The unique feature of staining for ALP and calcium is the weak activity for ALP and the complete absence of calcium deposits in undifferentiated hMSCs (PromoCell, 2008).

CHAPTER III

ANISOTROPIC TEMPERATURE SENSITIVE CHITOSAN-BASED INJECTABLE HYDROGELS MIMICKING CARTILAGE MATRIX

3.1. INTRODUCTION

Cartilage could be ravaged by various diseases and regular physical activities, and damaged cartilage has to be replaced due to limited healing capacity. Tissue engineering or regeneration techniques offer alternative strategies. In particular, injectable hydrogels have been extensively explored more recently because they offer a minimally invasive alternative to arthroscopic surgeries and ease of incorporation of cells and biologically active agents (Slaughter, Khurshid Ss Fau - Fisher, Fisher Oz Fau - Khademhosseini, Khademhosseini A Fau - Peppas, & Peppas, 2010). High water content of hydrogels mimics the biphasic (solid and fluid compartments) environment of cartilage; cartilage consists of 2 to 3% chondrocytes and nearly 15% of extracellular matrix (ECM) consists of collagen type II, proteoglycans (PG), and elastins, and the rest is water (Kock, van Donkelaar, & Ito, 2012). Water content within the scaffold generates both mechanical and osmotic pressures which play a significant role in nutrient nourishment and removal of waste products.

Various biomaterials and their modifications have been tested for cartilage regeneration. In particular, chitosan, a biodegradable and biocompatible polysaccharide derived from chitin, has been intensely investigated due to favorable properties in cartilage regeneration (W. S. Toh, Lee Eh Fau - Cao, & Cao, 2011). Since chitosan lacks cell binding domains, collagen and gelatin that

possess cell binding domain have been added via ionic interactions (Y. Huang, Onyeri, Siewe, Moshfeghian, & Madihally, 2005). Further, glycosaminoglycans such as hyaluronic acid (HA) and chondroitin sulfates present in cartilage or their analogues have been combined with chitosan (Tillman, Ullm A Fau - Madihally, & Madihally, 2006). Thermosensitive chitosan hydrogels using β-glycerophosphate (GP) have been prepared (Yamane et al., 2005); the chitosan-GP solution remains in liquid phase at room temperature and gels irreversibly upon increasing to body temperature (Supper et al., 2013). Since chitosan hydrogels are mechanically weak, effects of chitosan concentration have been investigated (Song et al., 2010; Limin Wang & Stegemann, 2010); elastic properties of hydrogel have seen improvement with increased chitosan concentration (Patois et al., 2009). However, many of these formulations are isotropic in nature, unlike the anisotropic cartilage matrix architecture (Bhosale & Richardson, 2008), which requires depth-dependent mechanical properties for a properly functioning cartilage.

Many recent studies show that matrix mechanical properties such as stiffness and scaffold architecture (pore size and void fraction) affect cell shape, attachment, and function (Lawrence & Madihally, 2008). Chitosan-gelatin based scaffolds of different forms also showed variation in the cellular behavior and matrix generation (Iyer, Walker, & Madihally, 2012). Hence, developing scaffolds mimicking the *in vivo* matrix architecture is necessary to improve tissue regeneration. All constituents are distributed anisotropically in cartilage, giving a zonal structure (Bhosale & Richardson, 2008). In each zone, cellular content and morphology vary. More importantly, there are changes in extracellular matrix (ECM) content, organization, and mechanical properties (Aydelotte, Greenhill, & Kuettner, 1988; Aydelotte & Kuettner, 1988). HA provides charge density and compressive modulus, and its content increase with depth. The ability of HA to bind and retain water in the ECM gives the cartilage its unique capacity to absorb repetitive compressive forces (J. A. Burdick & Prestwich, 2011; Toole, 2004). Collagen content responsible for tensile and shear properties (Klein, Chaudhry, Bae, & Sah, 2007) varies in type

and fiber orientation; the superficial zone contains high levels of collagen type II, the transitional (also referred to as middle) zone has lower collagen type II content. The radial zone contains the higher concentration of GAGs. The calcified cartilage zone has high levels of collagen type X and calcium phosphate which help in integration of cartilage to subchondral bone.

Our objective was to test an injectable temperature sensitive hydrogel formulation mimicking architecture of cartilage ECM, using chitosan as the continuous phase. First, isotropic hydrogel systems were formulated by combining chitosan with gelatin, HA, and/or β-tricalcium phosphate (β-TCP) representing the superficial, radial, and calcified zones. Then they were combined to obtain anisotropic hydrogels. Confined mechanical (compressive and cyclical), rheological, and structural properties were examined for each layer. Gelation properties of the hydrogels were assessed *in vitro* and *in vivo* in a BALB/c mouse model. These results show significant potential in the use of injectable hydrogels for cartilage regeneration.

3.2. MATERIALS AND METHODS

3.2.1. Sources for Materials

Low molecular weight (LMW) chitosan (200-300 kDa and 75-85% deacetylation), gelatin type A (300 Bloom), glycerol 2-phosphate (2GP), bovine serum albumin (BSA), hyaluronic acid sodium salt (from Streptococcus equi) (HA),and tri-calcium phosphate (TCP) were purchased from Sigma Aldrich Co. (St. Louis, MO). Hydrochloric acid (HCl) and ethyl alcohol (EtOH) (200 proof) were obtained from Pharmco.

β-TCP was kindly provided by Mr. Lukasz Witek, prepared and characterized by the procedure described previously (Witek et al., 2013). In brief, β-TCP was formed through a sequence of processes beginning with calcining, attrition milling, and drying. TCP was calcined at 800°C and 975°C for eleven hours and milled in distilled water for thirty minutes. Milling was done in an

attrition mill at 120 RPM in a charge of 3mm diameter zirconia milling media. The slurry was removed from the milling media and dried at physiological conditions to produce dry β-TCP.

3.2.2. Isotropic and Anisotropic Hydrogel Fabrication

Three different formulations were prepared to represent the superficial, radial, and calcified layers of articular cartilage. Different preparation techniques were attempted to ensure that those components could co-exist without precipitating. Each technique included a combination of the following factors: stirring speed and time, altering the temperature of the solution, and sequence of introducing different components. A systematic approach was used to optimize formulation of the respective zone by changing the concentration of chitosan (C) from 0.5 to 4% (wt/v), gelatin (G) from 0.1 to 2% (wt/v), HA from 0.1 to 1% (wt/v) and β-TCP from 0.1 to 4% (wt/v). Three categories were chosen: i) ability to form homogeneous solution, ii) gelation at or below body temperature and iii) compressive strength. Chitosan was dissolved using HCl (12 N) and 2GP (0.56 g/mL) was added drop wise into the solution to adjust the pH between 7.2 and 7.4.

After obtaining solutions for individual zones, anisotropic hydrogels were formed by layering each of the zones. To identify each zone, different dyes were added to each zone: yellow for superficial zone formulation, blue for radial zone formulation, and red or no dye (i.e., white from β-TCP) for calcified zone formulations. Two methods were tested while forming anisotropic hydrogels with varying thickness: 1) solutions were suctioned using a 14G needle into a 3mL syringe in layers to understand handling the composite within a syringe; and 2) larger volume of solutions were layered in a 15 or 50 mL conical tubes and intermediate layers were also prepared by mixing equal volumes of formulations from each zone.

3.2.3. Thermal Gelation Analysis

Gelation characteristics were evaluated over a temperature gradient using 12 mL of sample solutions in a Bohlin CVOR controlled stress/strain rheometer (Bohlin Instruments, East

Brunswick NJ). Isotropic hydrogels optimized for the three zones were tested using a C25 concentric cylinders fitting at a shear rate of 1 Hz shear with no strain variability. Mineral oil covered the solutions to prevent evaporation during the measurements. Oscillatory measurements of elastic or storage modulus (G') and viscous or loss modulus (G") were collected while the temperature increased at a rate of 1°C/min between 5°C and 50°C. Thermal gelation was determined as the temperature where G' deviates from G'' (A. Chenite et al., 2000).

3.2.4. Mechanical and Physical Testing

Confined compression testing was performed on hydrogels using an INSTRON 5542 (INSTRON, Canton, MA) and a custom-built anvil (**Figure 3.1.a and 3.1.b**). A solid anvil of diameter fitting a 6-well tissue culture plate with less than 0.5 mm clearance was fabricated. Hydrogels were formed in situ in 6-well tissue culture plates by incubating 13 mL of solution for 6 hours in an oven maintained at 37°C and saturated humidity. Similarly, anisotropic hydrogels were layered inside the 6-well plate and tested for compression. This will be referred as z-direction i.e., when different layers are in series. In addition, another apparatus accommodating a 14 mm cube was custom-built with removable walls in the x and z directions to test the anisotropic hydrogel in parallel orientation (**Figure 3.1.c**). Anisotropic hydrogels were formed inside the apparatus by layering solutions from different zones. After forming anisotropic hydrogel, the wall in the x-direction was relocated to the z-direction permitting compression testing in the x-direction using a custom built anvil, 13 mm × 13 mm.

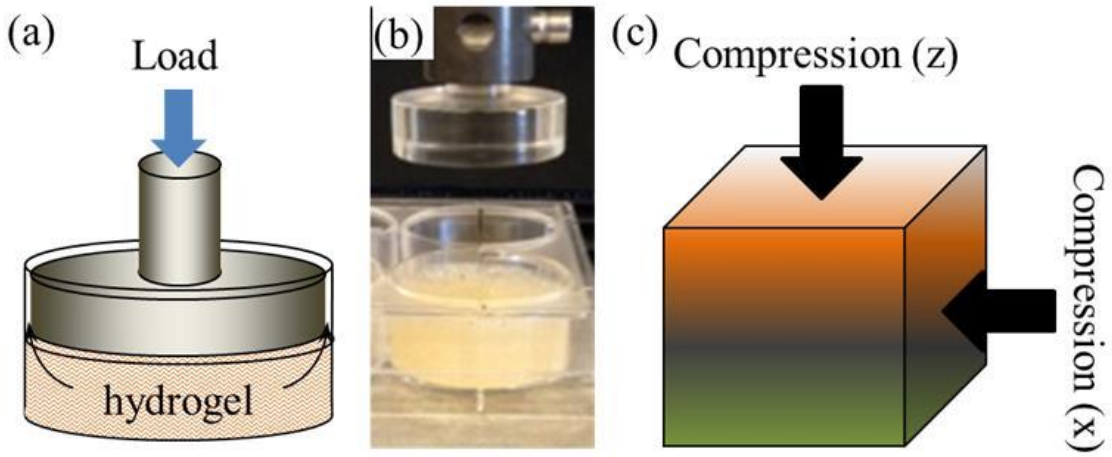

Figure 3.1. Confined compression testing of hydrogels. (a) Schematic of the setup with arrows showing mobility of fluid. (b) Photograph of the actual setup. (c) Schematic of hydrogel orientation along different axes.

Hydrogels were compressed at 1 mm/min crosshead speed. Data were exported to MS Excel and compressive modulus was calculated from the slope of the linear portion (20% to 80% strain range) of the stress-strain plot.

Based on the compression testing results, a strain range of 0 – 25% was selected for cyclical testing so that tests are performed below the yield point. Fresh hydrogels prepared in 6-well plates were subjected to five cycles of loading and unloading in the confined environment continuously at a frequency of 0.026 Hz, similar to previous reports (Kalyanam, Yapp Rd Fau - Insana, & Insana, 2009; Treppo et al., 2000). After testing, samples were examined for appearance by comparing to the fresh hydrogels.

All hydrogels were characterized for pore area, size, and number using dehydrated, cleared, paraffin-embedded, and 4 μm sectioned samples on an inverted microscope (Nikon TE2000, Melville, NY). Open pore area and shape factor of each hydrogel was assessed and calculated using digital micrographs and Sigma Scan Pro 5 (SPSS Science, Chicago, IL) software,

respectively. A minimum of 3 images/sample and more than 20 pores were analyzed for each condition. Pores with a shape factor value closer to 1 have circular geometry (Podichetty & Madihally, 2014). Geometrical features of a scaffold are best represented by permeability. Analytical formulas (Innocentini, Salvini, Macedo, & Pandolfelli, 1999; Truskey, Yuan, & Katz, 2009) or homogenization techniques (Hollister & Lin, 2007; Sanz-Herrera, Garcia-Aznar, & Doblare, 2009) are used to establish the permeability in biological scaffolds. Permeability was estimated using an analytical approach such as the Carmen – Kozeny relationship, which presents a relation between permeability and pore properties. From this method, an equation derived for cylindrical pores was used based on the shape factor value (Podichetty, Dhane, & Madihally, 2012). Thus, hydrogel permeability (κ) was calculated using **Equation 1**, where d is the pore diameter and n_A is the number of pores per unit area.

$$\kappa = \frac{\pi}{128} n_A d^4 \quad (1)$$

The structural integrity was evaluated by incubating 13 mL for 6 hours of hydrogel solution in a custom apparatus 26 mm in diameter with a removable bottom. The hydrogels were removed for evaluation. The diameters of the hydrogels were measured before and after removal from the apparatus to determine the structural integrity.

3.2.5. *In vivo* Mouse Model and Hydrogel Histology

Male BALB/c mice 8-10 weeks old (21-24 g) purchased from Charles River Laboratories (Wilmington, MA) were acclimatized for 3 to 4 days under ambient conditions (12-hour light/dark cycle and 25°C) with water and standard mouse chow ad libitum. Animal care was provided in accordance with the NIH guidelines and all procedures were performed with the approval of the Oklahoma State University Institutional Animal Care and Use Committee. Three animals per group were randomly assigned to either a control (sham) group, or a test group.

After measuring the body weight, they were anesthetized using isoflurane inhalation anesthetic administered via MDS Matrx (Versailles, OH). Then, the hair on the dorsal skin was clipped and surfaces were disinfected using surgical prep solution. The skin was separated from the underlying muscle. Sterile solutions (~0.5 mL) of chitosan-gelatin-2GP, chitosan- HA-2GP, and chitosan-HA-β-TCP-2GP were subcutaneously injected. Sham animals went through the same process, except 0.5 mL saline was injected instead of the hydrogels. After the procedure, animals were returned to individual cages. Animals were monitored regularly for appearance, activity, behavior, food and water intake, and infection at the injection site.

One and five days following injection of the hydrogels, mice were euthanized, and full thickness skin and subcutaneous tissue sections were retrieved from the site of administration along with adjoining tissues. These were processed by standard fixation and paraffin embedding to analyze histologically using H/E stain. Also, the liver and spleen were harvested for examination. In tandem, hydrogels were formed *in vitro* and used for the analyses along with *in vivo* samples.

Skin samples were fixed in a 3.7% buffered formalin solution and embedded in paraffin, and 4- m-thick sections were cut and stained with H/E. Digital photomicrographs were captured at representative locations using a CCD camera connected to an inverted microscope.

3.2.6. Statistical Analysis

Experiments were repeated three or more times. A one way analysis of variance (ANOVA) with a 99% confidence interval was used for evaluation for significant differences between two groups. Differences were considered statistically significant when $p<0.05$.

3.3. RESULTS

3.3.1. Isotropic and Anisotropic Hydrogel Formulations

Chitosan was used in the formation of different zones due to its unique characteristics such as gelation at body temperature and possibility to immobilize negatively charged molecules such as gelatin, HA, and β-TCP. Other materials were added mimicking the ECM chemical functional group distributions of cartilage.

Superficial zone hydrogel. In the superficial zone, there is an increased number of chondrocytes and collagen. To mimic this configuration, chitosan was blended with gelatin in solution and 2GP was added. Incorporation of gelatin with chitosan, without any cross linker, is shown to promote cell adhesion and spreading (Y. Huang et al., 2005). The chitosan-gelatin hydrogel had no problems during formulation, similar to many reports (Cheng et al., 2010). Gelatin did not alter the hydrogel formation and in fact, reduced the gelation temperature, similar to other reports (Cheng et al., 2010). However, others have reported the chitosan-gelatin hydrogel to be weak in mechanical strength relative to cartilage (Werkmeister et al., 2010). Thus, the polymer concentration was increased fourfold to improve the strength of the hydrogel for the superficial zone.

Radial zone hydrogel. Majority of the compressive forces are received by the radial zone, which has different composition to achieve this capability. To achieve this goal, HA was blended to chitosan as it i) assists in compressive resilience, ii) facilitates migration and condensation of hMSCs, iii) participates in joint cavity formation and iv) regulates bone remodeling by controlling osteoclast, osteoblast, and osteocyte behavior (Gentili & Cancedda, 2009). However, there were many obstacles to overcome during the chitosan-HA-gelatin tri-polymer composite hydrogel formulation. Multiple methods were attempted prior to adding 2GP and unsuccessful due to precipitation of the HA. The methods were tested at the lowest concentrations of HA at

0.1% (wt/v). Further, multiple concentrations of HA ranging from 0.1 to 1% (wt/v) were also tested to obtain the maximum dissolvable weight percent. Some of the techniques are as follows.

1. Chitosan/gelatin solution was prepared, then HA powder was added and stirred at room temperature (RT) for 12 hours. HA never dissolved into the solution at any tested weight fraction.
2. Chitosan/gelatin solution, and HA solution were prepared separately. Then HA solution was added drop wise into the chitosan/gelatin solution and stirred at RT for 12 hours. No homogeneous solution was obtained.
3. Alternatively, chitosan/HA solution and gelatin solution were prepared separately. Then gelatin solution was added drop wise into the chitosan/HA solution and stirred at RT for 12 hours. HA precipitated.
4. To understand the precipitation of HA was due to competitive electrostatic interaction of gelatin with chitosan, only chitosan solution was prepared first. Then HA powder was added and stirred at RT for 12 hours. HA never dissolved into the solution. This suggested that solubility of HA at RT may be the limiting factor.
5. To assess the role of temperature, water was steam sterilized at 121°C, chitosan/HA was added immediately and stirred at 500 RPM on a hot plate maintained at 45°C for 12 hours. HA never dissolved into the solution.
6. Finally, chitosan/HA mixture was steam sterilized at 121°C, immediately (in some cases gelatin was added) stirred at 1000 RPM on a hot plate maintained at 70°C for 3 hours. Stirring speed was reduced to 500 RPM and temperature was reduced to 50°C and solution was stirred for an additional 12 hours. Chitosan and HA dissolved into solution. There was a limitation on the amount of gelatin, up to 1.5% (wt/v), which could be dissolved in solutions containing greater than 0.2% (wt/v) HA. Increased amount of HA lead to precipitation of the solution. Without gelatin, addition of 2GP

to chitosan-HA did not show any precipitation. This methodology was selected for further use.

Calcified zone hydrogel. Mechanical stimulus and biological signals of cartilage are transmitted to underlying subchondral bone through the mineralized calcified cartilage zone. This zone begins the transition from the chondrogenic lineage into osteogenic lineage by the process of endochondral ossification. Previous studies have shown success with implants containing β-TCP and/or hydroxyapatite for use in repairing osteochondral defects (Amosi et al., 2012; Mayr et al., 2013). To facilitate and assist in this transition, a tri-polymer composite hydrogel was formulated with the composition of HA and β-TCP. Many methodologies and formulations were attempted while obtaining solutions with these mixtures. Some of these are described below.

1. Chitosan/β-TCP solution was prepared by stirring at 500 RPM on a hot plate maintained at 50°C for 12 hours. Although solution formed, addition of 2GP at RT resulted in precipitation of the solution. Addition of 2GP is shown to neutralize the charge on chitosan and could lead to premature precipitation (Supper et al., 2013).
2. We questioned whether mixing all three components (Chitosan, HA, and β-TCP) in the powder form and then steam sterilized at 121°C would work. This methodology was tested and immediately after removing the concoction, they were stirred at 500 RPM on a hot plate maintained at 50°C for 12 hours. Total solution never reached homogeneity.
3. Based on the success from the radial zone methodology, chitosan/HA solution was steam sterilized at 121°C, immediately β-TCP was added and stirred at 500 RPM on a hot plate maintained at 50°C for 12 hours. Solution formed, addition of 2GP at RT for adjusting the pH did not show any precipitation at lower concentrations of chitosan, HA and β-TCP. However, compressive tests (described below) showed poor results.

4. Chitosan/HA solution was steam sterilized at 121°C, immediately stirred at 1000 RPM on a hot plate maintained at 70°C for 3 hours. Then speed was reduced to 500 RPM and temperature was reduced to 50°C and solution was stirred for 12 hours. β-TCP powder was added and stirred for 12 hours at 500 RPM and 50°C. To the obtained solution, 2GP was added at RT very slowly while solution was constantly stirred. This methodology was selected for further use.

The optimized concentrations for the superficial, radial, and calcified zones were 2% C/1.5% G, 4% C/1% HA, and 2% C/1% HA/1% β-TCP, respectively. Optimized formulations for each layer (**Figure 3.2.**) showed the transition process before and after incubation at physiological temperatures and the ability of the hydrogels to form successfully.

Combining different zones to form anisotropic hydrogels. To mimic anisotropic cartilage matrix distribution, isotropic hydrogels were layered in the same sequence. Initially, they were layered in a syringe by suctioning sequentially (**Figure 3.2.c**). There was no difficulty in handling these solutions, except they had to be done slowly to avoid jetting of the subsequent solution into the previous layer. Other precautions were no different than handling viscous polymer solutions. Incubating the syringe at physiological condition caused gelation. Appearance of small bands of green color (mix of yellow and blue) and light blue (mix of blue and white) indicated formation of intermediate zones due to diffusion of constituents between zones in liquid phase.

As the cross-sectional area of the syringe was small (~8.5 mm in diameter), we tested layering on a larger surface areas (diameters of 15 mm and 26 mm, 15 and 50 mL tubes, respectively) to understand whether these intermediate zones form continuous phases. When the formed hydrogels were cut open (**Figure 3.2.d**), gradual changes in colors were observed unlike in the syringe. Also, there were no delamination issues suggesting minimal separation of the zones. Nevertheless, the dye could be diffusing faster than the polymers between the zones and observed

color gradation may not be a true indicator. Hence, hydrogels were formed by pre-mixing equal volumes of solutions from the two zones, and layered in between those. Further, red dye was used to better observe the calcified zone. Cross-sectional view of the formed hydrogel showed intermediate layers (**Figure 3.2.e**) represented by green (superficial to radial zones) and purple (radial to calcified zones) colors. Since the thickness of each layer in native cartilage is much smaller relative to the surface area, spreading the same volume of various zones would result in forming anisotropic hydrogels.

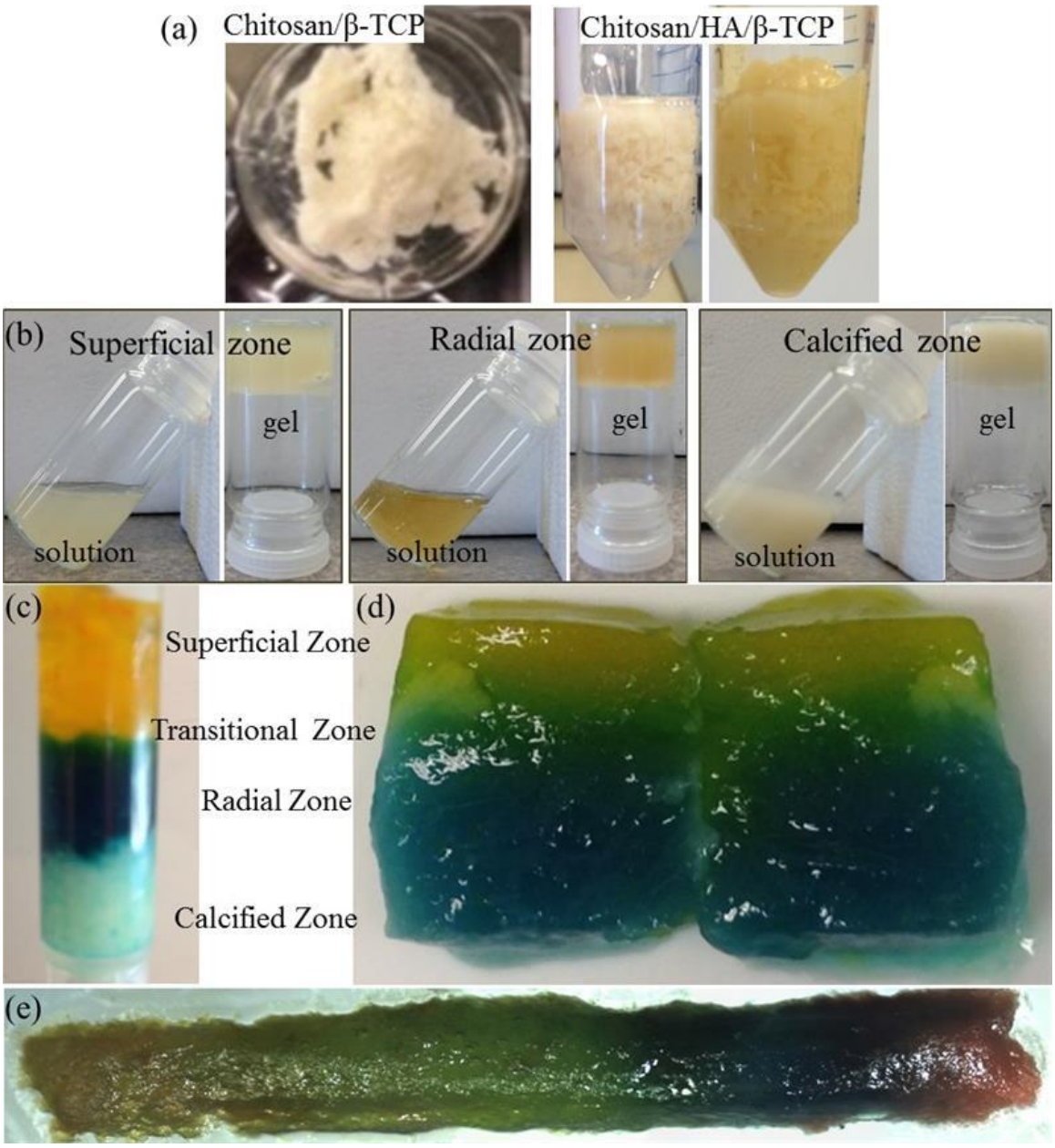

Figure 3.2. Photographs of solutions and hydrogels of different concoctions. (a) Conditions that showed precipitation in the calcified zone. (b) Optimized concentrations for each zone showing gelation at physiological condition. (c) Formation of anisotropic hydrogel with different food colors added to show the transition regions. (d) Cross-sectional view of the anisotropic hydrogel showing no delamination between different zones.

3.3.2. Thermal Gelation

Thermal gelation characteristics of the optimized hydrogels from corresponding zones were evaluated individually. Rheological analysis displayed gelation (**Figure 3.3.**) of all three zones below physiological temperatures. While optimizing the concentration of chitosan, we also observed that increasing the concentration of chitosan (data not shown) increases the rate of gelation coinciding with other reports (Cheng et al., 2010; Cheng, Yang, & Lin, 2011; Ngoenkam, Faikrua, Yasothornsrikul, & Viyoch, 2010). Slight reductions (6.9-7.1) of pH from the physiological pH (7.2-7.4) resulted in increased gelation temperatures, consistent with literature results (A. Chenite et al., 2000). The three optimized solutions showed similar behavior, but with slightly different sol/gel transition. The β-GP induced a sol-gel transformation around 25 °C, 30 °C, and 15 °C for superficial, radial, and calcified hydrogels, respectively. Below these sol/gel transition temperatures, the systems displayed viscoelastic liquid behavior, similar to pure chitosan (data not shown). The G′ and G″ were almost parallel straight lines below the gelation temperature and the value of G′ was more than 1 order of magnitude greater than that of G″ after the sol/gel transition. When the temperature was higher than the gelation point, elastic moduli G′ were higher than the viscous moduli G″ suggesting transition into the solid phase.

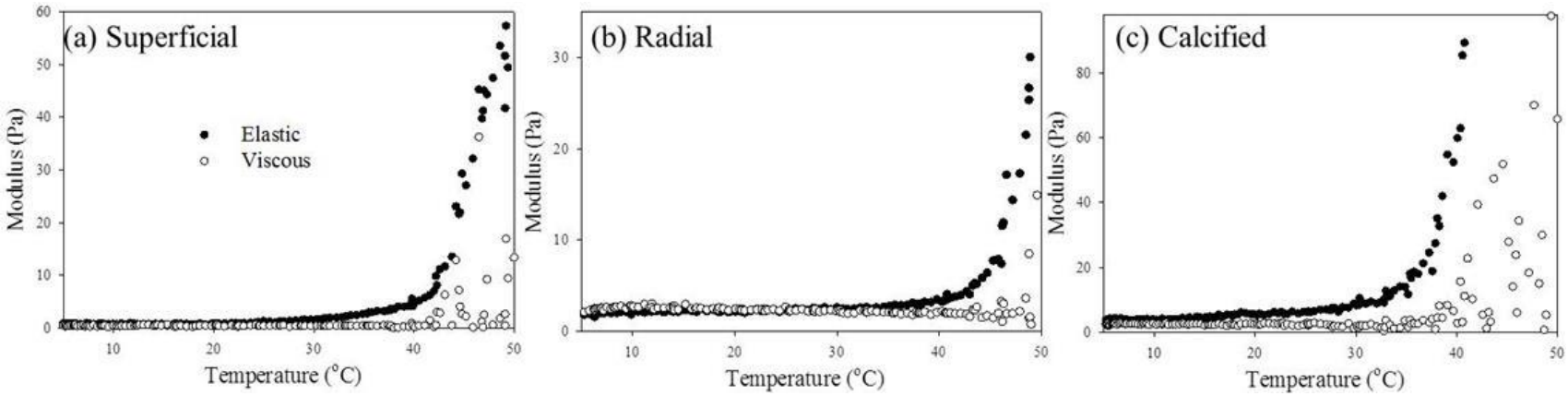

Figure 3.3. Thermal gelation of isotropic hydrogels. (a) Superficial, (b) Radial, (c) Calcified.

3.3.3. Confined Compressive Modulus

Apart from matrix composition, hydrogels with suitable mechanical properties are required for cartilage replacement. Compression testing was performed on preformed hydrogels in a confined environment to understand the mechanical characteristics of the hydrogel (Limin Wang & Stegemann, 2010). Confining the hydrogels during testing accounts for the role of fluid in the hydrogels. Using the custom-built anvil, fluid was allowed to escape around the periphery during the acquisition of stress-strain plot. Compressive modulus values calculated from the linear region of stress-strain plot (**Figure 3.4.**) showed values in the range of 10 to 12 kPa for superficial hydrogel. This is a significant improvement relative to previously reported compression strengths (Iyer et al., 2012). We also report that the gelatin component does not significantly contribute strength to the superficial hydrogel compared to the chitosan only hydrogel (**Figure 3.4.**). The compressive strength for the radial hydrogel increased seven fold in comparison to the superficial hydrogel (**Figure 3.4.**). The strength of the calcified hydrogel was similar to the superficial hydrogel. This was expected due to the chitosan composition similarities between the two hydrogels. The compressive modulus of anisotropic or combined hydrogel was the average of the three zones in the z direction. This further confirmed continuity between zones without separation or precipitation of various components. The higher water content from the superficial and calcified zones reduced the compressive strength of the radial zone consequently reducing the compressive modulus of the anisotropic hydrogel. However, when the anisotropic hydrogels were tested along the x-axis (when different zones were parallel), the hydrogels compressive modulus decreased relative to that in the z-direction, probably due to the dispersion of molecules from different zones. Compressive modulus was similar to that of chitosan alone. Significant reduction in break stress was obtained as the break strain also reduced. Distribution of components reduced the net thickness of each zone, resulting in reduced compressive modulus. This suggests that the formed hydrogels are anisotropic.

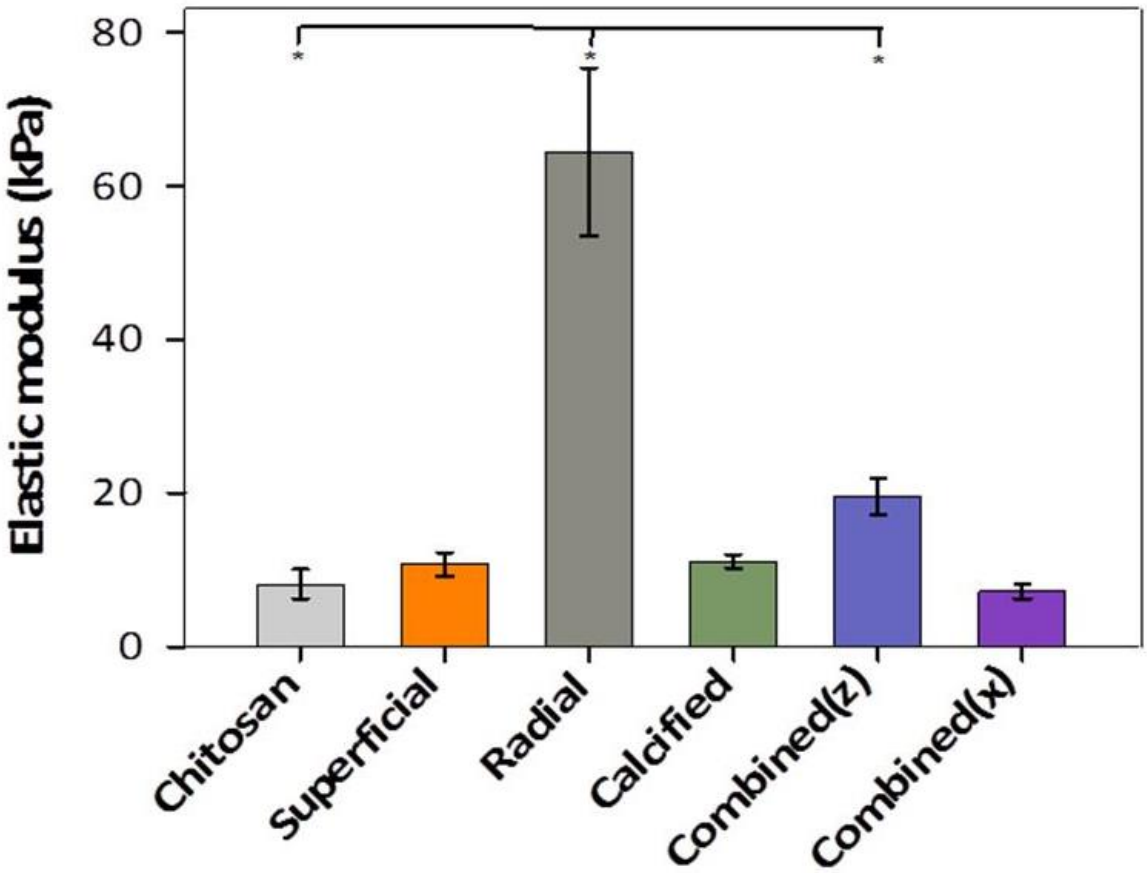

Figure 3.4. Compressive modulus calculated from the slope of the linear region of stress-strain curve obtained in confined condition. *p < 0.01 between the groups indicated.

3.3.4. Cyclical and Physical Testing

An average person takes approximately two million steps per year yielding in approximately one million load cycles per joint (Bellucci & Seedhom, 2001). These cyclic loads are delivered to the entire cartilage but are primarily distributed to the radial layer, which is the largest zone of natural cartilage (Wheeless, 2012). Therefore it is imperative to study the effects of cyclical loads on the hydrogel sections to determine durability, longevity, and deformity characteristics. In all

hydrogels, the maximum deformation was observed in the first cycle with no deformations in the subsequent cycles (**Figure 3.5.**).

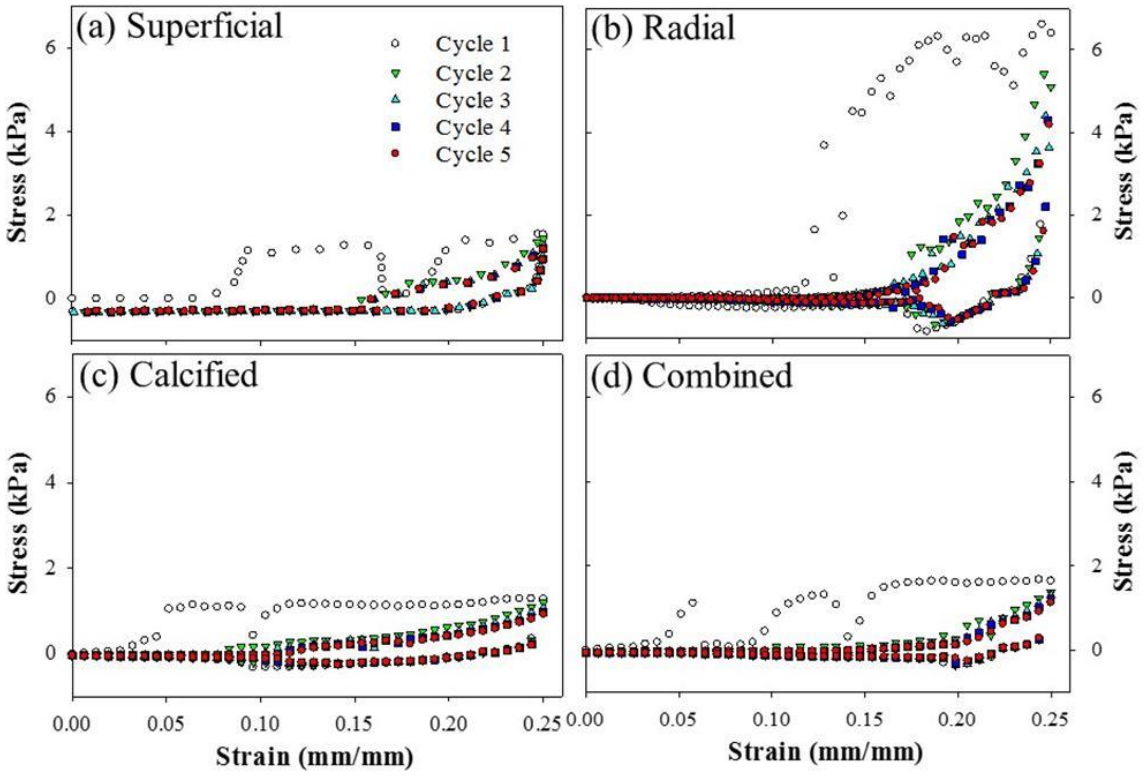

Figure 3.5. Effects of cyclic loading under confined condition on hydrogels at physiological conditions. (a) Superficial. (b) Radial. (c) Calcified. (d) Combined(z) corresponds to the anisotropic hydrogels when they are in series.

The negative stress in the relaxation period of each cycle is attributed to the creep deformation, which eventually disappears in the radial and calcified hydrogels but remains in the superficial and anisotropic hydrogels. The cyclical results of the radial and calcified zone hydrogels demonstrated repeatable strength and durability with no sign of failure in the cycle range. Stress relaxation experiments performed on chitosan-gelatin porous scaffolds showed nearly 10% accumulation of stress in each stage (Ratakonda, Sridhar, Rhinehart, & Madihally, 2012). Thus, observed creep deformation in superficial zone hydrogels containing only chitosan and gelatin are

consistent with other chitosan-gelatin scaffolds. This is also consistent with the anisotropic hydrogels due to the orientation of the experiment, which only affects for the top 25% of the hydrogel. The superficial zone may only take the blunt of the force. However, support from the radial zone could also be observed by nearly complete recovery from the creep deformation in each cycle. Since these changes were not observed in hydrogels which contained HA, complete recovery in radial and calcified zone hydrogels could be attributed to the presence of HA.

The permeability of the isotropic hydrogels was estimated based on cylindrical geometry determined by the shape factor. The permeability and shape factor displayed no statistical differences between the superficial, radial, and calcified hydrogels (**Figure 3.6**).

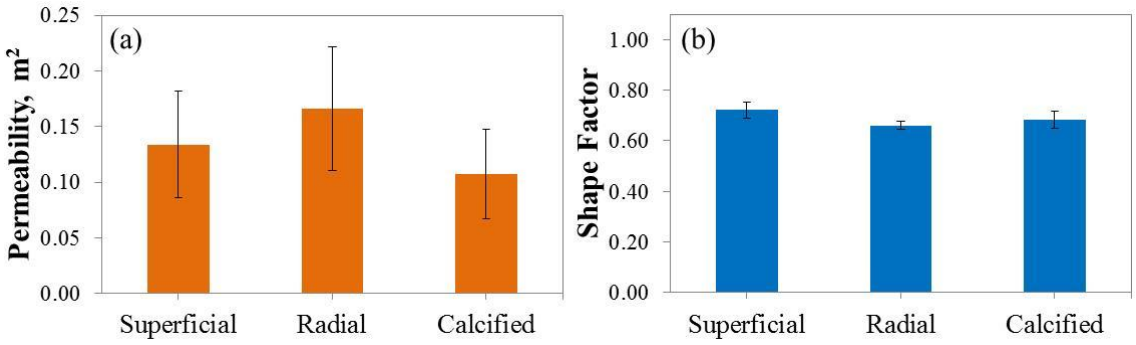

Figure 3.6. Permeability and shape factor for zonal chitosan–based hydrogels.

The structural integrity of hydrogels to keep the shape without using a container was assessed. All hydrogels kept the form of the apparatus with minimal deformation (**Figure 3.7.**). Upon removing the confinement, the superficial hydrogels showed the largest deformation at a ratio of 1:1.3 of the original length. The radial and calcified zones displayed deformation s at a ratio of 1:1.1. Structural integrity of the radial and calcified hydrogels could come from the addition of HA. Anisotropic hydrogels also showed similar changes, suggesting continuity in the phases. Further, similar behavior was observed in samples subjected to five cycles of compression. This

is consistent with native cartilage as HA provides the compressive resilience (Gentili & Cancedda, 2009).

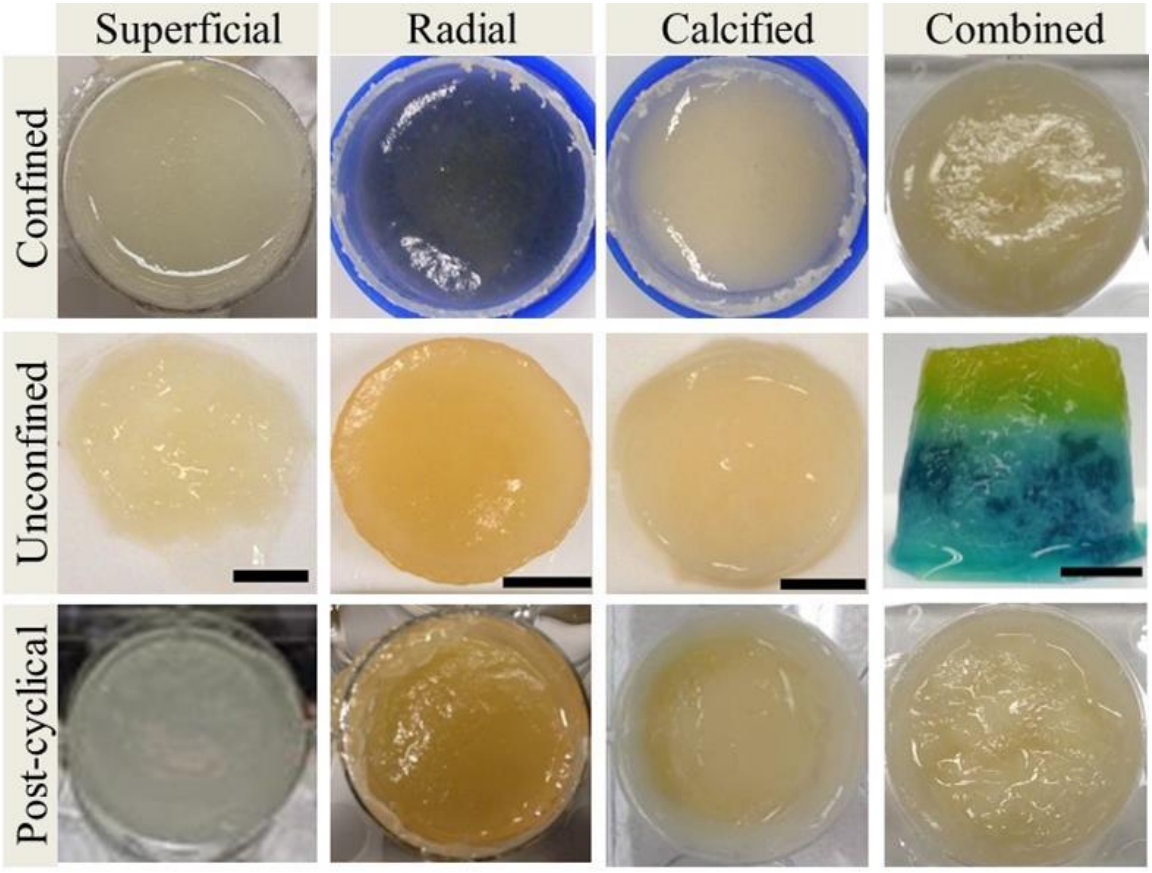

Figure 3.7. Photographs showing hydrogel characteristics in confined, unconfined and post-cyclical tests. Scale bar corresponds to 1 cm.

3.3.5. *In vivo* gelation characteristics

The isotropic solutions were injected into the subcutaneous region via 22G needle. All animals regained consciousness and no significant changes were observed in their behavior during the study period. All animals also showed normal mobility, stability and health through the duration of the study. Injected solution from all three zones rapidly gelled in the *in vivo* environment (**Figure 3.8.**). After the initial setting, no changes in shape were observed during the five day

period suggesting stability of the formed hydrogels. On the other hand, saline solution injected to sham animals disappeared in the first 24 h.

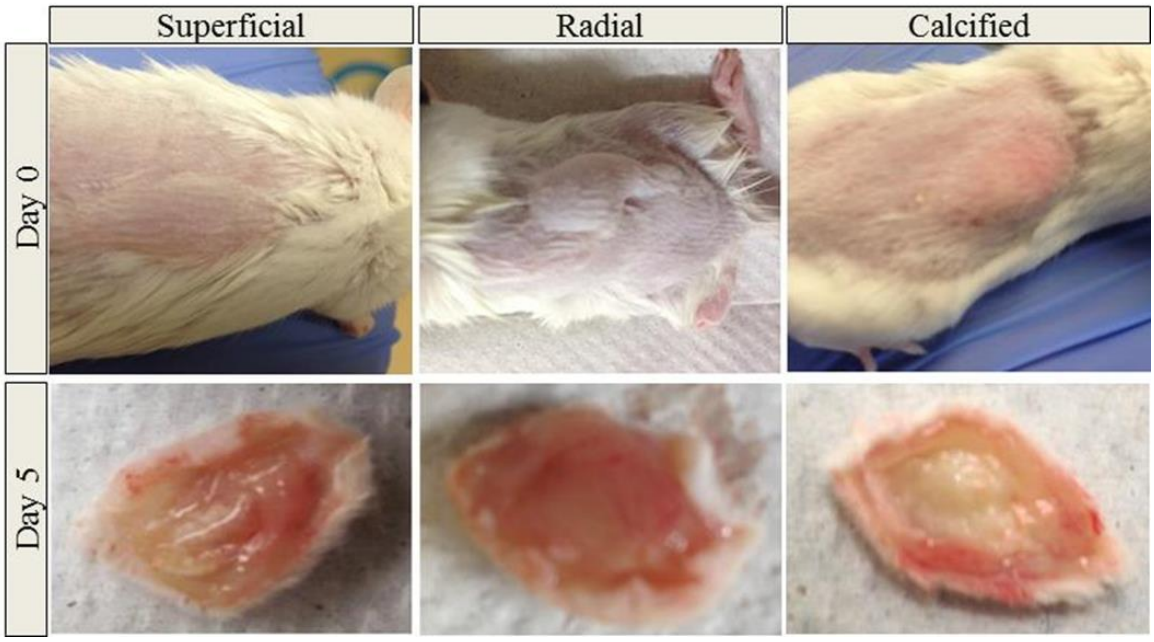

Figure 3.8. Photographs showing hydrogel in the dorsal region of the animal after injection of the solution and after retrieval from day 5.

After euthanization of animals from each group, various organs were evaluated. Overall, no gross changes in lymph nodes, spleen, heart, liver, kidney, and body weight were observed relative to sham controls. Also, hydrogels appeared intact in the injected area and color was similar to that formed *in vitro*, except in few locations where blood vessels had formed.

Histological (H/E) analysis of the injected hydrogels showed gelation and attachment of the hydrogel to the surrounding tissue. However, there was no neutrophil invasion in any of the hydrogels suggesting there were no bacterial infection. Also, no inflammatory cell invasion was found in the hydrogels in addition to no necrosis of adjoining tissues due to probable hyperosmotic conditions from the elution of 2GP before Day 1 (**Figure 3.9.**).

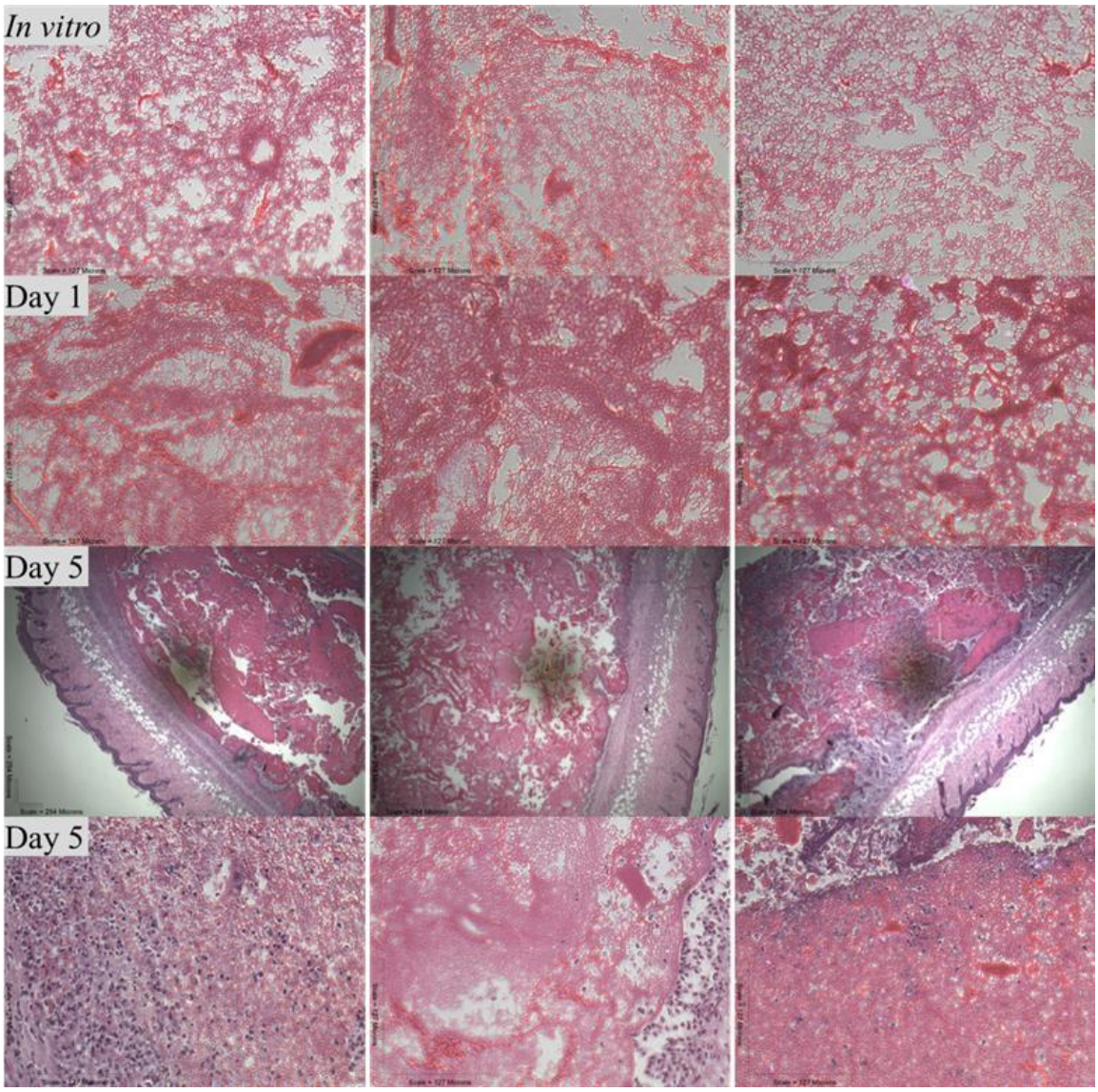

Figure 3.9. Morphology of hydrogels formed *in vitro* and *in vivo* conditions. Micrographs were obtained from H/E stained 4-µm thick sections.

Macrophage invasion was noticed at Day 5 in all hydrogels, which is expected as chitosan is known to activate macrophages (Vasconcelos et al., 2013). To confirm that the cells were not neutrophils, myeloperoxidase staining was performed using the Vector SK-4800 commercially available kit (data not shown). No cells were stained suggesting that these were macrophages. The superficial hydrogel experienced the highest density of macrophage invasion which may be

due to high porosity, presence of gelatin (denatured collagen) and weak mechanical strength. However, radial and calcified zone hydrogels showed presence of macrophages at the periphery and large portions of hydrogels remained acellular. Comparison of the micrographs with the *in vitro* gelled structures showed similar porous architecture. The hydrogels formed *in vitro* and *in vivo* appeared similar in material morphology after 5 days for all hydrogels.

3.4. DISCUSSION

Chitosan is biodegradable and biocompatible polymer utilized in various forms for tissue regeneration, drug delivery, and gene delivery. Others have evaluated the use of chitosan-gelatin-2GP systems for the regeneration of nucleus pulpus (Cheng et al., 2010; Cheng et al., 2011). Chitosan has a net positive charge for immobilizing negatively charged molecules such as glycosaminoglycans and gelatin but contains no cell-binding domain. Gelatin is used for the purposes of cell binding due to its Arg-Gly-Asp (RGD)-like sequence that promotes cell adhesion and migration (Y. Huang et al., 2005). In a previous study, a chitosan-gelatin mixture was found to support cell proliferation and viability of human foreskin fibroblast (hFF-1) cells (Iyer et al., 2012). Chondrogenic cell viability within the hydrogels, the amount of secreted collagen type II is reported on hyaluronan based hydrogel (W. S. Toh et al., 2011). Additionally, the shape of the cells encapsulated in the hydrogels closely resembled chondrocytes. Gelatin microspheres containing TGF-β3 are shown to promote mesenchymal stem cell differentiation to chondrocytes (Cheng et al., 2011; Fan et al., 2008; Gentili & Cancedda, 2009; Vasconcelos et al., 2013).

In this study, we developed chitosan-based hydrogels that mimic the native matrix architecture of cartilage. First, we optimized formulations based on three different zones in cartilage and then combined them to form an anisotropic hydrogel. We evaluated the hydrogels for multiple properties including confined compression testing, cyclical testing, stability, and *in vivo* gelation characteristics. Anisotropic hydrogels to mimic zonal organization of native cartilage tissue have

been recently explored. Photopolymerization has been the leading technique for developing the anisotropic hydrogels (Ng et al., 2009). The hydrogels are built in a layers using reactive crosslinking and allowing each layer to set up before constructing the next layer. Additionally, photopolymerization provides spatial and temporal control over the formation of the hydrogel (Kim et al., 2003; Nguyen et al., 2011; Piraino, Camci-Unal, Hancock, Rasponi, & Khademhosseini, 2012). While photopolymerization has its benefits; this technique is limited to preforming the hydrogels *in vitro* due to unavailability of photons to crosslink the hydrogels. One has to supply the photons using other sources of electromagnetic waves that can penetrate deep into the tissue uniformly, which have safety concerns. Nevertheless, this method does not facilitate a minimally invasive alternative to arthroscopic surgeries rather it coincides. Further, the authors did not discuss delamination issues of their hydrogels to any effect. Some have also utilized UV cross-linking in situ (Kloxin et al., 2009; Sharma et al., 2007). Others have formed anisotropic scaffolds using fabrication methods such as freeze drying and UV polymerization for use in cartilage repair (Nguyen et al., 2011). Although, elastic moduli are similar to native cartilage (ranges from 0.35 to 2.0 MPa (Werkmeister et al., 2010)), these methods require using highly invasive approaches with inherent safety concerns for regenerating or repairing the damaged cartilage. Building the hydrogels in layers could lead to believe the hydrogels have the ability to come apart layer by layer.

Our hydrogels, while the elastic moduli are below that of cartilage, contain considerable strength with the ability to be injected. Additional assistance such as casting or bracing would be necessary to use in a clinical setting until the tissue regenerates. Hence, this may not deter the applicability of the anisotropic hydrogel due to its similar material architecture, which could be influential for cell health, characterization, and proliferation to regenerate cartilage. The success with the isotropic formations also allows tailoring for patients that have only minor cartilage damage and may only need an isotropic layer to repair the lesion. Our technique for anisotropy

uses a continuous layering similar to the construction of widely used gels in molecular biology. The hydrogel is setup after all layers (superficial, transitional, radial, and calcified) are present to reduce the possibility of delamination. Further, anisotropy of the hydrogel has shown to be possible in syringes. The results for the cyclic compression, rheology, and structural integrity support the hydrogels' ability to be durable, injectable, and structurally sound with the applicability as an alternative for invasive cartilage surgeries. The *in vivo* analyses demonstrated results similar to *in vitro* results. The hydrogels were capable of injection via a 22G needle and were stable inside the body after five days.

In the knee, the articular cartilage is confined by the articular capsule. This capsule is a porous membrane allowing synovial fluid to flow in and out to retrieve nutrients. Due to this architecture, confined compression is a desired biomechanical property when exploring the strength of artificial alternatives. Confined compression has been performed in many different ways with unique techniques. Some methods include using a static compressive load with a step approach allowing fluid to flow through porous metal filters (Bertagnoli et al., 2005), a monotonic load until exceeding a specified force level in a piston-cylinder arrangement with hole to relieve air pressure (Sasson, Patchornik, Eliasy, Robinson, & Haj-Ali, 2012), and a constant strain rate until fracture in a rigid ring with porous metal plates (Borges, Bourban, Pioletti, & Månson, 2010). Our method is similar in the fact that we use non-strict confinement allowing minor amount of fluid escape along the circumference during compression. Many groups combine the confined compression with the non-confined compression. However, unconfined and confined compression tests are similar in evolution before reaching the inflection point (Borges et al., 2010). This area of the test is representing the hydrogel strength itself instead of the hydrostatic pressure.

We have previously shown cellular interactions with the chitosan-based hydrogels at lower concentrations (Iyer et al., 2012). Viability, differentiation, and proliferation studies were

performed with hFF-1 and human mesenchymal stem cell (hMSC) lineages. Similar trends were observed when hFF-1s and hMSCs were cultured in chondrogenic differentiation media after 28 days. Further support was provided by the cell morphology and collagen distribution studies where the cells and collagen were embedding in the chitosan-gelatin tissue. The cells would not be able to remain stable and viable in the previous hydrogels without nutrient transport from the media. The lack of statistical differences observed in the permeability of any of the hydrogels, suggests no nutrient supplementation issues. However, phenotypic and genotypic cellular analysis of the tissues studied in this paper need to be performed. Chondrocytes derived from superficial and deep zones differ significantly in morphology, rate of proliferation, and activity in secreting a proteoglycan-rich ECM. Nevertheless, utility of anisotropic hydrogels on cartilage regeneration needs be tested further with the incorporation of cell source, but is outside of the scope of this study.

3.5. CONCLUSIONS

Chitosan-based hydrogels with a similar distribution of various layers of cartilage were optimized by combining gelatin, HA and β-TCP. All formulations retained temperature sensitive gelation in both *in vitro* and *in vivo* conditions. Formed radial zone formulation had higher mechanical strength. Increasing compressive strength, durability, and rate of gelation of the hydrogels is suggested to be resultant of increasing chitosan concentration. Improved structural integrity was obtained in radial and calcified zones due to the addition of HA. Compressive modulus when different zones were in series was that of the average of different layers while that when different zones were in parallel was much less. Hydrogels were stable inside the body with minimal cell invasion in the radial and calcified hydrogels after five days. All *in vivo* hydrogel micro-architecture were comparable with the *in vitro* hydrogels.

3.6. ACKNOWLEDGEMENTS

Financial support was provided by the Oklahoma Center for Advancement of Science and Technology (HR12-023) and Edward Joullian Endowment. We would like to thank Mr. Curtis Andrew, Oklahoma Animal Disease and Diagnostic Laboratory (OADDL) for histological processing.

CHAPTER IV

CHONDROGENIC INDUCTION OF HUMAN FORESKIN FIBROBLASTS IN CARTILAGE MIMICKING ZONAL HYDROGELS

4.1. INTRODUCTION

Joint areas contain a capsule housing a tissue unlike any other in the body. The area known as the articular capsule gives residence to cartilage tissue. Cartilage is an avascular anisotropic soft tissue rich in layer specific extracellular matrix proteins and cells. Each layer represents a time sequence for the residing cartilage cells or chondrocytes. As cartilage progresses in depth, the chondrocytes mature and eventually reach the stage of apoptosis through the process of endochondral ossification (Gentili & Cancedda, 2009). At the outermost layer from bone, superficial zone, there is a combination of progenitor and chondrocyte cells, which are circular and in a random organization secreting multiple proteins with collagen type II being most dominant. The top middle layer, transition zone, the cells are spherical with random organization with a majority of collagen type II and aggrecan composing the surrounding ECM (Wilson et al., 2009). In the bottom middle layer, radial zone, the cells undergo columnar organization and begin hypertrophy while primarily secreting the proteoglycan, aggrecan. The bottom layer, calcified zone, consists of terminally hypertrophic chondrocytes which begin mineralizing and forming bone through alkaline phosphatase and collagen type X production (Gentili & Cancedda, 2009; Mow et al., 1999; Wilson et al., 2009). However, as the body ages, multiple factors could

cause damage to the cartilage tissue in turn producing tissue degrading enzymes known as matrix metalloproteinases (MMPs). Various diseases and regular physical activities could ravage cartilage; osteoarthritis (OA) is the most common joint disorder requiring significant medical aid. Injuries incurred by physical activity typically affect the younger population (Banzon, 2009), unlike OA which is more commonly seen in adults with advanced age ((NIAMS), 2013). The damaged cartilage must be replaced due to its inability to heal itself. Alternative strategies have been offered by tissue engineering or regeneration techniques. However, these methods require seeding immuno-compatible cells to colonize biodegradable scaffolds to circumvent immune rejection. The disadvantages of autologous chondrocytes are the difficulty in managing liquid and delicate chondrocyte culture solution, the need to create the hermetic periosteum suture, and the requirement of a second open surgical procedure. Other regenerative methods include using progenitor cells seeded in a natural or synthetic scaffold and implanted (Jin et al., 2009; Kloxin et al., 2009; Werkmeister et al., 2010). More recently, hydrogels have become popular for cartilage scaffolding because the gel offers an environment similar to native conditions. However, most of these methods require multiple invasive surgeries to isolate autologous progenitors and transplant regenerated cartilage.

Injectable hydrogels offer a minimally invasive alternative approach with the benefit of easy incorporation of cells and biologically active agents (J. A. Burdick & Prestwich, 2011; Kuo & Ma, 2001). In particular, thermo-sensitive chitosan-based hydrogels have received more attention due to chitosan's biocompatibility and biodegradability properties (Iyer et al., 2012; Lawrence & Madihally, 2008). Yet, there has been no study that introduces injectable zonal hydrogels to mimic the multi-layered morphology of natural cartilage with the inclusion of an autologous cell source that has potentiality to differentiate into the chondral cell line. Thus, the hypothesis was biologically inspired scaffolds mimicking the *in vivo* environment will serve as a permissive substrate for differentiation and biological function of a mature cell lineage. The hypothesis was

tested by assessing the differentiation and cellular responses of human foreskin fibroblasts (hFF-1s) suspended in injectable hydrogels mimicking cartilage zonal compositions (Walker & Madihally, 2015) for twenty eight days. Adult human mesenchymal stem cells (hMSC) known to differentiate into the chondrogenic lineage were used as a positive control. The cultures were performed in isotropic nature to evaluate the quality of tissue at each zone. Anisotropic formation of the hydrogels used was previously explored and can be used to form the complete cartilage tissue. Further, only the hydrogels representing the superficial and radial zones were assessed in this study since the chondrocytes in the calcified layer are terminally hypertrophic and at the very late stages of differentiation.

4.2. MATERIALS AND METHODS

4.2.1. Sources for Materials

hFF-1 cell line, Dulbecco's Modified Eagle's Medium (DMEM), and ATCC tested fetal bovine serum (FBS) were purchased from American Type Culture Collection (ATCC) (Manassas, VA). Adult hMSC cell line, Fibroblast Basal Medium supplemented with Fibroblast Growth Medium SingleQuot Kit and growth factors (FBM), Clonetics trypsin-EDTA for hMSC, Mesenchymal Stem Cell Basal Medium supplemented MSC Growth Medium SingleQuots (MSCBM), Chondrogenic Basal Medium supplemented with hMSC Chondrogenic SingleQuots Kit and Transforming Growth Factor-beta 3 (TGF-β3) were attained from Lonza Group Ltd. (Walkersville, MD). Ethyl alcohol (200 proof) (EtOH) was obtained from Pharmco. Formalde-Fresh (certified low odor 10% formalin) was obtained from Fisher Scientific (Pittsburgh, PA). Phosphate buffered saline (PBS), trypsin/EDTA (0.25% Trysin-0.53mM EDTA solution).

4.2.2. Hydrogel Formation

Two separate formulations, optimized using a systematic approach outlined in previous publication (Walker & Madihally, 2015), were prepared to represent the superficial and radial

zones of articular cartilage. Chitosan was dissolved using HCl (12 N) and glycerol 2-phosphate (2GP) (0.56 g/mL) was added drop wise to the superficial or radial hydrogel solution for pH adjustment (7.2 - 7.4) and induce gelation. For the superficial hydrogel, chitosan and gelatin were sterilized in a dry setting prior to the addition of water, HCL, and 2GP. Alternatively for the radial hydrogel, chitosan, hyaluronic acid (HA), and water were sterilized then HCL and 2GP were added to form a homogenous solution. The final superficial and radial hydrogel solution compositions prior to the addition of 2GP were 2%/1.5% wt% (chitosan/gelatin) and the 4%/1% wt% (chitosan/HA), respectively.

4.2.3. Cell Expansion Cultures and Population Maintenance

All cells were incubated at 37°C and 5% CO_2/95% Air atmosphere and medium was changed every 3 to 4 days. The hFF-1s and hMSCs were maintained and expanded in DMEM supplemented with 15% FBS and MSCBM, respectively. All cultures exhibited normal growth characteristics with respect to size, shape and confluency. Both cell lines were subcultured at a ratio of 1:3 plates. The culture flasks were washed with PBS and detached with 0.25% trypsin/0.53mM EDTA (hFF-1) and Clonetics trypsin-EDTA (hMSC). The trypsin/EDTA was neutralized using the respective media. The cells were centrifuged at 270×g (hFF-1) and 600×g (hMSC), then resuspended in the respective media and distributed.

Seven days prior to hFF-1 hydrogel cultures (cell encapsulated gelled hydrogel), DMEM with 15% FBS was replaced with FBM to remove serum proteins. Removal the FBS is pertinent due to the absence of FBS in humans and the necessity of having humanly innate cells at the time of experimentation. Further, this process is important to avoid constructing unrealistic experimental conditions and leaching of FBS into supernatant samples. At the time of experimentation, hFF-1 cells were detached using TrypLE™ Express enzyme (Life Technologies, Grand Island, NY). Cell preparation for experiments is explained in detail in the following sections.

4.2.4. Hydrogel Suspension Cultures

Cells were tested in three culture conditions in suspension cultures for the superficial and radial hydrogels and are represented in a concise manner in **Figure 4.1**.

1. hFF-1s in FBM, *hFF-1 control,*
2. hFF-1s in complete chondrogenic induction medium (CCM), *hFF-1 Induced*, and
3. hMSCs in CCM, *hMSC Induced*.

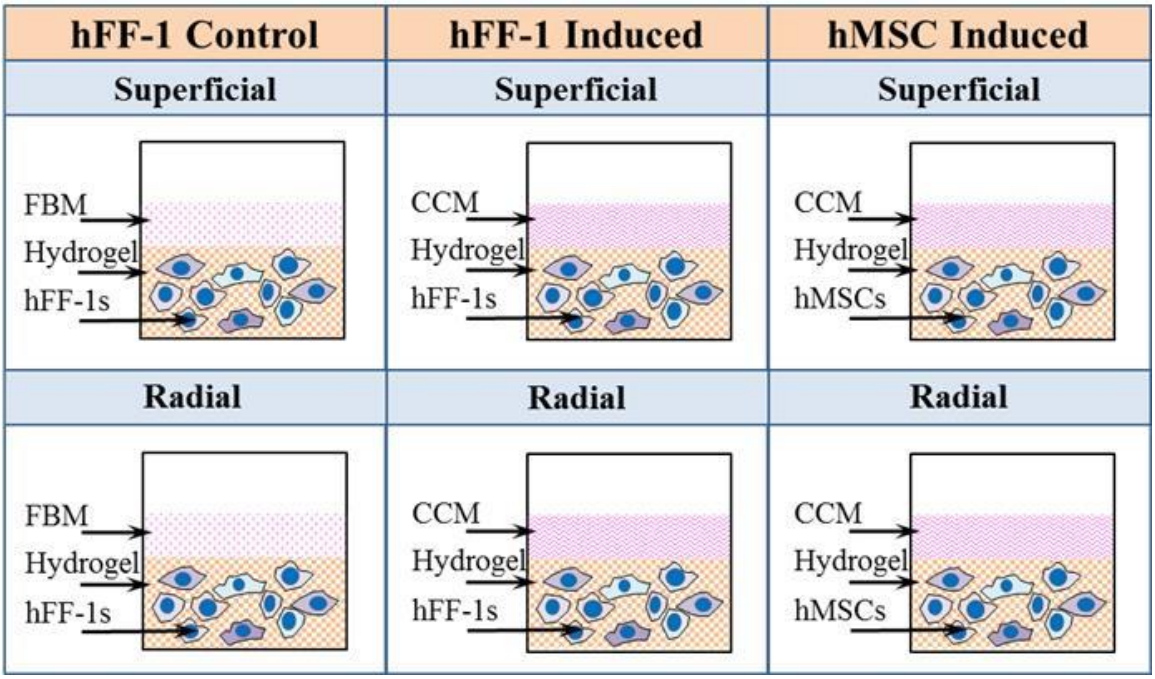

Figure 4.1. Schematics of the different culture conditions and the reference name used in the study.

Incomplete chondrogenic induction medium (ICM) was prepared by supplementing the Chondrogenic Basal Medium with hMSC Chondrogenic SingleQuots Kit. Lyophilized TGF-β3 was reconstituted in 4mM HCl supplemented with 1 mg/mL bovine serum albumin (BSA) to a concentration of 20μg/mL. The CCM was prepared by adding TGF-β3 to ICM to a concentration of 10ng/mL before each use. At the time of experimentation, cells were obtained from methods

previously described. The hFF-1s and hMSCs were counted, aliquoted to the different conditions, and washed twice with FBM (hFF-1 control) or ICM (induced conditions). hFF-1 control and induced conditions were centrifuged between washes at 270×g and 150×g, respectively.

Superficial or radial hydrogel solution was dispensed into wells of a 6-well plate. Then 500,000cells/mL were dispensed and mixed in crisscross patterns for uniform distribution. The cell containing-mixture was allowed to reach gelation by incubating at 37°C for 2 hours prior to adding the respective media. All hydrogel cultures were incubated at 37°C and 5% CO2 in air and media was changed twice a week. Culture supernatants were collected and preserved at -80°C for analyses of total protein and aggrecan content, and MMP activity. After 28 days, the hydrogel cultures were analyzed via histology and IHC. Biological triplicates of all conditions were performed to ensure repeatability of the experiments.

4.2.5. Assays

Preserved supernatants from the hydrogel cultures were tested for the production of aggregan and MMPs. Supernatants were centrifuged at 1800×g for 20 minutes prior to use in assays. The total amount of protein present in the spent medium was assessed using BCA Protein Assay Kit (Pierce Chemical Co, Rockford, IL) following vendor's protocol. Concentration of total protein in the medium exposed structures without cells was subtracted as blank. Measured activity was normalized using the total protein content. Absorbance and fluorescence were measured using a Molecular Devices EMax Precision and SpectraMax Gemini XS Precision Microplate Readers (Molecular Devices, LLC, Sunnyvale, CA), respectively.

Aggrecan ELISA. Cell culture supernatants from the hydrogel cultures were tested for aggregan content using human ELISA kit from Life Technologies (Grand Island, NY) following vendor's protocol. In brief, the microplate was loaded with standard, control, or supernatant sample

followed by incubation buffer into each well. The plate was gently tapped to ensure mixing and incubated at room temperature (RT) for 2 hours. The plate was then aspirated and washed three times. Conjugate solution was added to each well. The plate was tapped, covered, and incubated for 1 hour at RT. The wells were once more washed, and Chromogenic Solution was then pipetted into each well. The plate was covered, incubated, and protected from light for 15 minutes. The reaction was stopped and the plate was read for absorbance at 450 nm.

MMP Activity Assay. MMP activity in supernatants and fresh media was analyzed fluorogenic substrates MMP-1 (DNP-Pro-Cha-Abu-Cys(Me)-His-Ala-Lys(N-Me-Abz)), MMP-2/MMP-9 (DNP-Pro-Leu-Gly-Met-Trp-Ser-Arg-OH), and MMP-13 (MCA-Pro-Cha-Gly-Nva-His-Ala-Dpa-NH_2), as described previously (Iyer et al., 2012). All substrates were purchased from EMD Millipore, Billerica, MA. In brief, activity was measured by mixing 1:1 volume ratio of cell culture supernatant with respective 100µM fluorogenic peptide solution and incubated at 37°C for 20 minutes. The MMP-1 fluorescence was measured at 460nm emission and 355nm excitation, whereas, MMP-2/MMP-9 and MMP-13 fluorescence was measured at 405nm emission and 320nm excitation.

4.2.6. Histology and Immunohistochemistry

The hydrogel cultures were harvested after 28 days and fixed with 3.7% paraformaldehyde. The samples were dehydrated, cleared, paraffin-embedded, and sectioned at 4 µm. Sections were stained with haematoxylin and eosin (H/E) to evaluate morphology and alcian blue stain (pH 1.0) to assess the GAG content in the matrix. Immunohistochemistry (IHC) specimens were unmasked with 0.1% pepsin in 0.01N HCl for 15 min and blocked with 1% BSA in PBS for 60 min. Sections for aggrecan and collagen IHC were treated with 5 µg/ml primary antibody (mouse IgG1-aggrecan (4F4), goat IgG-collagen type I (D-13), or rabbit IgG-collagen type II (H-300))/1% BSA in PBS for 30 min. Horseradish peroxidase (HRP) secondary antibodies, goat

anti-mouse IgG1 (aggrecan), swine anti-goat IgG (type I), or goat anti-rabbit IgG (type II), were applied for 30 min, followed by a peroxidase substrate for 15 min to allow sufficient color to develop. All primary antibodies were purchased from Santa Cruz Biotechnology, Inc., Dallas, TX. Aggrecan and collagen secondary antibodies were purchased from Bio-Rad Labs, Inc., Raleigh, NC and Fisher Scientific, Pittsburgh, PA, respectively. All substrates were purchased from Vector Laboratories, Burlingame, CA.

4.2.7. Assessment of Quantitative Polymerase Chain Reactions (qPCR)

hMSCs (MSCBM) and hFF-1s (FBM) from the expansion cultures were used as controls against the hydrogel cultures. The control pellets and small hydrogel cultures were harvested at Day 0 and Day 28 of culture, respectively. Total RNA from the controls was isolated using the RNeasy kit (Qiagen), following vendors's protocol. Different techniques were attempted to isolate RNA from cells embedded in the hydrogels. Each method included a tissue pretreatment and isolation strategy. The RNA concentration and nucleic acid quantitation (260/280) was assessed using NanoDrop ND-1000 (NanoDrop Technologies, Inc., Wilmington, DE).

4.2.8. Statistical Analysis

Statistical analysis was done by repeating experiments three or more times and collecting samples in triplicate. A one way analysis of variance (ANOVA) with a 99% confidence interval was used for evaluation for significant differences between two groups. Differences were considered statistically significant when $p<0.05$.

4.3. RESULTS

4.3.1. Matrix Accumulation

Cellular morphologies and the distribution of aggrecan, collagen types I and II, and GAGs were evaluated to understand the quality of the tissue as well as differentiation of the induction

cultures. Similar material morphology, matrix accumulation, and cell distribution were observed in the superficial and radial hydrogels after H/E staining in all conditions (**Figure 4.2.**). The cellular morphology was similar in all conditions except the radial hydrogel hFF-1 control, where the cells display spreading consistent with fibroblastic responses to stiffer substrates (**Figure 4.2.**). In contrast, the round morphology and increased nuclear size relative to the cytoplasm of the induction cultures suggest differentiation into the chondrogenic lineage (**Figure 4.2.**). Also, hFF-1 cultures showed small cell size relative to hMSCs, which could be attributed to the initial cell sizes.

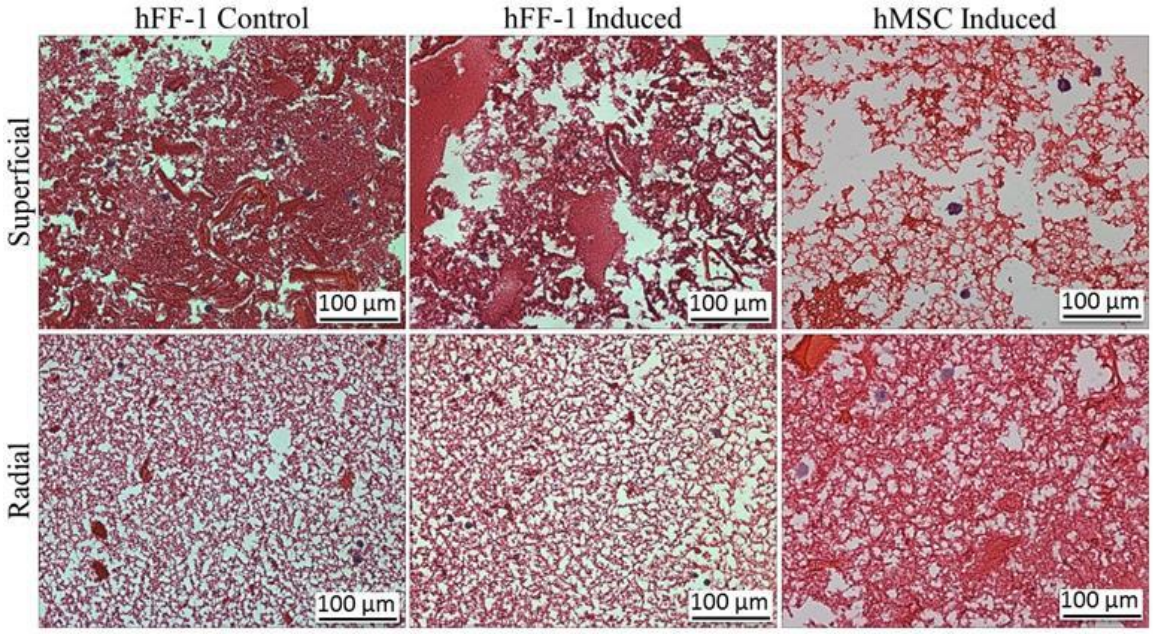

Figure 4.2. Representative H/E stained micrographs of various conditions from 28-day cultures.

4.3.2. Cartilage Specific Extracellular Matrix Analysis

More than 80% of cartilage (dry weight basis) matrix is composed of two major elements, aggrecan and collagen type II (Gentili & Cancedda, 2009). Aggrecan is a cartilage specific PG and the largest and most abundant of all PGs found in cartilage. Since a hallmark of chondrocyte

differentiation is the production of aggrecan, it is used as a marker in determining differentiation of cells into the chondrogenic lineage. Thus, aggrecan content was measured in the supernatants of the superficial and radial zone hydrogel cultures. All cultures exhibited a similar content throughout the culture duration except the induced hFF-1 superficial hydrogel culture (**Figure 4.3.**). The induced hFF-1 superficial hydrogel cultures showed an increasing trend until day 28 where the aggrecan content decreased. The hFF-1 control displayed elevated levels in the day 0 medium and in the hydrogel culture supernatants compared to the day 0 induction medium and day 28 culture supernatants (**Figure 4.3.a**). Further, the hFF-1 control of the radial hydrogel contained the highest aggrecan content, nearly fifteen fold higher than the induction cultures. The induction cultures showed no significant differences after day 7 for both hydrogels (**Figures 4.3.b and 4.3.c**).

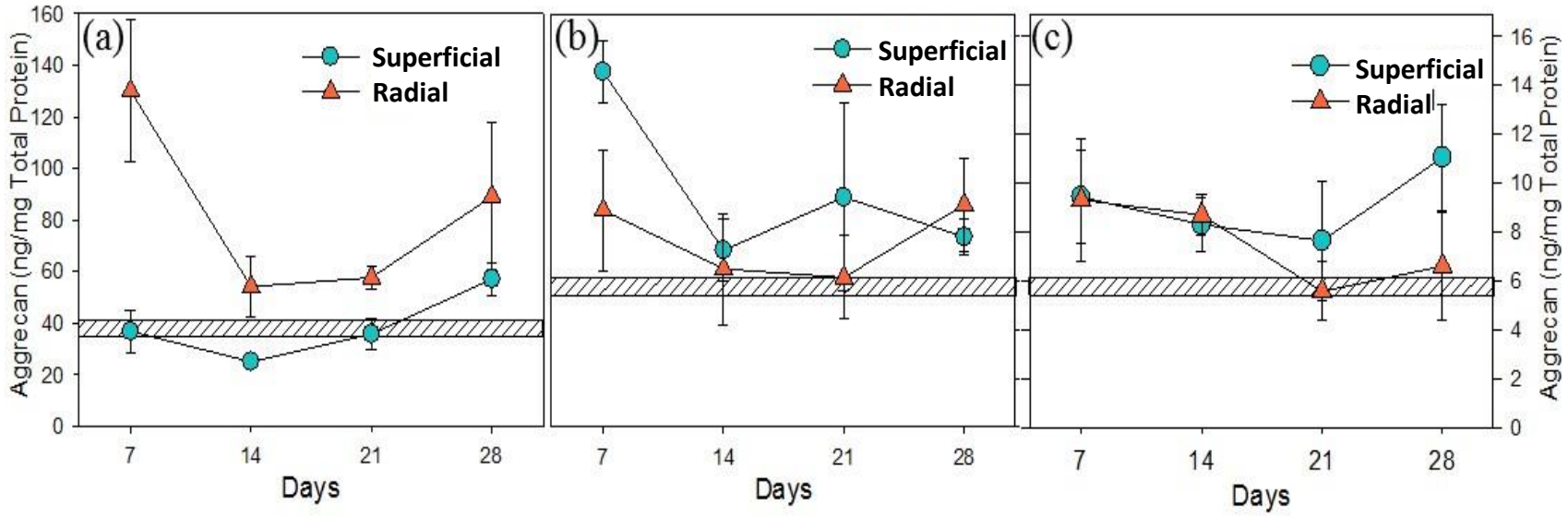

Figure 4.3. Aggrecan content in media supernatants. (a) hFF-1 control. (b) hFF-1 induced. (c) hMSC induced. Rectangular box corresponds to that present in fresh medium.

Since higher aggrecan content were present in controls rather than hFF-1 cells, we questioned the aggrecan content in the matrix. Small accumulations of aggrecan content were noticed in the induction cultures as represented by the bluish staining. However, the content in the hFF-1 control cultures was minimal or absent (**Figure 4.4.**).

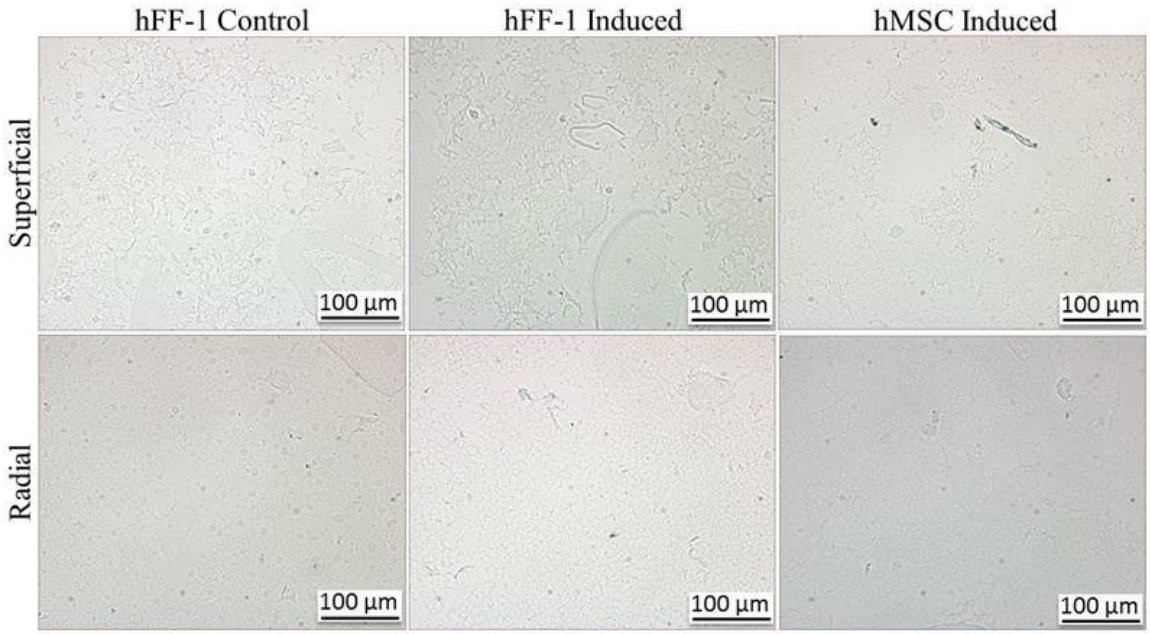

Figure 4.4. Representative micrographs from the immunohistochemical stains for aggrecan after 28-day culture.

In order to better understand, tissue sections were also stained with alcian blue stain (pH 1.0) to evaluate the distribution of GAGs in the tissue. GAGs are hydrophilic branches connected to a PG central core protein such as aggrecan and are a strong indicator of cartilage matrix (Gentili & Cancedda, 2009). The alcian blue stain on the superficial and radial hydrogel cultures demonstrated similar GAG distribution in the induction cultures and absence of GAGs for the hFF-1 control cultures (**Figure 4.5.**). This suggested that the hFF-1 control cultures are not induced for assembly of aggrecan in the matrix.

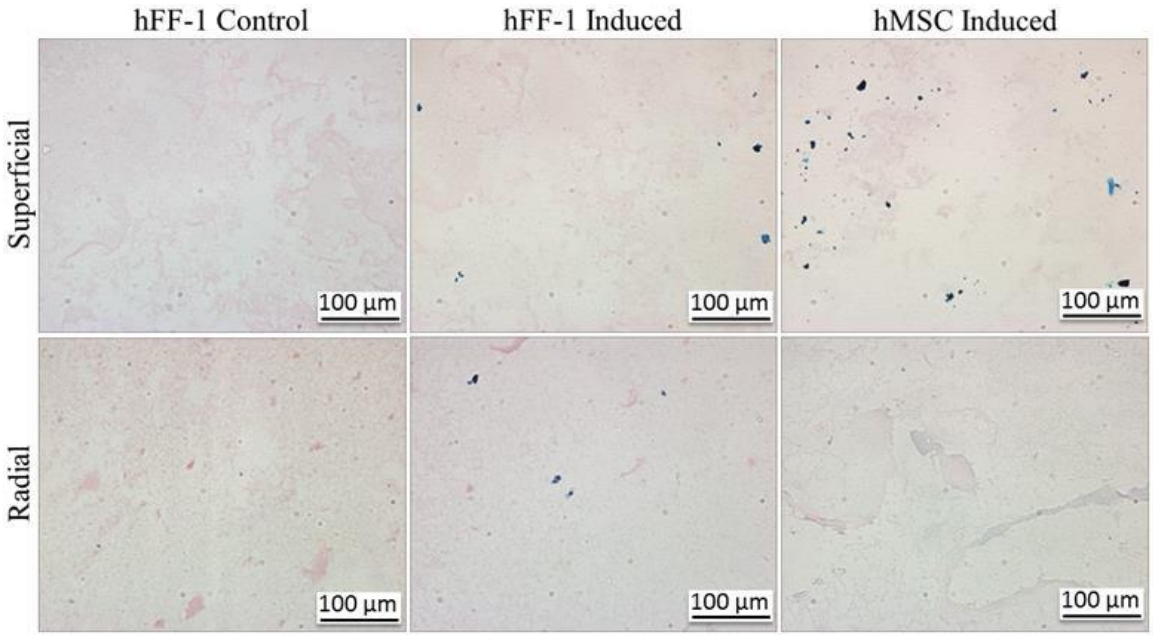

Figure 4.5. Representative alcian blue (pH 1.0) stained micrographs of various conditions after 28-day culture.

Large accumulations of collagen type II were noticed in the induction cultures but were minimal or absent in the hFF-1 control cultures (**Figure 4.6.**). This is consistent with the aggrecan and GAG content noticed in the induction cultures. Additionally, collagen type I is identified with fibroblastic cultures (Barry et al., 2001; Kaveh, 2011), and used as a marker of fibroblasts. In order to better understand the state of fibroblasts in the induction cultures compared to hFF-1 controls, we assessed collagen type I. These results showed negligible collagen type I in the induction cultures (**Figure 4.7.**), unlike hFF-1 control cultures. In particular, the radial hydrogel induction cultures had no observable collagen type I content. This suggested that fibroblasts had changed their phenotypic characteristics towards chondrocytes, similar to hMSCs in the induction cultures.

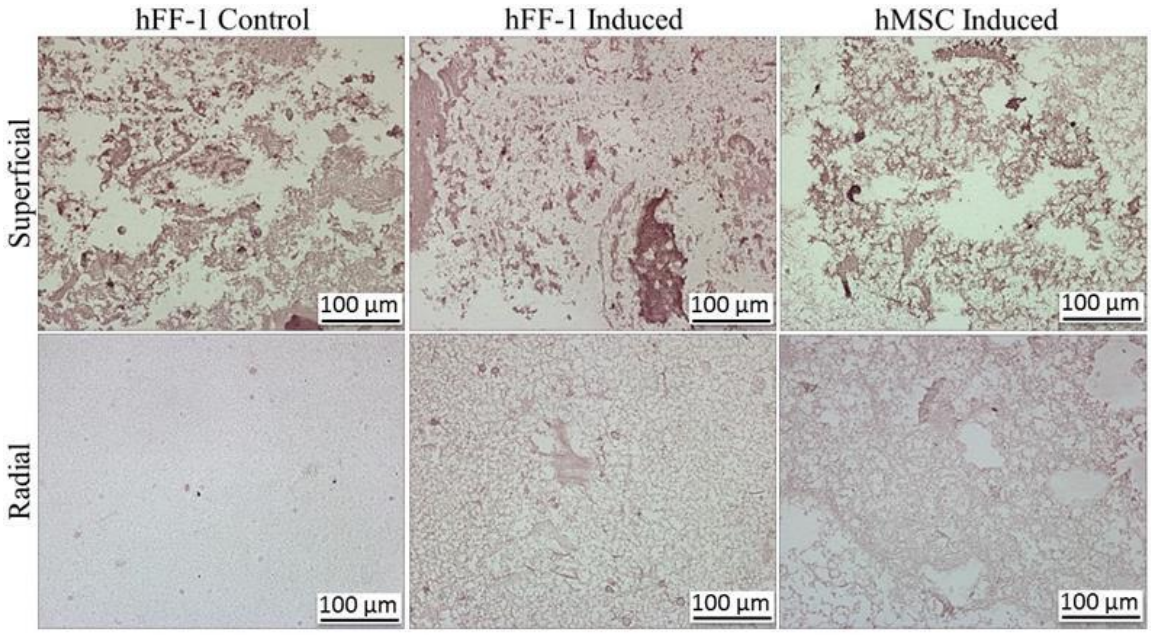

Figure 4.6. Representative micrographs from the immunohistochemical stains for collagen type II after 28-day culture.

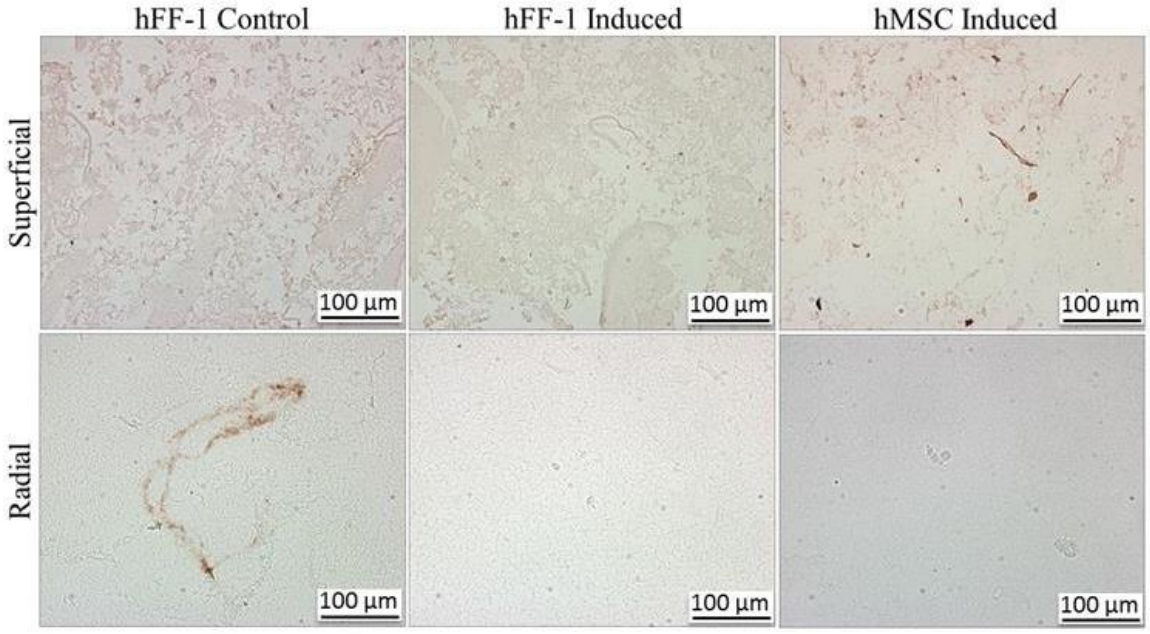

Figure 4.7. Representative micrographs from the immunohistochemical stains for collagen type I after 28-day culture.

4.3.3. MMP Activity

To better understand the cellular responses from the hydrogel cultures and the stage of differentiation of the induction cultures, activity of MMP-1, MMP-2/MMP-9, and MMP-13 were measured in the media supernatants. The MMP-1 content of the superficial and radial hydrogels housing the hFF-1 control condition displayed significant differences up to day 21 (**Figure 4.8.a**). The hFF-1 control superficial hydrogel cultures displayed no MMP-1 content throughout the duration, whereas the MMP-1 activity of the radial hydrogel cultures was significantly upregulated until day 21. The MMP-1 content for the induction cultures followed similar trends on both hydrogel and cellular bases (**Figures 4.8.b and 4.8.c**). However, the MMP-1 content for both (hFF-1 and hMSC) radial hydrogel induction cultures showed significant increases from the medium line up to day 21. The superficial hydrogel induction cultures contained no significant MMP-1 content for the hFF-1 and hMSC induction conditions after day 7 and 14, respectively. The MMP-1 content for the radial hydrogel induction cultures was significantly upregulated compared to the superficial induction cultures for the hFF-1 condition up to day 21, whereas the hMSC condition was only significantly different at day 7.

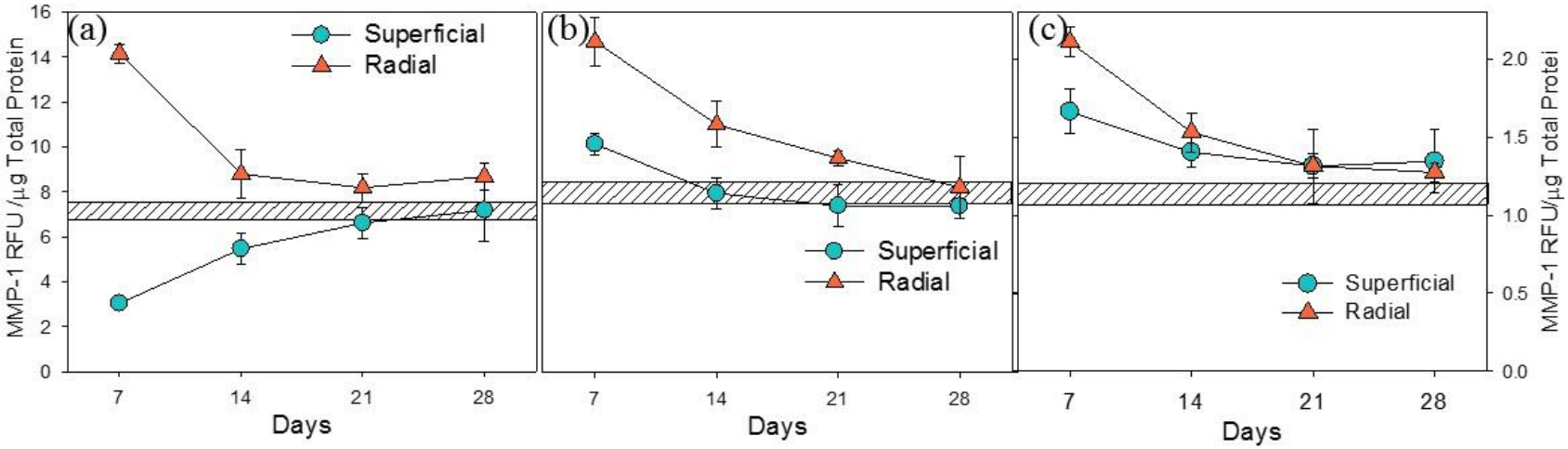

Figure 4.8. MMP-1 secretion into the medium. (a) hFF-1 control. (b) hFF-1 induced. (c) hMSC induced. Rectangular box corresponds to that present in fresh medium.

There was a significant difference in the MMP-2/MMP-9 content in the hFF-1 control and the induction cultures (**Figures 4.9.**). Additionally, only the hFF-1 control cultures displayed significantly increased quantities of MMP-2/MMP-9 activity above the medium line as seen on day 21. At all other time points, no significant activity was observed with the exception of the radial hydrogel culture at day 7 (**Figure 4.9.a**). The induction cultures followed similar trends on a hydrogel and cellular basis. Also, there were no significant differences observed between the induction cultures on hydrogel and cellular bases (**Figures 4.9.b and 4.9.c**). Further, no significant MMP-2/MMP-9 activity produced by the induction cultures as no time points have activity significantly above the medium line.

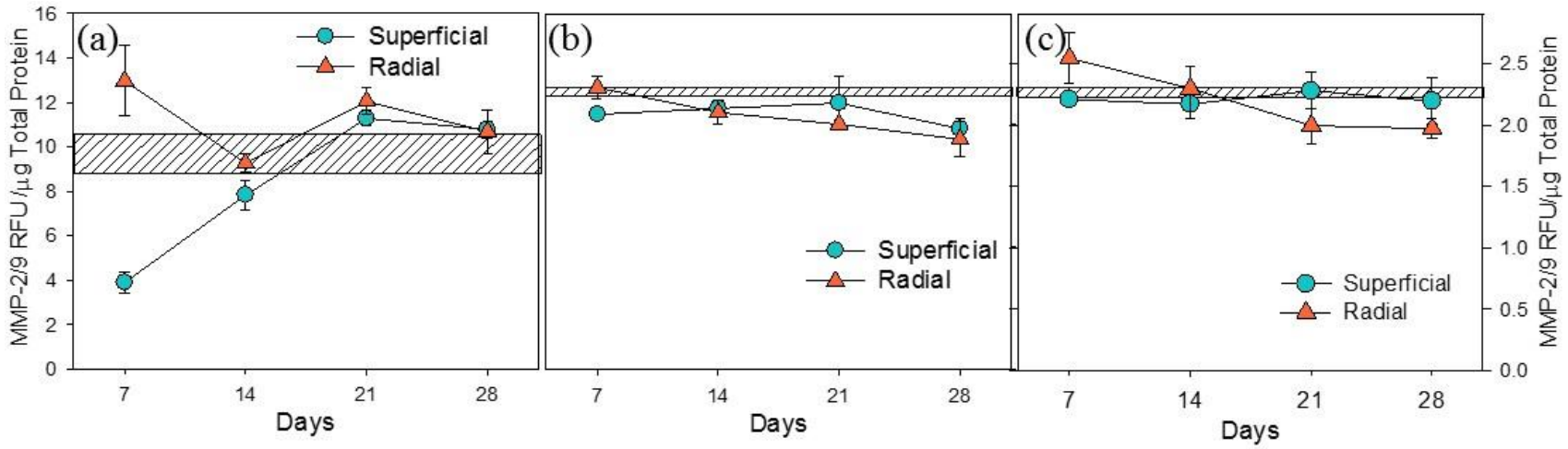

Figure 4.9. MMP-2/MMP-9 secretion into the medium. (a) hFF-1 control. (b) hFF-1 induced. (c) hMSC induced. Rectangular box corresponds to that present in fresh medium.

Alternatively, the MMP-13 content of the hFF-1 control observed significant differences between the superficial and radial hydrogels (**Figure 4.10.a**). The superficial hydrogel cultures displayed no MMP-13 content throughout the duration, whereas the radial hydrogel cultures secreted a copious quantity at each time point. Additionally, there is almost a tenfold content difference between the hFF-1 control and induction cultures. Similarly to the MMP-2/MMP-9 content, the MMP-13 content for the induction cultures followed similar trends on both hydrogel and cellular bases (**Figures 4.10.b and 4.10.c**). However, the MMP-13 content for the radial hydrogel induction cultures displayed significant increases from the medium line at day 7 only, which was not seen in the MMP-2/MMP-9 content. The superficial hydrogel contained no significant MMP-13 content for either induction condition.

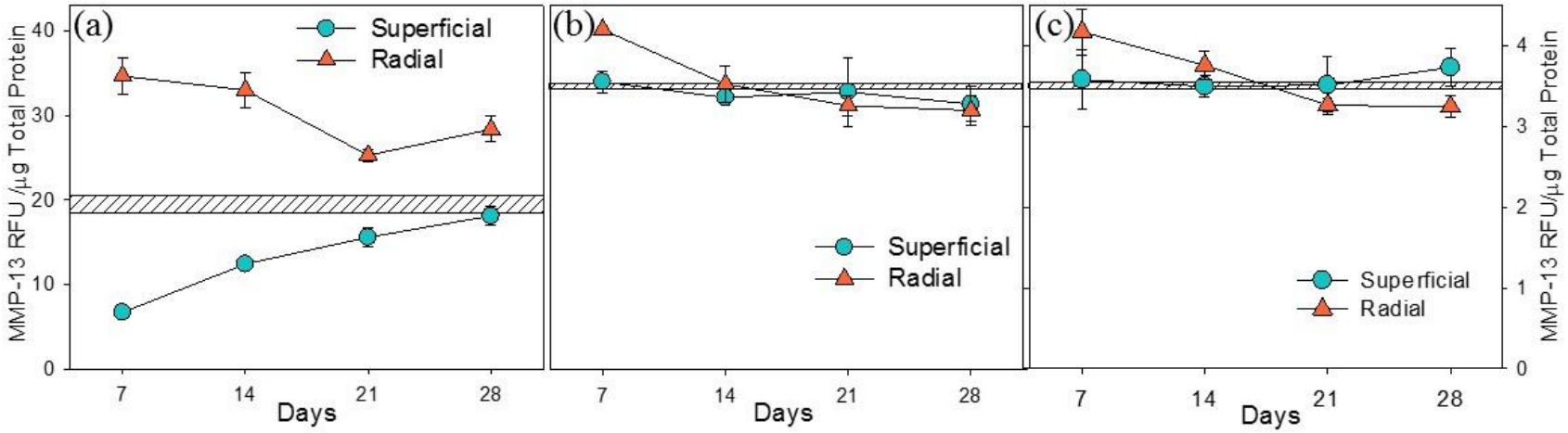

Figure 4.10. MMP-13 secretion into the medium. (a) hFF-1 control. (b) hFF-1 induced. (c) hMSC induced. Rectangular box corresponds to that present in fresh medium.

4.3.4. Genetic Analysis

In order to understand whether the observed changes are at that genetic level, we opted to use qPCR. Initial approaches of harvesting RNA using TRIzol (Life Technologies) yielded no measurable amount most likely due to the low cell density and possibility of DNA and protein contamination during the phase separation. Hence, multiple methods were attempted to isolate RNA from the cultures. First, the RNeasy kit (Qiagen) was used as the process employed spin columns to reduce the loss of genetic material. This method did not yield any RNA, probably due to the blockage of the columns from the hydrogel. Multiple tissue processing methods were used as either alone or in combination including homogenizing and cryo-pulverization with a mortar and pestle. Both TRIzol and the RNeasy kit were used again after the tissue pretreatment, yet no detectable RNA was present. We questioned whether this is attributed to the chemical characteristics of chitosan in different environments. Chitosan protonates in acidic environment (Ma, Lavertu, Winnik, & Buschmann, 2009; Supper et al., 2013), which could bind negative charged nucleic acids, resulting in the absence of RNA from the samples. Hence, caustic lysis buffers at pH 7.5 and 11 were tested in combination with the tissue pretreatment. Since the RNA was irretrievable from the hydrogels, alternative approach was to retrieve intact cells from the hydrogel followed by lysis to isolate RNA. Two enzymatic methods were utilized to isolate the cells from the hydrogel, which were trypsin to unbind the cell and chitosanase to digest chitosan. However, material loss and prolonged incubation time with the trypsin and chitosanase methods yielded no RNA. This suggested that increasing cell density is necessary, as the used cell densities were two orders of magnitude lower than that of reports in RNA isolation methods (Carrion, Janson, Kong, & Putnam, 2014; H. Huang et al., 2014; Yu, Young, Russo, Amsden, & Flynn, 2013). Used cell density was based on hMSC pellet cultures rather than RNA isolation technique.

4.3.5. Increased Cell Density Analysis

In order to understand the effect of increased cell density, hFF-1 induction cultures were performed with fourfold increase in cell density. Increased ECM accumulations were seen in both hydrogel with the radial hydrogel containing the largest increases (**Figure 4.11.**). Also, increased protein content was observed in both hydrogels for all proteins when compared to the lower cell density counterparts (**Figure 4.11.**). Collagen type I content was present due to the early stages of the induction process as fibroblasts secrete collagen type I. The increased cell number may have influences of collagen type I production from responses of neighboring cells. Further, experiments evaluating the effect of cell density in hFF-1 cultures are necessary to better understand the role of cell to matrix ratio on the differentiation into chondrocytes.

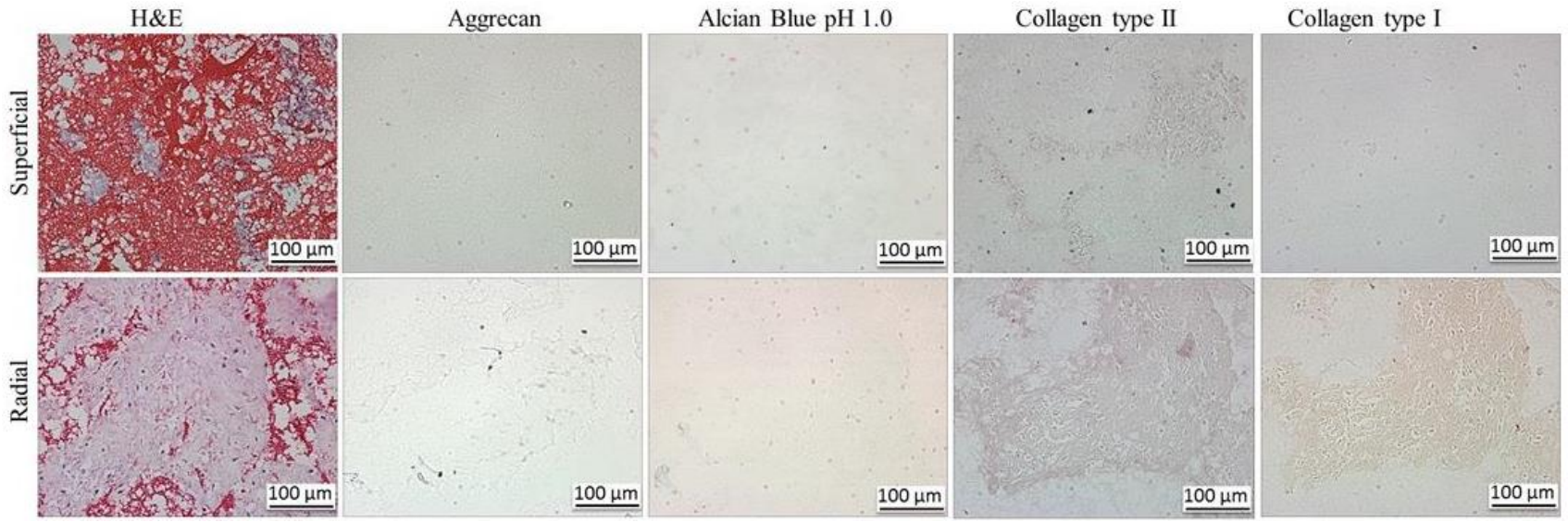

Figure 4.11. Increased cell density of hFF-1 induced 28-day cultures were processed for morphology via histology and immunohistochemistry, similar to previous descriptions. Representative micrographs are shown for each stain.

4.4. DISCUSSION

In this study, we explored the cellular responses to biologically inspired zonal hydrogels in regards to promoting differentiation of a mature fibroblastic cell line. Multiple techniques were used to assess the cellular responses and the resulting tissue quality after 28 days. Aggrecan and MMP content was used to evaluate phenotypic alterations during the culture period. Increased aggrecan content was observed in the radial hydrogel for the hFF-1 control group. Since the hFF-1 control group is not undergoing induction i.e., should not secrete aggrecan, this could be due to the leaching of HA from the radial hydrogels. The cause of the HA leaching could be due to matrix degradation from the fibroblasts not undergoing induction thus destabilizing the immobilized HA. This is also supported by the lack of aggrecan content in superficial hydrogels, which contains no HA (Y. Huang et al., 2005; Iyer et al., 2012). Alternatively, the radial hydrogel induction cultures do not reveal any leaching suggesting tissue maturation.

Increased activity of MMPs in cartilage and the synovial tissues has been found in patients suffering from OA and rheumatoid arthritis (Nagase & Kashiwagi, 2003). Chitosan-based scaffolds have been used to treat these diseases and known to influence the release of collagenase and gelatinase MMPs during tissue remodeling (Okamura, Nomura, Minami, & Okamoto, 2005). Collagen and aggrecan degradation in cartilage is mediated by MMP-1, MMP-3, MMP-13, and MMP-14. Interstitial collagenase, MMP-1, is activated by MMP-3 and expressed in multiple tissues housing cells such as macrophages, fibroblasts, and chondrocytes (Pei, Harvey, Yu, Chandrasekhar, & Thirunavukkarasu, 2006). MMP-1 plays a role in the breakdown of collagen types I, II, III, VII, and X and a broad range other matrix proteins (Monfort et al., 2006; Vincenti & Brinckerhoff, 2002), whereas MMP-3 and aggrecanases degrade PGs through the proteolytic cleavage of the aggrecan core in the early stages of OA (Monfort et al., 2006). The high MMP-1 activity present at day 7 could an indication of MMP-3 expression by the fibroblasts as a response mechanism to the HA containing hydrogel, which is foreign to the native fibroblastic conditions.

Therefore, the hFF-1s could be secreting MMP-3 which is cleaving the HA from the radial hydrogels causing the non-specific detection in the aggrecan ELISA. The MMP-1 activity observed in the induction cultures could be due to the cells acclimatizing to the environment as the activity steadily declines throughout the culture period. Gelatin turnover is mediated either by MMP-2 or MMP-9 (Makowski & Ramsby, 1998). MMP-2 is expressed by MSCs but the activity is inhibited by tissue inhibitors of metalloproteases (Lozito & Tuan, 2011). Additionally, MMP-1 and MMP-2 activity in fibroblasts is regulated by the mechanical strength of gels (Petersen, Joly, Bergmann, Korus, & Duda, 2012; Tomasek et al., 1997). The increased strength of the radial hydrogel could explain the cause of increased expression of the MMP-1 and MMP-2/MMP-9 in the hFF-1 control of the radial hydrogel but not the gelatin containing superficial hydrogel, which has much lower mechanical strength (Walker & Madihally, 2015). MMP-13, which is produced by chondrocytes, can cleave native fibrillar collagen as well as several other ECM components. MMP-13 also contains a RUNX2 binding element, and both, MMP-13 and RUNX2 have been found to co-localize in cartilage during chondrogenesis and OA. Overexpression of RUNX2 was shown to induce transcription of MMP-13 but had no effect on the expression of MMP-1 (Pei et al., 2006). Therefore, MMP-1 and MMP-13 could play separate roles in the degradation of osteoarthritic cartilage (Kevorkian et al., 2004). MMP-13 is also expressed by fibroblasts in chronic cutaneous ulcers but not in normally healing acute dermal wounds (Ravanti, Heino, Lopez-Otin, & Kahari, 1999). This may explain the high MMP-13 expression levels observed for the hFF-1 control radial hydrogels as another fibroblastic response to the foreign environment. Alternatively, fibroblasts cultured in collagen type I gels express mRNAs of MMP-13 but not in monolayer cultures without TGF-β. Adding TGF-β induces MMP-13 expression which could be the cause of the initial increase in expression of the induction cultures. Interestingly, after day 7, MMP-13 content decreased with no significant differences noticed for all induction cultures. This decrease in expression could be attributed to the differentiation of cells into the chondrogenic lineage coinciding with cell attachment and responsive construction of the ECM

rather than degradation of the hydrogels. Further, the absence of MMP-13 at the later days suggests the cells are not proceeding into the hypertrophic and apoptotic stages of the chondrogenesis, but instead are going through the chondrogenic stages consistent with the superficial and radial cartilage layers.

Histological and IHC staining gave valuable insight into the cellular and material morphologies of the cultures allowing for quality assessment of the tissues. Multiple stains for common cartilage proteins (aggrecan, GAGs, and collagen type II) were incorporated as well as a protein not primarily (collagen type I) found in cartilage. The H/E stain was utilized to observe the material morphology and cell distribution between the conditions. All conditions displayed similar material morphology and cell distribution considering the cell density to previous reports using similar hydrogel components and cell lines (Klangjorhor et al., 2012; Liu et al., 2004; C. C. Wang et al., 2014). Additionally, the alcian blue micrographs of the induction cultures exhibited similar GAG accumulation and distribution in hydrogels similar to radial hydrogel (Wei Seong Toh et al., 2010) as well as high density chondrocyte micromasses (Dehne et al., 2010). As expected, the aggrecan and collagen type II IHC micrographs of induction cultures showed similar staining characteristics with progenitor micromasses (Barry et al., 2001; Dehne et al., 2010) and hydrogels containing hyaluronan (Wei Seong Toh et al., 2010; Yamane et al., 2005), gelatin (C. C. Wang et al., 2014), or alginate (Xu et al., 2008), whereas the hFF-1 control did not display aggrecan and collagen type II content. However, the hFF-1 control cultures did exhibit large accumulations and distributions of collagen type I which consistent with the native cellular function of fibroblasts (Ivarsson, McWhirter, Borg, & Rubin, 1998). The induction cultures were absent or contained small areas of collagen type I content similar to other reports (C. C. Wang et al., 2014; Yamane et al., 2005). However, all superficial hydrogel cultures (induced and control) contained collagen type I content most likely due to non-specific binding of the secondary antibody to gelatin causing a false positive. While the lower cell density hydrogels displayed

similar characteristics with the multiple previous reports, the fourfold hFF-1 induced cultures displayed almost identical representations to the histological and IHC micrographs of many of the previously referenced articles. However, the increased cell density also displayed production of collagen type I, which is a deviation from the lower density induction cultures. This production of the collagens may follow in a temporal fashion; wherein the early stages of chondrogenesis, the fibroblasts are still expressing their dominant cellular and molecular signals and functions followed by the increasing production of collagen type II and reduction of collagen type I as chondrogenesis continues (Barry et al., 2001; Wei Seong Toh et al., 2010; Wilson et al., 2009). Together these micrographs display an image of an alternative tissue for cartilage produced *in vitro*. The key elements (aggrecan, collagen type II, and GAGs) are all present in the induction cultures with the absence of collagen type I, similar to native cartilage. Furthermore, this study has presented a mature cell source as an alternative to progenitor cells that functions and differentiates in similar fashion.

4.5. CONCLUSIONS

In summary, we present suggestive evidence to support the possibility of fibroblast differentiation into the chondrogenic lineage. Throughout each of the methods, the induced fibroblasts followed similar trends with no significant differences as well as exhibiting similar protein and cellular morphology to the induced hMSC control. Further, the induced fibroblasts show phenotypic deviations from the fibroblast control through the duration of the culture period. The combined observations of the study show similarities to native cartilage suggesting complete differentiation of the fibroblast lineage into the chondrogenic lineage. This study proposes a new viable cell source requiring a less invasive isolation procedure for use in academic and clinical orthopedic applications.

4.6. ACKNOWLEDGEMENTS

Financial support was provided by the Oklahoma Center for Advancement of Science and Technology (HR12-023) and Edward Joullian Endowment. Authors would like to thank Mr. Curtis Andrew, Oklahoma Animal Disease and Diagnostic Laboratory (OADDL) for histological processing.

CHAPTER V

DIRECT DIFFERENTIATION OF ADULT HUMAN FIBROBLASTS INTO OSTEOBLASTS BY INDUCED FACTORS

5.1. INTRODUCTION

Developments in cell biology have focused on a two-step process for reprogramming mature cells into stem cells using genetic factors and then differentiating them into required mature lineage (Szabo et al., 2010). This is based on the possibility of reprogramming skin fibroblast cells into induced pluripotent stem (iPS) cells in two-dimensional (2D) tissue cultures using transduction fragments (G. Gong, D. Ferrari, C. N. Dealy, & R. A. Kosher, 2010). Using dermal fibroblasts has been attractive due to the less invasive surgical procedure to harvest a skin biopsy, and expanding them in serum free medium. iPS cells exhibit properties typical of embryonic stem cells (K. Okita, T. Ichisaka, & S. Yamanaka, 2007) and could give rise to adult chimeras capable of germline transmission, showing the possibility of redifferentiating mature cells. Genetic reprogramming was demonstrated without viral vectors (Okita, Nakagawa, Hyenjong, Ichisaka, & Yamanaka, 2008) and converting fibroblasts without confirming the pluripotency (P. Huang et al., 2011). While iPS cells provide many advantages, they pose many hurdles to overcome before being clinically safe and efficient. Primary concerns with the iPS cells are low conversion efficiency (~10%) (Okita & Yamanaka, 2010), and general concerns related to artificial genetic manipulations (Apostolou & Hochedlinger, 2011). Autologous iPS cells derived by both viral vectors and episomal approaches were found to be immunogenic to the host in a murine models

(Zhao, Zhang, Rong, & Xu, 2011). These downfalls regress to using autologous adult stem cells as the primary and prominent source for clinical cellular therapies.

Mesenchymal stem cells (MSCs) are commonly explored due to the multipotency and residence in a diverse host of tissues (Kaveh, 2011; Tuan, Boland, & Tuli, 2003). Of these tissues, bone marrow has the highest yield of MSCs besides adipose tissue, blood stream, and omentum. Also, due to substantial demand in musculoskeletal tissues and identified role of hMSCs in those tissues, many approaches have been developed to differentiate hMSCs. For example, MSCs differentiate to osteoblasts during natural bone formation and osteogenic differentiation using common chemical pathways for adult hMSCs. Differentiated osteoblasts build mineralized bony tissues, leading to adult skeletal formation, growth, and repair (Ducy, 2000; Gentili & Cancedda, 2009). Many have demonstrated the possibility of differentiating hMSCs into various mature lineages using inducible factors in 2D tissue culture. However, a considerable limitation of MSCs is the inability to obtain autologous cell source, leading to long time immunosuppressive therapies with the use of allogeneic cells (Kaveh, 2011). Thus focusing on autologous cell sources would be useful.

Fibroblasts have been used as a base cell for differentiation purposes through genetic modification. This begs the question of why fibroblasts could not differentiate using similar pathways of somatic stem cells if they have much of the machinery to revert to a pluripotent stage through genetic modification. Further, fibroblasts and osteoblasts share many of the same qualities; some even suggested that they are indistinguishable except osteoblast mineralized ECM outside the cell (Ducy, 2000). Thus, we questioned whether inductive signals used to differentiate adult hMSCs into osteoblasts would differentiate human fibroblasts (hFF-1) without needing genetic modification. A hepatocellular carcinoma cell line (HepG2), which is known to endogenously express alkaline phosphatase (ALP), was used assess if differentiation was limited to closely related lineages. From developmental biology, we know that the liver primarily

originates from the reorganization of endoderm, unlike the bone, which originates from mesoderm. Although, relatively little is known about the endoderm reorganization and subsequent organ formation due to the absence of suitable *in vitro* models; hepatocytes and hematopoiesis (process of blood cell formation) are known to share a common ancestral lineage (Zanjani, Ascensao, & Tavassoli, 1993). Recent advances show that cell-cell and cell-matrix interactions in three-dimensional (3D) systems are crucial to integrate the extensive signaling pathways, biophysics, and biomechanics that regulate the development, homeostasis, and regeneration of tissues. In order to evaluate the effect of 3D structures, a hydrogel scaffold was used to test differentiation and maturation. These results show similarities in the differentiation of hFF-1s to osteoblasts, similar to hMSCs.

5.2. MATERIALS AND METHODS

5.2.1. Sources for Materials

Human foreskin fibroblast (hFF-1), hepatocellular carcinoma cell line HepG2 (HB-8065), Dulbecco's Modified Eagle's Medium (DMEM), Eagle's Minimum Essential Medium (EMEM), and fetal bovine serum (FBS) were purchased from ATCC (Manassas, VA). Human mesenchymal stem cells (hMSC), normal human osteoblasts (NHOst), Fibroblast Basal Medium supplemented with Fibroblast Growth Medium SingleQuot Kit and growth factors (FBM), trypsin-EDTA for hMSCs, Mesenchymal Stem Cell Basal Medium (MSCBM) supplemented MSC Growth Medium SingleQuots, HEPES buffered saline (HEPES-BSS), trypsin/EDTA NHOsts, trypsin neutralizing solution, OBM, and Osteogenic basal medium supplemented with hMSC osteogenic SingleQuots Kit (referred hereafter as induction medium) were obtained from Lonza Group Ltd. (Walkersville, MD). Ethyl alcohol (200 proof) (EtOH) was obtained from Pharmco. Formalde-Fresh (certified low odor 10% formalin) was obtained from Fisher Scientific (Pittsburgh, PA).

5.2.2. Cell Expansion Cultures

All cells were incubated in respective media (**Table 1**) at 37°C and 5% CO_2/95% air atmosphere and medium was changed every 3 to 4 days. All cultures exhibited normal growth characteristics with respect to size, shape and confluency. Once confluent, all cell types were subcultured at a ratio of 1 plate: 3 plates. The cells were centrifuged for 5 minutes, then resuspended in the respective media and distributed.

Seven days prior to experimentation in serum free conditions, hFF-1 and NHOst cultures weaned off serum by feeding with FBM instead of DMEM with 15% FBS and serum-free OBM instead of the serum containing OBM, respectively. Serum free hFF-1 cultures were detached using TrypLE™ Express enzyme (Life Technologies, Grand Island, NY). Serum free NHOsts cultures were detached using the method described in **Table 1**. Confluent cells were subcultured using detachment enzyme and centrifugation following vendors protocol (**Table 5.1.**). Viable cells were counted using trypan blue dye exclusion assay.

Table 5.1. Culture conditions for maintaining different cell types.

Cells	Source	Maintenance medium	Centrifuge	Subculture process
NHOst	Lonza	Osteogenic Basal Medium with 10% FBS	220×g	washed with HEPES-BSS, detached with trypsin/EDTA, neutralized with trypsin neutralizing solution
hFF-1	ATCC	DMEM with 15% FBS	270×g	Washed with PBS and detached with 0.25% trypsin/0.53mM EDTA and Clonetics trypsin-EDTA, respectively. The trypsin/EDTA was neutralized using the respective media.
hMSC	Lonza	MSCBM with MSCGM	600×g	
HepG2	ATCC	EMEM with 10% FBS	125×g	Washed with PBS, detached using trypsin/EDTA, and neutralized with growth media

5.2.3. 2D Differentiation Using Induction Medium

For testing differentiation, all cells were centrifuged at 150×g for 5 minutes. 250,000 viable cells per culture were seeded into 6-well plates. The cells undergoing induction were washed with Osteogenic Basal Medium supplemented with induction medium prior to seeding on the TCPS. To induce differentiation, hFF-1s, hMSCs, and HepG2 cells were incubated with 2-mL of induction medium. In tandem, same number of cells were seeded into 6-well plates and supplemented with maintenance media (both with and/or without serum containing media) of respective cell line and were used as controls. NHOsts cultures were used as positive controls. Induction medium was prepared fresh prior to cell culturing. Triplicate samples were prepared per condition and per cell type. All cultures were incubated at 37°C and 5% CO2 in air and media was changed twice a week. Culture supernatants were collected and preserved at -80°C for analyses of alkaline phosphatase activity. Every week, phase contrast micrographs were obtained at representative locations using an inverted microscope (Nikon TE2000, Melville, NY) outfitted with a Hamamatsu C4742-95-12ERG CCD camera.

5.2.4. 3D Differentiation in Hydrogel Suspension Cultures

Differentiation in a 3D culture was evaluated using chitosan-hyaluronic acid-beta tri-calcium phosphate (β-TCP) hydrogels prepared as described previously (Walker & Madihally, 2015). In brief, chitosan, HA, and water were sterilized, then HCl (12 N) was added to dissolve chitosan and the solution was stirred to homogeneity. Thereafter, sterile β-TCP was added and mixed until homogeneity. The final hydrogel solution composition was 2%/1%/1% wt% (chitosan/HA/ β-TCP). Glycerol 2-phosphate (0.56 g/mL) was added drop wise to the hydrogel solution for pH adjustment (7.2 - 7.4) and assistance with gelation.

The hydrogel solution was dispensed into each well of a 6-well plate. Then 500,000cells/mL were dispensed and mixed in crisscross patterns for uniform distribution. The cell containing-

mixture was allowed to reach gelation by incubating at 37°C for 2 hours prior to adding the respective media. All hydrogel cultures were incubated at 37°C and 5% CO2 in air and media was changed twice a week. Culture supernatants were collected and preserved at -80°C for analyses of total protein content, alkaline phosphatase activity, and MMP activity. After 28 days, the hydrogel cultures were analyzed via histology and IHC.

5.2.5. Alkaline Phosphatase (ALP) Activity

Supernatants from the TCP cultures and the hydrogel cultures were tested for ALP activity using the Alkaline Phosphatase Assay Kit (Abcam, Inc., Cambridge, MA), following vendor's protocol. In brief, the reagents and supernatants were brought to room temperature. The hydrogel supernatants were centrifuged for three minutes at 100×g to remove hydrogel particulates. Into each of the wells in 96-well plates, 80μL of supernatants were added. Fresh media was used as the background control. 50μL of 5 mM pNPP (p-nitrophenyl phosphate) prepared in assay buffer was added, thoroughly mixed and incubated at room temperature (RT) for one hour in darkness. ALP converts the pNPP substrate to an equal amount of colored pNP (p-nitrophenol). 20μL of stop solution was added to terminate the reaction. Absorbance was measured at 405nm using a Molecular Devices EMax Precision Microplate Reader (Molecular Devices, LLC, Sunnyvale, CA). Absorbance was converted to ALP activity using the standard curve prepared using lyophilized ALP with assay buffer and diluting the pNPP solution with assay buffer to 1 mM. pNPP was added to the wells at different volumes (0, 4, 8, 12, 16, and 20nmol/well) followed by the addition of the ALP resulting in a standard curve with concentrations of 0, 20, 40, 60, 80, and 100nmol/mL.

5.2.6. qPCR Analysis

Total RNA from cell cultures was isolated using the Qiagen RNeasy mini kit (Qiagen Sciences Inc., Frederick, MD). DNase treatment was performed using DNase I, Amplification Grade kit

(Life Technologies, Grand Island, NY). cDNA was synthesized using SuperScript™ III First-Strand Synthesis SuperMix for qRT-PCR kit (Life Technologies, Grand Island, NY) and MultiGene™ OptiMax Thermal Cycler (Labnet International, Inc., Edison, NJ). The cDNA was amplified using SYBR GreenER™ qPCR SuperMix Universal kit (Life Technologies, Grand Island, NY) and Applied Biosystems 7500 Fast real-time PCR thermocycler (Life Technologies, Grand Island, NY). Primer sequences (Integrated DNA Technologies, Coralville, IA) and annealing temperatures used are listed in **Table 5.2**. The expression of beta-actin (*β-actin*) in each condition was used as the housekeeping gene. Relative quantification of marker gene expression was preformed applying the using 2-ΔCt method.

Table 5.2. Primer Sequences and Annealing Temperatures

Primers	Gene ID	GenBank Accession	Sequence	Annealing Temp, °C
Osterix (F) Osterix (R)	*SP7*	NM_001173467	5'-TAATGGGCTCCTTTCACCTG-3' 5'-CACTGGGCAGACAGTCAGAA-3''	51
Osteopontin (F) Osteopontin (R)	*SPP1*	NM_001040058	5'-CCTGGGCAACGGGGATGG-3' 5'-TGATGGCCGAGGTGATAGTGTGGT-3'	58
Osteocalcin (F) Osteocalcin (R)	*BGLAP*	NM_199173 NM_000711	5'-ATGAGAGCCCTCACACTCCTC-3' 5'-CGTAGAAGCGCCGATAGGC-3'	55
Osteonectin (F) Osteonectin (R)	*SPARC*	NM_003118	5'-AGTAGGGCCTGGATCTTCTT-3' 5'-CTGCTTCTCAGTCAGAAGGT-3'	51
Collagen I (F) Collagen I (R)	*COL1A1*	NM_000088	5'-CCACCAATCACCTGCGTACAGAAC-'3 5'-GGCACGGAAATTCCTCCGGTTGAT-3'	55
Sox-9 (F) Sox-9 (R)	*SOX9*	NM_000346	5'-TGGCAGACCAGTACCCGCATCT-3' 5'-TCTTTCTTGTGCTGCACGCGC-3'	58
beta-actin (F) beta-actin (R)	*β-actin*	NM_001101	5'-TGGCACCACACCTTCTACAATGAG-3' 5'-GCACAGCTTCTCCTTAATTGTCACGC-3'	55
Runx2 (F) Runx2 (R)	*RUNX2*	NM_001024630	5'-ATCCATCCACTCCACCACGC-3' 5'-AAGGGTCCACTCTGGCTTTGG-3'	55
ALP (F) ALP (R)	*ALPL*	NM_000478	5'-CTCGTCGACACCTGGAAGAGCTTCAAACCG-3' 5'-GGATCCGTCACGTTGTTCCTGTTCAGC-3'	58
BSP (F) BSP (R)	*IBSP*	NM_004967	5'-TCAGCATTTTGGGAATGGCC -3' 5'-GAGGTTGTTGTCTTCGAGGT-3'	51

5.2.7. Histology

The hydrogel cultures were harvested after 28 days and fixed with 3.7% formaldehyde for 30 minutes at RT. The samples were washed thrice with PBS and stored in EtOH. The samples were paraffin-embedded, sectioned, and stained with haematoxylin and eosin (H/E) and von Kossa. Digital photomicrographs were captured at representative locations using a Nikon TE2000 microscope using Metamorph image analysis software (Universal Imaging, West Chester, PA) and a CCD camera.

5.2.8. MMP Activity

Matrix metalloproteinase (MMP) activity in supernatants from the hydrogel cultures and fresh media was analyzed using fluorogenic substrates (DNP-Pro-Leu-Gly-Met-Trp-Ser-Arg-OH), as described previously (Iyer et al., 2012). In brief, the supernatants were centrifuged at 100×g for 3 minutes prior to running the assay. A 1:1 volume ratio of 100μM fluorogenic peptide solution and cell supernatant was mixed and incubated at 37°C for 20 minutes. The fluorescence was measured at 405nm emission and 320nm excitation using Molecular Devices SpectraMax Gemini XS Precision Microplate Reader (Molecular Devices, LLC, Sunnyvale, CA). The total amount of protein present in the medium exposed to cells was assessed using BCA Protein Assay Kit (Pierce Chemical Co, Rockford, IL) following vendor's protocol. Obtained MMP activity was normalized using the total protein content from respective culture conditions.

5.2.9. Assessment of Hydrogel Stability

Hydrogels containing no cells were subjected to serum free OBM and induction medium with β-GP removed for 28 days. Identical culture procedure to the cell containing hydrogels was followed for consistency. This was done to reveal the cause of the breakdown which could be due to either the media constituents or enzymatic responses to the environment by the cells.

Instability/breakdown was assessed by the presence of the hydrogel in the supernatant during media exchange. Additionally, micrographs were taken at days 0, 7, 14, 21, and 28 to observe any breakdown occurring in the hydrogels. After the 28 days, the hydrogels were removed from containment and observed for stability and structural integrity.

5.2.10. Statistical Analysis

Statistical analysis was done by repeating experiments three or more times and collecting samples in triplicate. A one way analysis of variance (ANOVA) with a 99% confidence interval was used for evaluation for significant differences between two groups. Differences were considered statistically significant when $p<0.05$.

5.3. RESULTS.

5.3.1. Differentiation through soluble factors on tissue culture plastic.

Osteoblasts arise following the process, endochondral ossification, whereupon vascularization invades the cartilage periphery, and terminally differentiated hypertrophic chondrocytes mineralize subsequently becoming apoptotic. The effects of soluble factors known to induce differentiation of hMSCs into osteoblasts were tested on hFF-1s and HepG2 cell cultures at similar cell densities. The normal human osteoblasts (NHOsts) controls were cultured with Osteoblast basal medium supplemented with Osteoblast growth medium SingleQuot Kit and growth factors (OBM) supplemented with serum and without serum. During the culture period, micrographs were acquired to observe changes in morphology and cell number at different conditions (**Figure 5.1.**). In NHOsts cultures with serum, cell clusters which lead to nodules appeared as early as seven days and persisted for the rest of the culture duration. However, NHOsts cultures without serum showed reduction in cell numbers relative to NHOsts cultures with serum, and no clusters were observed probably attributed to decreased cell numbers. When hMSCs were cultured in induction medium, as shown by others (Dolatshahi-Pirouz et al., 2014),

multiple cell clusters appeared similar to NHOsts with serum and persisted for the rest of the duration. Interestingly, cell clusters were also observed in hFF-1 induction cultures at times delayed by a week. This is in contrast to the hFF-1 control cultures where no clustering and nodule formation was observed. On the contrary no such clustering was observed in HepG2 cultures with induction medium. Overall, there seemed to be a reduction in number of cells compared to HepG2 control cells cultured for the same period of time. In all cultures, no morphological differences were observed in the cells except the clustering.

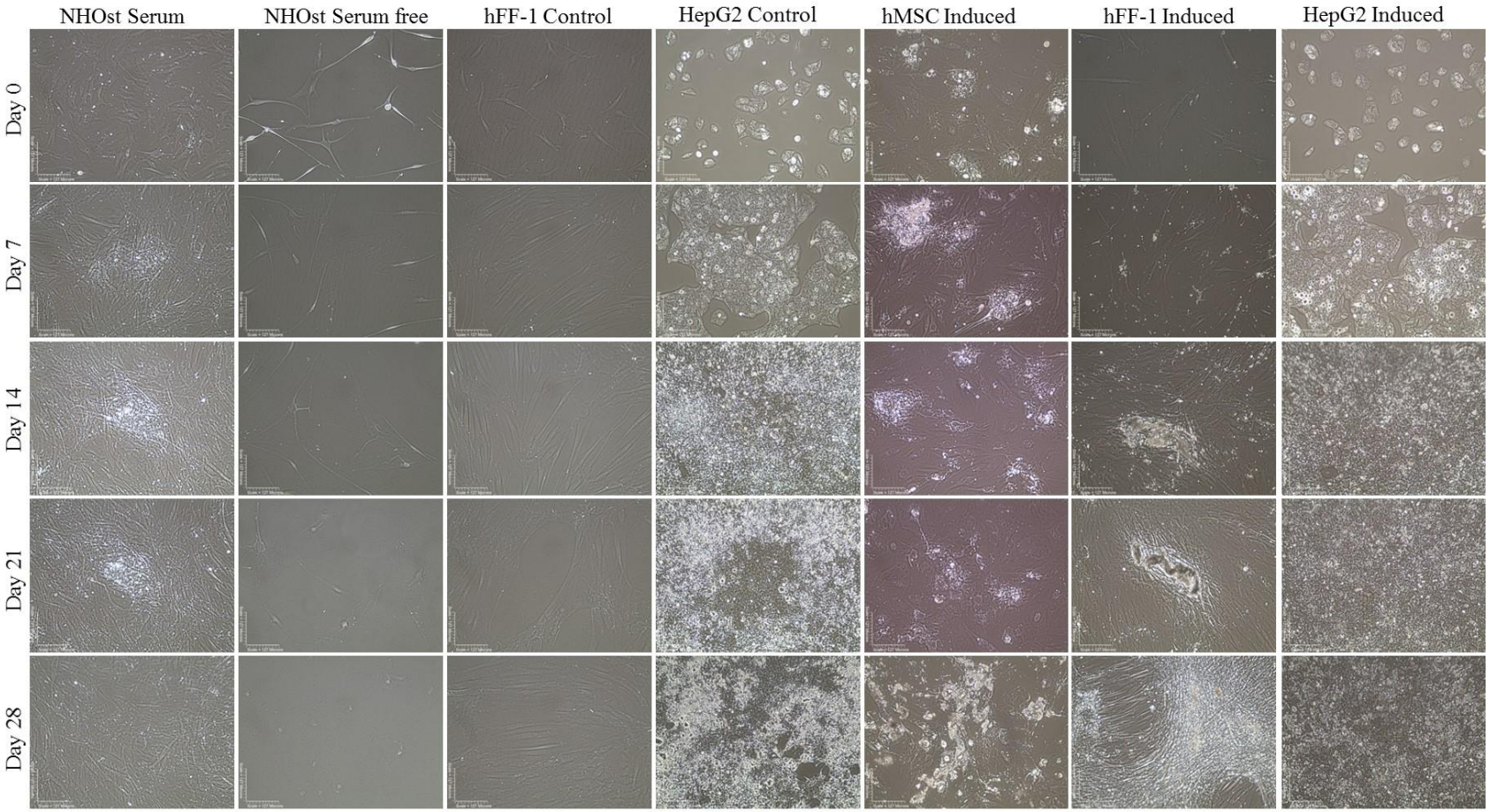

Figure 5.1. Represented phase-contrast micrographs showing the morphological changes during the culture period.

5.3.2. ALP Activity

ALP is expressed during osteogenic differentiation and bone matrix maturation. ALP helps improve the availability of phosphates for calcification and an early indicator for the osteoblast lineage (Kaveh, 2011). ALP activity is known to have higher expression during osteogenic differentiation and bone matrix formation, and lower during the new bone formation from osteoprogenitors and osteoblast transformation to osteocytes. ALP activity has been used as an indicator of osteoblast differentiation, bone therapies, and tissue engineering applications (Baylan et al., 2013; Chen, Deng, & Li, 2012; Frohbergh et al., 2012; Peter, Lu, Kim, & Mikos, 2000; Stratford et al., 2014). In order to understand the clusters formed in the cell cultures particularly in induced hFF-1 cultures, supernatants were analyzed for ALP activity. Elevated levels of ALP activity were observed in all conditions except the serum free NHOst control. Also, the normally cultured hFF-1 control, which was not supplemented with induction medium, exhibited no activity (**Figure 5.2.**). However, induced hFF-1 showed significant increase in ALP activity even at day 7. The activity levels persisted throughout the culture period. ALP activity levels in induced hFF-1 cells were similar to induced hMSCs and NHOst serum containing cultures. HepG2 cells endogenously express ALP due to its involvement in various metabolic functions. As expected, HepG2 control cells showed very high ALP activity. However, the induced HepG2 condition showed reduction by nearly half the ALP activity compared to the HepG2 control cultures throughout the 28 days. This was substantially less than induced hFF-1 and hMSC cultures. This suggests that induction medium differentially regulates ALP activity based on the type of cells.

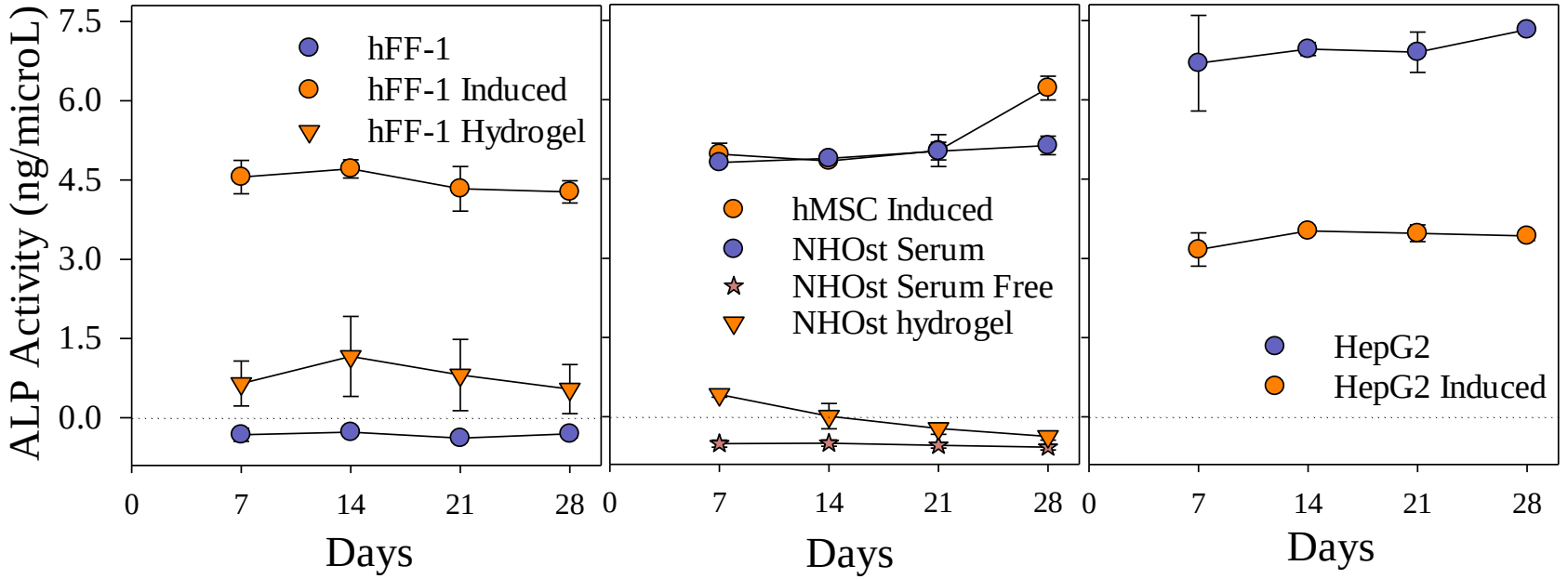

Figure 5.2. Differences in ALP activity between cell lineages.

5.3.3. qPCR Analysis

To better understand the observed changes in cell clusters formed at different times and altered ALP activity, changes in cDNA expressions corresponding to osteogenic genes transcribed during differentiation were assessed. At different stages of osteogenesis, osteoprogenitors differentiating into osteoblasts transcribe genes such as *ALPL*, *COL1A1*, *IBSP*, *RUNX2*, *SP7*, *BGLAP*, *SPARC*, *SPP1*, and *SOX9* as well as many others (Dalle Carbonare, Innamorati, & Valenti, 2012; Koo et al., 2014; Villarreal, Mann, & Long, 1989; Zhu, Friedman, Luo, Woolf, & Hankenson, 2012). In terms of their functions, bone sialoprotein (BSP) plays a role in the nucleation of hydroxyapatite crystals. Osteopontin anchors cells via their $\alpha_V\beta_3$ integrin to the mineralized bone surface. Osteocalcin activates both osteoclasts and osteoblasts during early bone formation. Collagen type I is the major organic component in bone extracellular matrix, secreted by osteoblasts. The expression of genes at different time points creates a map to follow the progression of osteogenesis. Thus, RNA was isolated from different cultures after 28 days and their expression levels in different cultures were compared. However, at this time point, the induced cultures must be in mature stages of the osteogenic differentiation. Hence, the late expressed genes are *RUNX2*, *SPARC*, *BGLAP*, and *SP7* were first compared. These results showed (**Figure 5.3.**) similar expressions between the induced hFF-1s and the NHOst control cultures. Further, the genes that are expressed earlier including *COL1A1*, *ALPL*, and *SPP1* exhibited reduced expressions in the induced hFF-1 cells relative to the hFF-1 control cells, while showing similarities to the NHOst control. The hFF-1 control cells exhibited significant increases in expressions of all cDNA expressions except *SP7* and *BGLAP* (**Figure 5.3.**). Similar expression levels were observed between the induced hFF-1s and the NHOsts, except *ALPL* and *SPP1*. *ALPL* expression in hFF-1 control cells was high despite negligible activity in the media supernatants. Upon induction and differentiation, *ALPL* cDNA expressions decreased in hFF-1 induced cultures relative to hFF-1 control cells while the ALP activity increased.

cDNA expressions from the HepG2 control cells had little overlap with that of the NHOst control except in the *RUNX2* gene. The *COL1A1*, *ALPL*, and *SPARC* expression of the HepG2 control were down-regulated compared to the NHOst control while other cDNA expressions were upregulated. Also, the induced HepG2 condition showed no similarities in any of the cDNA expressions compared to the NHOst control. *ALPL* expression in the induced HepG2 cultures was similar to that in HepG2 controls.

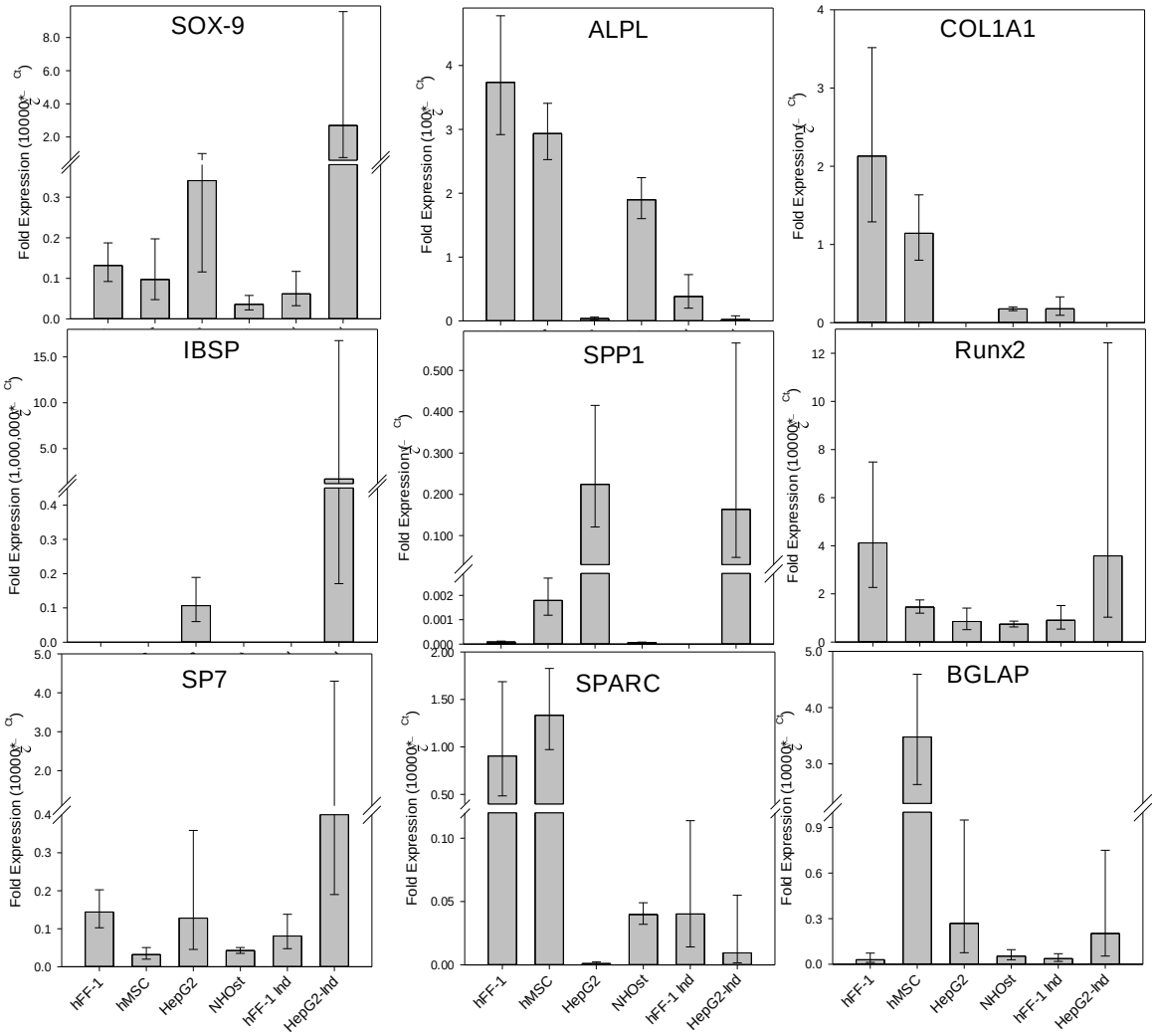

Figure 5.3. Changes in the cDNA expression of various genes.

5.3.4. Differentiation on Hydrogels

Next, we questioned the effect of 3D environment on fibroblast differentiation in addition to induction medium using an injectable hydrogel formulation containing β-TCP. These materials have shown to form a hydrogel at body temperature and remain intact in the absence of cells during cyclical tests. Further, at five days the hydrogel showed minimal immune reaction in a murine dorsal dermal model (Walker & Madihally, 2015). First, after 28 days in culture, cells were analyzed by histological staining using H/E and von Kossa to assess the cell and matrix distribution and calcium phosphate deposition. In tandem, hydrogels without cells were used as a control. **Figure 5.4.** shows the distribution of the cells and extracellular matrix (ECM) for all conditions after 28 days of culture. Similar cell distributions and cell morphologies were observed in all cell lineages (**Figure 5.4.**). Notably, the hFF-1 and hMSC induction cultures displayed similar mineralization to the NHOst culture after 28 days. Size of nodules corresponded to the cell cluster sizes observed in 2D cultures. Further, increased mineral deposition was observed in all cell seeded hydrogels when compared to the no cell control.

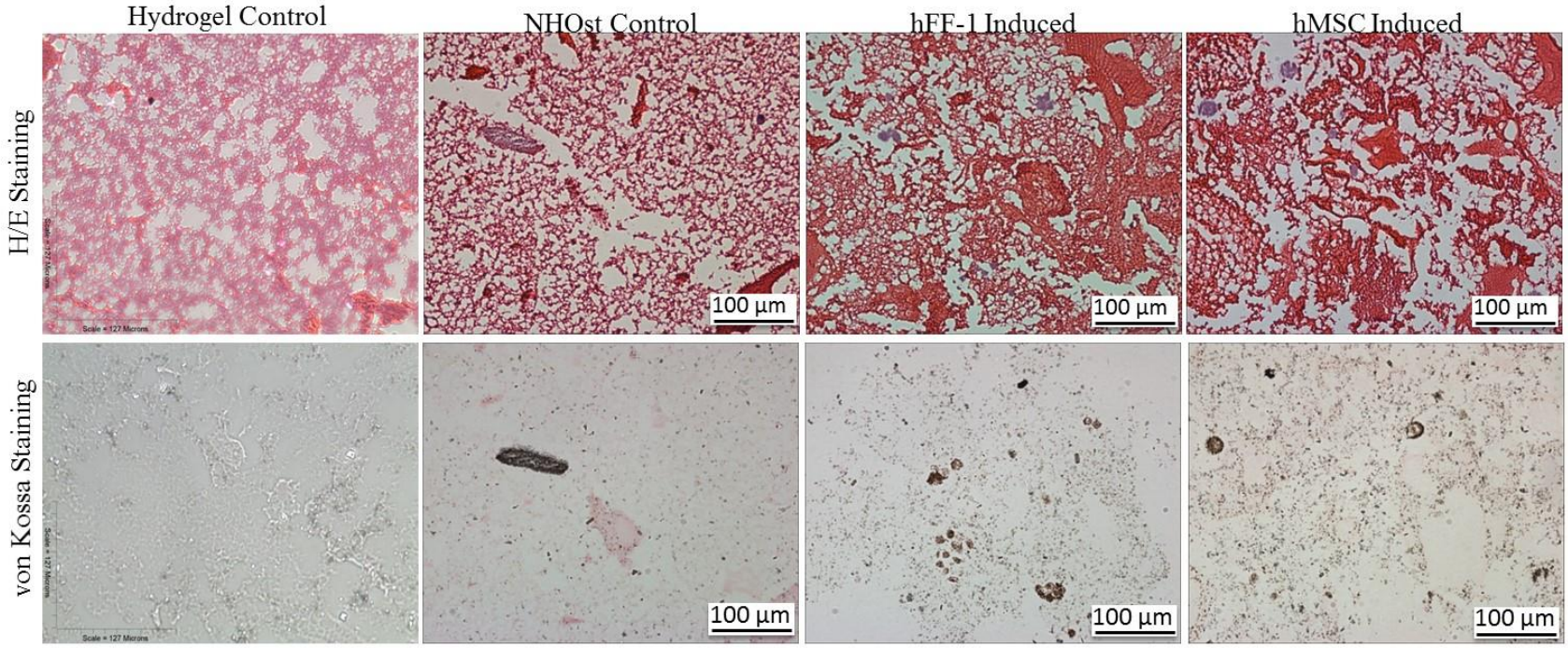

Figure 5.4. Differentiation on 3D Hydrogels. Representative H/E and von Kossa stained micrographs of various conditions from 28-day cultures.

ALP activity was also assessed in the hFF-1 induced condition and NHOst serum free condition in a 3D hydrogels (**Figure 5.2.**). The induced hFF-1s in the 3D hydrogels followed a similar trend to the 2D TCP induced hFF-1 condition and displayed significant increases in ALP content from the hFF-1 control until day 28. The ALP activity of the serum free NHOst in the 3D hydrogels steadily declined throughout the culture period until the activity reached that in 2D serum free NHOst cultures at day 28. The increased ALP activity of the induced hFF-1 conditions in both 2D and 3D cultures compared to the hFF-1 control and the similar activity level of the hFF-1 induced 2D cultures with the induced hMSCs and serum NHOsts indicate differentiation using identical chemical pathways as an osteoprogenitor such as MSCs.

5.3.5. Hydrogel Stability Issues

Hydrogel-based approaches to local delivery of cells have shown poor performance due to attrition of cells. This could be attributed to the stability of the hydrogels due to various reasons such as premature degradation of the hydrogel and deprived nutrient environment. Since histological analysis and ALP activity show presence of functional cells, stability of the hydrogel in presence of cells could be an issue in certain conditions. In this regard, we noticed that when the hydrogel cell cultures were harvested at day 28, only the serum free NHOst hydrogel cultures remained stable. Other hydrogel cultures containing hFF-1 and hMSC induction medium exhibited noticeable breakdown. The instability continued throughout the 28 day period resulting in uncertainty in these samples. This could be due to either media constituents or endogenous proteases secreted by the cells. First, the supernatants of the hydrogel cultures were assessed for the presence of matrix metalloprotease (MMP)-2/MMP-9 activity. MMP-2 is expressed by MSCs but the activity is inhibited by tissue inhibitors of metalloproteases (Lozito & Tuan, 2011). Additionally, MMP-2 activity in fibroblasts is regulated by the mechanical strength of gels (Tomasek et al., 1997). These results showed (**Figure 5.5.**) no significant difference to the fresh medium except at day 7 for the induced hFF-1 and hMSC cultures. A marginal increase in the

MMP-2/MMP-9 expression was observed in the NHOst cultures relative to the fresh medium initially and gradually declined as the cultures progressed. The steady decline was also observed in the ALP activity for the NHOst hydrogel cultures. This decline in ALP and MMP activity may be due to the progression of cell death over the culture period similarly observed in the micrographs.

Next, hydrogels without cells were prepared and cultured with serum free OBM and osteoblast induction medium to determine whether the media component was the influential factor. **Figure 5.5.c** shows a representation of the hydrogels cultured without cells in different media with and without stability issues. Since β-glycerophosphate was used in the formulation of the hydrogels, and is also present in the induction medium, we thought that the breakdown could be due to excess presence of phosphate groups altering the pH and stability of the hydrogel. To test the role of β-glycerophosphate, the hydrogels were cultured with β-glycerophosphate free osteoblast induction medium and showed instability at an earlier time (between day 0 and 7) than previous cultures, which was between day 7 and day 14 (data not shown). Further, progression of the breakdown was observed in the hydrogels subjected to the induction medium throughout the culture period. After 28 days, the hydrogels were removed and placed in PBS to show the structural integrity of the hydrogels. The hydrogels subjected to induction medium displayed breakdown with the appearance of the opaqueness of PBS whereas the hydrogel subjected to serum free OBM was intact in Day 28 Harvest. This suggested that the breakdown was not due to β-glycerophosphate and probably due to the proteases present in the serum. Hence while developing formulations for differentiation of cells, it is important to consider the impact on serum proteases and their effect on scaffolds used in injectable formulations.

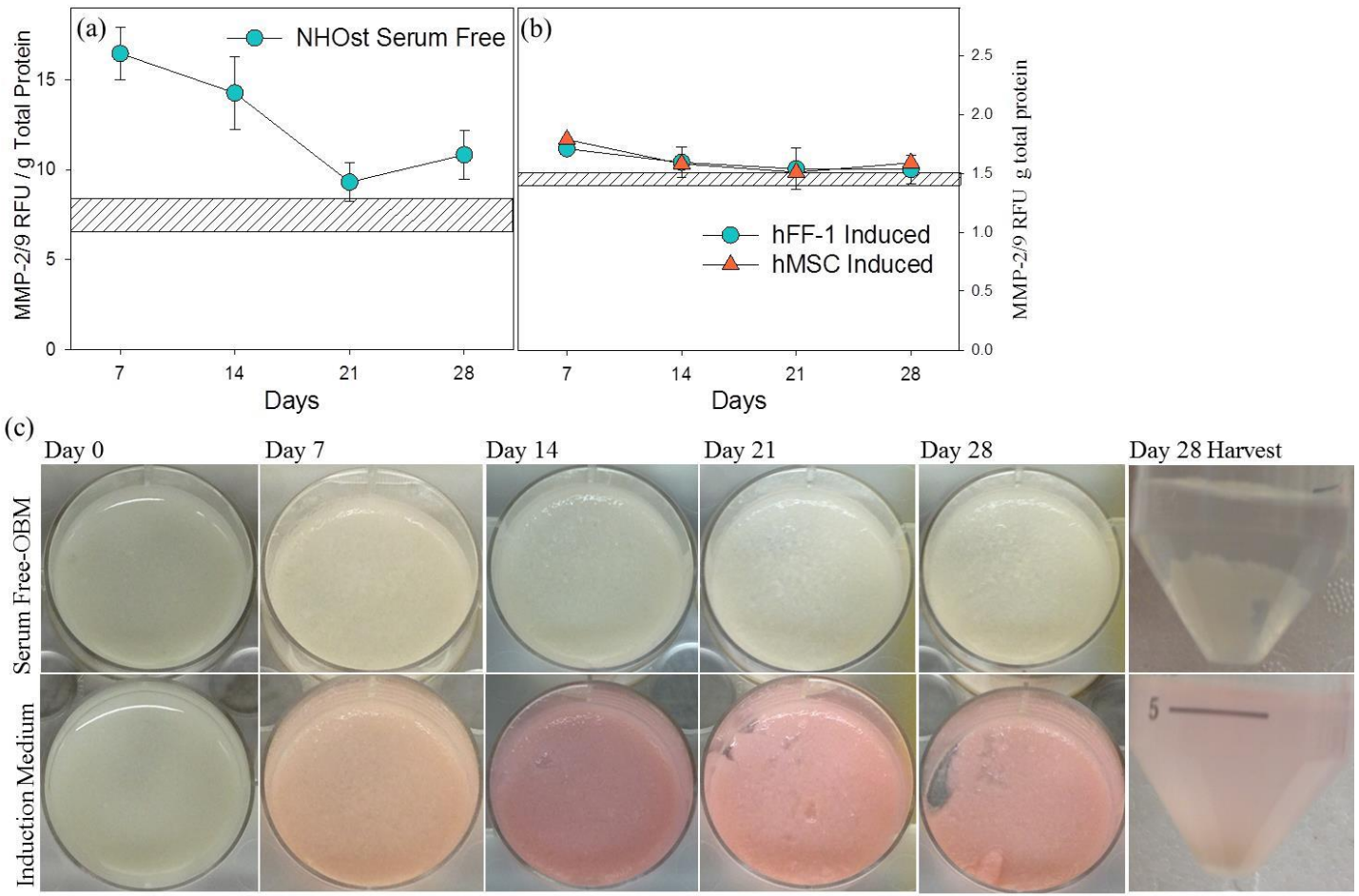

Figure 5.5. MMP-2/MMP-9 secretion into the medium. (a) Osteoblast control. (b) hFF-1 induced and hMSC induced. Rectangular box corresponds to activity present in fresh medium. (c) Photographs showing the stability of the hydrogel in two different media.

5.4. DISCUSSION

In this study, we investigated the effect of soluble factors and environmental effects on differentiation of mature hFF-1s into osteoblasts. However, osteogenic differentiation can be initiated from one or a combination of chemical (Majumdar, 2001; Sila-Asna et al., 2007), environmental (Koo et al., 2014), magnetic/electrical (Lohmann et al., 2000; Tsai et al., 2009), and mechanical (32, 33) stimuli; we used chemical stimulus of a well-known and used medium concoction. The inductive signals known and used to influence osteogenic differentiation are dexamethasone, ascorbate, and β-glycerophosphate (Czekanska et al., 2012; Kaveh, 2011). Each condition was cultured on 2D tissue culture plastic (TCPS) and in a hydrogel designed with similarities to calcified articular cartilage and bone for a period of 28 days. Thereafter, the cells and tissues were harvested and assessed for differentiation using phenotypic and genetic analyses.

ALP has been widely used as a detector for early stages of osteogenic differentiation and mineralization in the extracellular matrix. Examining each of the conditions, the hFF-1 control displayed no ALP activity as expected. Alternatively, the induced hFF-1s showed increased ALP expression similar to induced hMSCs and the NHOsts. The induced hFF-1s exhibit a reduction in expression beginning on day 14, which is consistent with osteoblast-like cells in other reports (Czekanska et al., 2012; Frohbergh et al., 2012). This reduction may indicate cellular maturation into the osteogenic lineage (Frohbergh et al., 2012). The ALP activity in the NHOst control had no statistically significant changes throughout the 28 day period. This effect was also seen in 7F2 cells cultured under similar conditions (Frohbergh et al., 2012). Alternatively, the induced hMSCs exhibited a continual increase of expression of the culture period, peaking at day 28 similar with other reports (Peter et al., 2000). Similar to cultures on 2D TCPS, the induced hFF-1s in the 3D hydrogels followed a similar trend and displayed significant increases in ALP content from the hFF-1 control. This suggests the cells in the 3D hydrogel respond similarly to the chemical stimulus. Alternatively, the serum free NHOst conditions exhibited no ALP

activity on the 2D TCPS and a gradual decline in ALP activity in 3D hydrogel condition during the culture period. A similar decline was also observed in the MMP activity for the NHOst hydrogel cultures. This decline in ALP and MMP activity may be due to the progression of cell death over the culture period similarly observed in the micrographs. This is expected as the hydrogels do not contain a vascular system to constantly supply nutrients to the osteoblast similar to bone tissue.

To understand the effects of chemical stimulation on the fibroblastic plasticity, osteogenic genes transcribed during differentiation were assessed. Multiple changes in gene expression occur during osteogenic differentiation. At the early stages of the endochondral ossification process, the genes *SOX9* (Gentili & Cancedda, 2009; Majumdar, 2001), *COL10A1* (Gentili & Cancedda, 2009; Richardson et al., 2010), and *RUNX2* (Ducy, 2000; Komori, 2010; Sila-Asna et al., 2007) are expressed. These genes, primarily *RUNX2*, activate the subsequent genes or transcription factors expressed in the early stages of osteogenesis, which are *ALPL* (Baylan et al., 2013; Kaveh, 2011; Richardson et al., 2010), *COL1A1* (Sila-Asna et al., 2007), *IBSP* (Sila-Asna et al., 2007), and *SPP1* (Frohbergh et al., 2012; Kaveh, 2011; Komori, 2006; Mostafa et al., 2011). At later stages of the differentiation process *BGLAP* (Ducy, 2000; Kaveh, 2011; Komori, 2010; Qi et al., 2003; Sila-Asna et al., 2007), *SPARC* (Czekanska et al., 2012; Frohbergh et al., 2012; Mostafa et al., 2011; Sila-Asna et al., 2007), and *SP7* (Komori, 2006) are expressed. Since the genetic analysis was performed at day 28, the induced hFF-1s could be entering the late stages of the osteogenic maturation as suggested by the reduced *ALPL* expression consistent with literature (Kaveh, 2011). Interestingly, the hFF-1 control lineage contained the gene *ALPL* but does not naturally have the influence to continue the complete formation of the enzyme exogenously, whereas, the induced hFF-1 condition experienced the exogenous ALP formation due to the influence by soluble factors as evidenced by the ALP assay. The late genes (*RUNX2*, *SP7*, *BGLAP*, and *SPARC*) of the induced hFF-1s follow a similar pathway to the breakdown time

analysis for the gene expression. Further, the hFF-1 induced and control conditions displayed significant differences in the earlier expressed genes (*ALPL*, *COL1A1*, and *SPP1*) suggesting the induced hFF-1 condition has transformed out of the fibroblastic lineage. These similarities of the induced hFF-1s to the NHOst control and deviations from the hFF-1 control suggest a genetic transformation into the osteogenic lineage. However, the exact pathway responsible for fibroblastic plasticity cannot be determined in this study since the genes necessary to determine certain pathways were not tested. Alternatively, the induced HepG2 displayed no similarities to the osteoblast control, suggesting no differentiation potential.

The physical environment used was a chitosan based hydrogel containing β-TCP and hyaluronic acid (Walker & Madihally, 2015). The lack in MMP activity in the induction cultures and the presence of the breakdown in the no cell hydrogel cultures suggests the cells were not responsible for the breakdown. The induction medium contained common constituents known to support differentiation such as dexamethasone, ascorbate, mesenchymal cell growth supplement (MCGS), and β-glycerophosphate (Kaveh, 2011). The differences in the media formulation used for inducing differentiation could have led to the stability issues of the hydrogel. The two main differences observed between osteoblast induction medium and other medium, which possibly causes the breakdown, were MCGS (serum) and β-glycerophosphate. Since β-glycerophosphate is used for hydrogel formation, the hydrogel could be oversaturated with the salt causing a pH imbalance resulting in precipitation of chitosan. Therefore, β-glycerophosphate was removed from the osteoblast induction medium; the β-glycerophosphate free osteoblast induction medium was used to test the chitosan precipitation theory and serum free OBM was used as a control. The earlier instability of the hydrogels suggests the stability issues were not due to β-glycerophosphate concentration but rather due to the presence of serum. MCGS may contain enzymes that could be leading to the instability of the hydrogels. Additionally, the hydrogels cultured with serum free OBM showed no instability issues, strengthening this theory. However,

further analysis of the MSGS constituents is necessary to better understand the mechanism.

5.5. CONCLUSIONS

In summary, we present the efficacy of differentiating hFF-1s into the osteogenic lineage using chemical factors alone. The induced fibroblasts show many similarities to the NHOst control from a phenotypic and genotypic standpoint. The induced fibroblasts also showed considerable deviations from the fibroblast control at the genetic level. Although the exact cellular signaling pathways were not studied at earlier time points during induction, this study suggests that mature cells could play a role in the regenerative process apart from stem cells.

5.6. ACKNOWLEDGEMENTS

Financial support was provided by the Edward Joullian Endowment. Authors would like to thank Mr. Curtis Andrew, Oklahoma Animal Disease and Diagnostic Laboratory (OADDL) for histological processing.

CHAPTER VI

CONCLUSIONS AND RECCOMENDATIONS

6.1. CONCLUSIONS

This research focused on the fundamental concepts of tissue engineering wherein cells interact with biocompatible 3D hydrogel scaffolds comparable to native cartilage ECM. The objectives sought in this study were i) construction of an anisotropic scaffold mimicking cartilage architecture and ECM, ii) *in vitro* chondrogenic induction of human foreskin fibroblasts via chemical and physical stimuli, iii) *in vitro* osteogenic induction of human foreskin fibroblasts via chemical and physical stimuli.

Scaffold architecture plays an important role in regulating cell-cell and cell-matrix interactions through signaling pathways provided by the cellular responses. Providing the proper chemical and physical environment can promote cell adhesion and proliferation, and ultimately regeneration of the tissue. However, if the essential physical and chemical characteristics are not in place, the signals necessary to control cellular fate may be arrested resulting in an undesirable outcome. The cell type capable of providing similar phenotypic and genotypic cues is also preferred to warrant the desired response. Some of the conclusions of the three studies follow.

6.1.1. Anisotropic chitosan-based hydrogels mimicking cartilage matrix

Chitosan-based hydrogels containing gelatin, HA and β-TCP were used to develop an anisotropic hydrogel, mimicking the various layers of cartilage matrix. All formulations were tested in

in vitro and *in vivo* environments and retained temperature sensitive gelation. The radial hydrogel exhibited elevated compressive strength relative to the superficial and calcified hydrogels. Increasing chitosan concentration was shown to increase mechanical, physical and rheological properties of the hydrogels. Structural integrity of the hydrogels was best supported in the radial and calcified hydrogels most likely due to the presence of HA. Compressive strength of the anisotropic hydrogel in the series orientation was observed to be the average of the isotropic hydrogels. When anisotropic hydrogel was tested in parallel orientation, the mechanical strength was observed to be much less than all hydrogels suggesting anisotropy. The hydrogels injected into the mouse model showed no changes in shape throughout the duration of the study suggesting stability and appeared intact in the injected area. Minimal macrophage invasion was observed in the radial and calcified hydrogels after five days inside the body. Similarities in micro-architecture were noticed in the *in vivo* and *in vitro* hydrogels.

6.1.2. Chondrogenic induction of fibroblasts in cartilage mimicking hydrogels

The superficial and radial hydrogels combined with chondrogenic induction medium were utilized as physical and chemical stimuli to induce chondrogenesis in fibroblasts (hFF-1) and hMSCs. Analysis of aggrecan content in the media revealed significant similarities between the hFF-1 and hMSC induction cultures. Further, phenotypic analysis of the cultures through morphological appearance and cartilage–specific protein presence showed fibroblast deviation from the native phenotype relating more closely to the chondrogenic phenotype. This was confirmed by the comparable aggrecan, collagen types I and II, and GAG content observed in both hydrogels' conditions (hFF-1 and hMSC) undergoing induction. This was more prevalent in the radial hydrogels as this condition was able to repress expression of collagen type I in the induction cultures. Genetic information through qPCR was to be tested; however, RNA isolation was not possible due to the low cell density. A methodical approach was incorporated to analyze the hydrogel systems in an attempt to successfully isolate RNA. None of the methods used were

able to successfully isolate any genetic material. However, the combination of the phenotypic observations is still suggestive of successful differentiation of the fibroblast line into the chondrogenic lineage; although more supportive evidence in the form of genetic profiling of the cartilage-specific genes is necessary to determine fibroblast plasticity.

6.1.3. Osteogenic induction of human foreskin fibroblasts for bone mineralization

Osteogenic induction medium was used to impress osteogenic induction upon a fibroblast lineage (hFF-1) because fibroblasts and osteoblasts share many genotypic and phenotypic similarities. After 28 days of culture, genotypic and phenoptyic alterations were observed in the induced hFF-1s and in many osteoblast-specific genes (RUNX2, BGLAP, SPP1, SP7, and SPARC) were more closely related to the osteoblastic lineage (NHOst). Further, at 28 days, the early osteogenic marker and highly expressed fibroblastic gene (COLIA1) was observed to be downregulated, which is more constant with mature osteoblasts. ALP content secreted into the media exhibited significant deviations between the hFF-1 control and induced hFF-1 conditions. The induced hFF-1s were observed to have no significant difference in ALP content with the induced hMSC and NHOst controls until the 28th day indicative of mature osteoblasts. These results convey a strong indication of the fibroblast plasticity into the osteogenic lineage. Osteogenic induction of the hFF-1s and hMSCs was also attempted using the induction medium with the calcified hydrogel. However, hydrogel dissociation occurred in the induced hydrogel cultures. Assessment of the dissociation suggested serum in the media concoction contained enzymes capable of degradation. Nodule formation was observed in small sections of the induced hydrogel cultures after 28 days via von Kossa staining.

6.2. RECOMMENDATIONS

6.2.1. Cell behavior to increased cell density in zonal hydrogels

Alterations in cellular phenotype and genotype were evaluated in this research. However, the cartilage-specific proteins exhibited small accumulations matrix formation. This could be due to the reduced cell density used for proof of concept. Increasing the cell density to a more widely used quantity or to physiologic conditions may activate an improved cellular response from increased cell-cell interactions from the reduced cellular network proximity. Additionally, this would allow for genetic material to escape from binding to the chitosan hydrogel and provide us the genetic information to fully assess chondrogenic induction of the fibroblast lineage. This would be very beneficial in understanding the regeneration capabilities and cellular responses of the resultant tissue formation

6.2.2. Exploration of cellular signaling pathways for induced hFF-1s

Genetic analyses were performed in this study but only to the extent of observing the specific chondrogenic and osteogenic genes. Alternatively, it would be beneficial to understand whether the fibroblasts follow the same signaling pathways as hMSCs using the same induction strategies. Signaling pathways for both chondrogenic (Mahmoudifar & Doran, 2012) and osteogenic (Robubi et al., 2014) differentiation of hMSCs has been studied previously displaying the essential genes needed to uncover the signaling pathways making fibroblast plasticity possible.

6.2.3. Study of cellular responses to load stresses in anisotropic hydrogel

Mechanical loads were addressed for each of the isotropic and anisotropic hydrogels; however, the mechanical load was not assessed while the hydrogels were embedded. In theory, the cells would secrete ECM proteins which would construct a physically durable tissue. Additionally, mechanical stresses are known to play a role in chondrogenesis and matrix assembly. Therefore,

cellular and mechanical responses to different load stresses should be explored since the hydrogel could experience this if used in a clinical setting. Mechanical stimulus has been performed on cartilage explants previously to study the mechano-electrochemical events occurring during loading (Mow et al., 1999).

6.2.4. Characterization of hydrogel degradation profile

Typically, implantable and injectable tissues are used for purposes of regenerating defective tissues. When a defect occurs, enzymes such as MMPs are produced to degrade the ECM proteins and participate in homeostasis. Therefore, the hydrogels would immediately experience an enzymatic environment when implanted or injected into the body. Inducing degradation using physiologic enzymes would be beneficial to study the structural competency of the physical and cellular networks as well as characterize the degradation profile.

6.2.5. *In vivo* evaluation of tissue growth in cell embedded hydrogels

In this research, the isotropic hydrogels were evaluated on the gelation characteristics, morphological similarities, and immune responses in an *in vivo* mouse model. This study provided invaluable information about the physical characteristics of each of the hydrogels. Yet, analysis of the tissue growth was not possible due to the type of model used and the lack of cells. Therefore, incorporation of an immuno-deficient model and cell embedded hydrogels will provide the environment necessary to assess tissue growth. Ultimately, learning the tissue ingrowth capabilities will give real world applicability to the hydrogels.

REFERENCES

(NIAMS), N. I. o. A. a. M. a. S. D. (2013). Osteoarthritis. Retrieved December 2014, 2014, from http://www.niams.nih.gov/Health_Info/Osteoarthritis/.

Ahmadi, R., & de Bruijn, J. D. (2008). Biocompatibility and gelation of chitosan-glycerol phosphate hydrogels. *J Biomed Mater Res A, 86*(3), 824-832. doi: 10.1002/jbm.a.31676.

Amosi, N., Zarzhitsky, S., Gilsohn, E., Salnikov, O., Monsonego-Ornan, E., Shahar, R., & Rapaport, H. (2012). Acidic peptide hydrogel scaffolds enhance calcium phosphate mineral turnover into bone tissue. *Acta Biomater, 8*(7), 2466-2475. doi: 10.1016/j.actbio.2012.04.003.

Apostolou, E., & Hochedlinger, K. (2011). Stem cells: iPS cells under attack. *Nature, 474*(7350), 165-166. doi: 10.1038/474165a.

Association, A. H. (2013). Heart disease and stroke continue to threaten U.S. health: American Heart Association Annual Statistical Update. Retrieved December 2014, 2014, from http://newsroom.heart.org/news/heart-disease-and-stroke-continue-to-threaten-u-s-health.

Aydelotte, M. B., Greenhill, R. R., & Kuettner, K. E. (1988). Differences between sub-populations of cultured bovine articular chondrocytes, II. Proteoglycan metabolism. *Connective Tissue Research, 18*(3), 223-234.

Aydelotte, M. B., & Kuettner, K. E. (1988). Differences between sub-populations of cultured bovine articular chondrocytes, I. morphology and cartilage matrix production. *Connective Tissue Research, 18*(3), 205-222.

Bae, J. S., Gutierrez, S., Narla, R., Pratap, J., Devados, R., van Wijnen, A. J., . . . Javed, A. (2007). Reconstitution of Runx2/Cbfa1-null cells identifies a requirement for BMP2 signaling through a Runx2 functional domain during osteoblast differentiation. *J Cell Biochem, 100*(2), 434-449. doi: 10.1002/jcb.21039.

Banzon, M. T. (2009). Total Knee Replacement ... or Not? Retrieved November 2010, 2010, from http://advancedorthosports.com/Documents/News/aosmi_pr06232009-2.pdf.

Barry, F., Boynton, R. E., Liu, B., & Murphy, J. M. (2001). Chondrogenic differentiation of mesenchymal stem cells from bone marrow: differentiation-dependent gene expression of matrix components. *Exp Cell Res, 268*(2), 189-200. doi: 10.1006/excr.2001.5278.

Baylan, N., Bhat, S., Ditto, M., Lawrence, J. G., Lecka-Czernik, B., & Yildirim-Ayan, E. (2013). Polycaprolactone nanofiber interspersed collagen type-I scaffold for bone regeneration: a unique injectable osteogenic scaffold. *Biomed Mater, 8*(4), 045011. doi: 10.1088/1748-6041/8/4/045011.

Bellucci, G., & Seedhom, B. B. (2001). Mechanical behaviour of articular cartilage under tensile cyclic load. *Rheumatology (Oxford), 40*(12), 1337-1345.

Bertagnoli, R., Sabatino, C. T., Edwards, J. T., Gontarz, G. A., Prewett, A., & Parsons, J. R. (2005). Mechanical testing of a novel hydrogel nucleus replacement implant. *The Spine Journal, 5*(6), 672-681. doi: 10.1016/j.spinee.2004.12.004.

Bhosale, A. M., & Richardson, J. B. (2008). Articular cartilage: structure, injuries and review of management. (1471-8391 (Electronic)).

Blasi, A., Martino, C., Balducci, L., Saldarelli, M., Soleti, A., Navone, S. E., . . . Alessandri, G. (2011). Dermal fibroblasts display similar phenotypic and differentiation capacity to fat-derived mesenchymal stem cells, but differ in anti-inflammatory and angiogenic potential. *Vasc Cell, 3*(1), 5. doi: 10.1186/2045-824X-3-5.

Bobick, B. E., Chen, F. H., Le, A. M., & Tuan, R. S. (2009). Regulation of the chondrogenic phenotype in culture. *Birth Defects Research Part C: Embryo Today: Reviews, 87*(4), 351-371. doi: 10.1002/bdrc.20167.

Borges, A. C., Bourban, P. E., Pioletti, D. P., & Månson, J. A. E. (2010). Curing kinetics and mechanical properties of a composite hydrogel for the replacement of the nucleus pulposus. *Composites Science and Technology, 70*(13), 1847-1853. doi: 10.1016/j.compscitech.2010.07.018.

Burdick, J. A., Peterson, A. J., & Anseth, K. S. (2001). Conversion and temperature profiles during the photoinitiated polymerization of thick orthopaedic biomaterials. *Biomaterials, 22*(13), 1779-1786. doi: 10.1016/s0142-9612(00)00347-1.

Burdick, J. A., & Prestwich, G. D. (2011). Hyaluronic acid hydrogels for biomedical applications. *Adv Mater, 23*(12), H41-56. doi: 10.1002/adma.201003963.

Carrion, B., Janson, I. A., Kong, Y. P., & Putnam, A. J. (2014). A safe and efficient method to retrieve mesenchymal stem cells from three-dimensional fibrin gels. *Tissue Eng Part C Methods, 20*(3), 252-263. doi: 10.1089/ten.TEC.2013.0051.

Center, J. H. A. (2012). Role of Body Weight in Osteoarthritis. Retrieved December 2014, 2014, from http://www.hopkinsarthritis.org/patient-corner/disease-management/role-of-body-weight-in-osteoarthritis/#obesity.

Chen, G., Deng, C., & Li, Y. P. (2012). TGF-beta and BMP signaling in osteoblast differentiation and bone formation. *Int J Biol Sci, 8*(2), 272-288. doi: 10.7150/ijbs.2929.

Cheng, Y. H., Yang Sh Fau - Su, W.-Y., Su Wy Fau - Chen, Y.-C., Chen Yc Fau - Yang, K.-C., Yang Kc Fau - Cheng, W. T.-K., Cheng Wt Fau - Wu, S.-C., . . . Lin, F. H. (2010). Thermosensitive chitosan-gelatin-glycerol phosphate hydrogels as a cell carrier for nucleus pulposus regeneration: an in vitro study. (1937-335X (Electronic)).

Cheng, Y. H., Yang, S. H., & Lin, F. H. (2011). Thermosensitive chitosan-gelatin-glycerol phosphate hydrogel as a controlled release system of ferulic acid for nucleus pulposus regeneration. *Biomaterials, 32*(29), 6953-6961. doi: 10.1016/j.biomaterials.2011.03.065.

Chenite, A., Buschmann, M., Wang, D., Chaput, C., & Kandani, N. (2001). Rheological characterisation of thermogelling chitosan/glycerol-phosphate solutions. *Carbohydrate Polymers, 46*(1), 39-47. doi: 10.1016/S0144-8617(00)00281-2.

Chenite, A., Chaput C Fau - Wang, D., Wang D Fau - Combes, C., Combes C Fau - Buschmann, M. D., Buschmann Md Fau - Hoemann, C. D., Hoemann Cd Fau - Leroux, J. C., . . . Selmani, A. (2000). Novel injectable neutral solutions of chitosan form biodegradable gels in situ. (0142-9612 (Print)).

Cho, J., Heuzey, M. C., Begin, A., & Carreau, P. J. (2005). Physical gelation of chitosan in the presence of beta-glycerophosphate: the effect of temperature. *Biomacromolecules, 6*(6), 3267-3275. doi: 10.1021/bm050313s.

Czekanska, E. M., Stoddart, M. J., Richards, R. G., & Hayes, J. S. (2012). In search of an osteoblast cell model for in vitro research. *Eur Cell Mater, 24*, 1-17.

Daily, S. (2013). Knee replacement surgery may lead to weight gain. Retrieved December 2014, 2014, from http://www.sciencedaily.com/releases/2013/01/130114153428.htm.

Dalle Carbonare, L., Innamorati, G., & Valenti, M. T. (2012). Transcription factor Runx2 and its application to bone tissue engineering. *Stem Cell Rev, 8*(3), 891-897. doi: 10.1007/s12015-011-9337-4.

Danisovic, L., Varga, I., & Polak, S. (2012). Growth factors and chondrogenic differentiation of mesenchymal stem cells. *Tissue Cell, 44*(2), 69-73. doi: 10.1016/j.tice.2011.11.005.

Das, S., Pati, F., Chameettachal, S., Pahwa, S., Ray, A. R., Dhara, S., & Ghosh, S. (2013). Enhanced redifferentiation of chondrocytes on microperiodic silk/gelatin scaffolds: toward tailor-made tissue engineering. *Biomacromolecules, 14*(2), 311-321. doi: 10.1021/bm301193t.

de Crombrugghe, B., Lefebvre, V., & Nakashima, K. (2001). Regulatory mechanisms in the pathways of cartilage and bone formation. *Curr Opin Cell Biol, 13*(6), 721-727.

Declercq, H., Van den Vreken, N., De Maeyer, E., Verbeeck, R., Schacht, E., De Ridder, L., & Cornelissen, M. (2004). Isolation, proliferation and differentiation of osteoblastic cells to study cell/biomaterial interactions: comparison of different isolation techniques and source. *Biomaterials, 25*(5), 757-768.

Dehne, T., Schenk, R., Perka, C., Morawietz, L., Pruss, A., Sittinger, M., . . . Ringe, J. (2010). Gene expression profiling of primary human articular chondrocytes in high-density micromasses reveals patterns of recovery, maintenance, re- and dedifferentiation. *Gene, 462*(1-2), 8-17. doi: 10.1016/j.gene.2010.04.006.

Di Martino, A., Sittinger, M., & Risbud, M. V. (2005). Chitosan: a versatile biopolymer for orthopaedic tissue-engineering. *Biomaterials, 26*(30), 5983-5990. doi: 10.1016/j.biomaterials.2005.03.016.

Diekman, B. O., Estes, B. T., & Guilak, F. (2010). The effects of BMP6 overexpression on adipose stem cell chondrogenesis: Interactions with dexamethasone and exogenous growth factors. *Journal of Biomedical Materials Research Part A, 93A*(3), 994-1003. doi: 10.1002/jbm.a.32589.

Discher, D. E., Janmey, P., & Wang, Y.-l. (2005). Tissue Cells Feel and Respond to the Stiffness of Their Substrate. *Science, 310*(5751), 1139-1143. doi: 10.1126/science.1116995.

Dolatshahi-Pirouz, A., Nikkhah, M., Gaharwar, A. K., Hashmi, B., Guermani, E., Aliabadi, H., . . . Khademhosseini, A. (2014). A combinatorial cell-laden gel microarray for inducing osteogenic differentiation of human mesenchymal stem cells. *Sci Rep, 4*, 3896. doi: 10.1038/srep03896.

Du, M., Liang, H., Mou, C., Li, X., Sun, J., Zhuang, Y., . . . Dai, J. (2014). Regulation of human mesenchymal stem cells differentiation into chondrocytes in extracellular matrix-based hydrogel scaffolds. *Colloids Surf B Biointerfaces, 114*, 316-323. doi: 10.1016/j.colsurfb.2013.10.001.

Ducy, P. (2000). The Osteoblast: A Sophisticated Fibroblast under Central Surveillance. *Science, 289*(5484), 1501-1504. doi: 10.1126/science.289.5484.1501.

Elisseeff, J., McIntosh, W., Anseth, K., Riley, S., Ragan, P., & Langer, R. (2000). Photoencapsulation of chondrocytes in poly(ethylene oxide)-based semi-interpenetrating networks. *J Biomed Mater Res, 51*(2), 164-171.

Elisseeff, J. H. Repairing Knee Joints by Growing New Cartilage Using an Injectable Hydrogel. Retrieved December 2010, 2010, from http://www.datlof.com/8Axamal/docs/Marketing/jhu/JE/index.htm.

Eyre, D. (2002). Collagen of articular cartilage. *Arthritis Res, 4*(1), 30-35.

Fan, H., Zhang C Fau - Li, J., Li J Fau - Bi, L., Bi L Fau - Qin, L., Qin L Fau - Wu, H., Wu H Fau - Hu, Y., & Hu, Y. (2008). Gelatin microspheres containing TGF-beta3 enhance the chondrogenesis of mesenchymal stem cells in modified pellet culture. (1526-4602 (Electronic)).

Federation, W. H. Obesity. Retrieved December 2014, 2014, from http://www.world-heart-federation.org/cardiovascular-health/cardiovascular-disease-risk-factors/obesity/.

Foundation, A. Osteoarthritis and Obesity: More than just overloading joints, obesity can lead to fat cells taking aim at joints. Retrieved December 2014, 2014, from http://www.arthritistoday.org/about-arthritis/types-of-arthritis/osteoarthritis/who-gets-oa-and-why/osteoarthritis-and-obesity.php.

Fox, A. J. S., Bedi, A., & Rodeo, S. A. (2009). The Basic Science of Articular Cartilage: Structure, Composition, and Function. *Sports Health: A Multidisciplinary Approach, 1*(6), 461-468. doi: 10.1177/1941738109350438.

Franceschi, R. T., & Xiao, G. (2003). Regulation of the osteoblast-specific transcription factor, Runx2: responsiveness to multiple signal transduction pathways. *J Cell Biochem, 88*(3), 446-454. doi: 10.1002/jcb.10369.

Fritz, J. R., Pelaez, D., & Cheung, H. S. (2009). Current Challenges in Cartilage Tissue Engineering: A Review of Current Cellular-Based Therapies. *Current Rheumatology Reviews, 5*(1), 8-14.

Frohbergh, M. E., Katsman, A., Botta, G. P., Lazarovici, P., Schauer, C. L., Wegst, U. G., & Lelkes, P. I. (2012). Electrospun hydroxyapatite-containing chitosan nanofibers crosslinked with genipin for bone tissue engineering. *Biomaterials, 33*(36), 9167-9178. doi: 10.1016/j.biomaterials.2012.09.009.

Gentili, C., & Cancedda, R. (2009). Cartilage and Bone Extracellular Matrix. *Current Pharmaceutical Design, 15*(12), 1334-1348. doi: 10.2174/138161209787846739.

Goldring, M. B. (2012). Chondrogenesis, chondrocyte differentiation, and articular cartilage metabolism in health and osteoarthritis. *Ther Adv Musculoskelet Dis, 4*(4), 269-285. doi: 10.1177/1759720X12448454.

Goldring, M. B., Tsuchimochi, K., & Ijiri, K. (2006). The control of chondrogenesis. *Journal of Cellular Biochemistry, 97*(1), 33-44. doi: 10.1002/jcb.20652.

Gong, G., Ferrari, D., Dealy, C. N., & Kosher, R. A. (2010). Direct and progressive differentiation of human embryonic stem cells into the chondrogenic lineage. *Journal of Cellular Physiology, 224*(3), 664-671. doi: 10.1002/jcp.22166.

Gong, G., Ferrari, D., Dealy, C. N., & Kosher, R. A. (2010). Direct and progressive differentiation of human embryonic stem cells into the chondrogenic lineage. *J Cell Physiol*. doi: 10.1002/jcp.22166 [doi].

Grogan, S. P., Barbero, A., Diaz-Romero, J., Cleton-Jansen, A.-M., Soeder, S., Whiteside, R., . . . Mainil-Varlet, P. (2007). Identification of markers to characterize and sort human articular chondrocytes with enhanced in vitro chondrogenic capacity. *Arthritis & Rheumatism, 56*(2), 586-595. doi: 10.1002/art.22408.

Guweidhi, A., Kleeff, J., Adwan, H., Giese, N. A., Wente, M. N., Giese, T., . . . Friess, H. (2005). Osteonectin influences growth and invasion of pancreatic cancer cells. *Ann Surg, 242*(2), 224-234.

Health, N. I. o. (2012). A View of the U.S. Obesity Epidemic. Retrieved December 2014, 2014, from http://directorsblog.nih.gov/tag/epidemic/.

Healthline. (2012a). Knee Replacement & Your State of Mind. Retrieved December 2014, 2014, from http://www.healthline.com/health/total-knee-replacement-surgery/insomnia-depression.

Healthline. (2012c). Knee Replacement Statistics Infographic. Retrieved December 2014, 2014, from http://www.healthline.com/health/total-knee-replacement-surgery/statistics-infographic.

Healthline. (2012e). Risks and Complications of Total Knee Replacement Surgery. Retrieved December 2014, 2014, from http://www.healthline.com/health/total-knee-replacement-surgery/risks-complications#4.

Healthline. (2012g). Understanding Knee Replacement Costs: What's On the Bill? Retrieved December 2014, 2014, from http://www.healthline.com/health/total-knee-replacement-surgery/understanding-costs#2.

Heywood, H. K., Knight, M. M., & Lee, D. A. (2010). Both superficial and deep zone articular chondrocyte subpopulations exhibit the Crabtree effect but have different basal oxygen consumption rates. *J Cell Physiol, 223*(3), 630-639. doi: 10.1002/jcp.22061.

Hoang, Q. Q., Sicheri, F., Howard, A. J., & Yang, D. S. (2003). Bone recognition mechanism of porcine osteocalcin from crystal structure. *Nature, 425*(6961), 977-980. doi: 10.1038/nature02079.

Hollister, S. J., & Lin, C. Y. (2007). Computational design of tissue engineering scaffolds. *Computer Methods in Applied Mechanics and Engineering, 196*(31–32), 2991-2998. doi: http://dx.doi.org/10.1016/j.cma.2006.09.023.

Hong, S. H., Lu, X., Nanes, M. S., & Mitchell, J. (2009). Regulation of osterix (Osx, Sp7) and the Osx promoter by parathyroid hormone in osteoblasts. *J Mol Endocrinol, 43*(5), 197-207. doi: 10.1677/JME-09-0012.

Hootman, J. M., & Helmick, C. G. (2006). Projections of US prevalence of arthritis and associated activity limitations. *Arthritis Rheum, 54*(1), 226-229. doi: 10.1002/art.21562.

Huang, H., Zhang, X., Hu, X., Dai, L., Zhu, J., Man, Z., . . . Ao, Y. (2014). Directing chondrogenic differentiation of mesenchymal stem cells with a solid-supported chitosan thermogel for cartilage tissue engineering. *Biomed Mater, 9*(3), 035008. doi: 10.1088/1748-6041/9/3/035008.

Huang, P., He, Z., Ji, S., Sun, H., Xiang, D., Liu, C., . . . Hui, L. (2011). Induction of functional hepatocyte-like cells from mouse fibroblasts by defined factors. *Nature, 475*(7356), 386-389. doi: 10.1038/nature10116.

Huang, Y., Onyeri, S., Siewe, M., Moshfeghian, A., & Madihally, S. V. (2005). In vitro characterization of chitosan–gelatin scaffolds for tissue engineering. *Biomaterials, 26*(36), 7616-7627. doi: 10.1016/j.biomaterials.2005.05.036.

Hunter, G. K., & Goldberg, H. A. (1993). Nucleation of hydroxyapatite by bone sialoprotein. *Proc Natl Acad Sci U S A, 90*(18), 8562-8565.

Idelevich, A., Rais, Y., & Monsonego-Ornan, E. (2011). Bone Gla protein increases HIF-1alpha-dependent glucose metabolism and induces cartilage and vascular calcification. *Arterioscler Thromb Vasc Biol, 31*(9), e55-71. doi: 10.1161/ATVBAHA.111.230904.

Innocentini, M. D. M., Salvini, V. R., Macedo, A., & Pandolfelli, V. C. (1999). Prediction of ceramic foams permeability using Ergun's equation. *Materials Research, 2*, 283-289.

Ivarsson, M., McWhirter, A., Borg, T. K., & Rubin, K. (1998). Type I collagen synthesis in cultured human fibroblasts: regulation by cell spreading, platelet-derived growth factor and interactions with collagen fibers. *Matrix Biol, 16*(7), 409-425.

Ivaska, K. K., Hentunen, T. A., Vaaraniemi, J., Ylipahkala, H., Pettersson, K., & Vaananen, H. K. (2004). Release of intact and fragmented osteocalcin molecules from bone matrix during bone resorption in vitro. *J Biol Chem, 279*(18), 18361-18369. doi: 10.1074/jbc.M314324200.

Iyer, P., Walker, K. J., & Madihally, S. V. (2012). Increased matrix synthesis by fibroblasts with decreased proliferation on synthetic chitosan–gelatin porous structures. *Biotechnology and Bioengineering, 109*(5), 1314-1325. doi: 10.1002/bit.24396.

Jin, R., Moreira Teixeira, L. S., Dijkstra, P. J., Karperien, M., van Blitterswijk, C. A., Zhong, Z. Y., & Feijen, J. (2009). Injectable chitosan-based hydrogels for cartilage tissue engineering. *Biomaterials, 30*(13), 2544-2551. doi: 10.1016/j.biomaterials.2009.01.020.

Kalyanam, S., Yapp Rd Fau - Insana, M. F., & Insana, M. F. (2009). Poro-viscoelastic behavior of gelatin hydrogels under compression-implications for bioelasticity imaging. (0148-0731 (Print)).

Kapustin, A. N., & Shanahan, C. M. (2011). Osteocalcin: a novel vascular metabolic and osteoinductive factor? *Arterioscler Thromb Vasc Biol, 31*(10), 2169-2171. doi: 10.1161/ATVBAHA.111.233601.

Kaveh, K., Rashid Ibrahim , Md. Zuki Abu Bakar and Tengku Azmi Ibrahim. (2011). Mesenchymal Stem Cells, Osteogenic Lineage and Bone Tissue Engineering: A Review. *Journal of Animal and Veterinary Advances, 10*(17), 2317-2330. doi: 10.3923/javaa.2011.2317.2330.

Kawakami, T., Antoh, M., Hasegawa, H., Yamagishi, T., Ito, M., & Eda, S. (1992). Experimental study on osteoconductive properties of a chitosan-bonded hydroxyapatite self-hardening paste. *Biomaterials, 13*(11), 759-763.

Kevorkian, L., Young, D. A., Darrah, C., Donell, S. T., Shepstone, L., Porter, S., . . . Clark, I. M. (2004). Expression profiling of metalloproteinases and their inhibitors in cartilage. *Arthritis & Rheumatism, 50*(1), 131-141. doi: 10.1002/art.11433.

Kim, T. K., Sharma, B., Williams, C. G., Ruffner, M. A., Malik, A., McFarland, E. G., & Elisseeff, J. H. (2003). Experimental Model for Cartilage Tissue Engineering to Regenerate the Zonal Organization of Articular Cartilage☆. *Osteoarthritis and Cartilage, 11*(9), 653-664. doi: 10.1016/s1063-4584(03)00120-1.

Klangjorhor, J., Nimkingratana, P., Settakorn, J., Pruksakorn, D., Leerapun, T., Arpornchayanon, O., . . . Pothacharoen, P. (2012). Hyaluronan production and chondrogenic properties of primary human chondrocyte on gelatin based hematostatic spongostan scaffold. *J Orthop Surg Res, 7*, 40. doi: 10.1186/1749-799X-7-40.

Klein, T. J., Chaudhry, M., Bae, W. C., & Sah, R. L. (2007). Depth-dependent biomechanical and biochemical properties of fetal, newborn, and tissue-engineered articular cartilage. *Journal of Biomechanics, 40*(1), 182-190. doi: 10.1016/j.jbiomech.2005.11.002.

Kloxin, A. M., Kasko, A. M., Salinas, C. N., & Anseth, K. S. (2009). Photodegradable hydrogels for dynamic tuning of physical and chemical properties. *Science, 324*(5923), 59-63. doi: 10.1126/science.1169494.

Kock, L., van Donkelaar, C. C., & Ito, K. (2012). Tissue engineering of functional articular cartilage: the current status. *Cell Tissue Res, 347*(3), 613-627. doi: 10.1007/s00441-011-1243-1.

Komori, T. (2006). Regulation of osteoblast differentiation by transcription factors. *J Cell Biochem, 99*(5), 1233-1239. doi: 10.1002/jcb.20958.

Komori, T. (2010). Regulation of osteoblast differentiation by Runx2. *Adv Exp Med Biol, 658*, 43-49. doi: 10.1007/978-1-4419-1050-9_5.

Koo, K. T., Lee, S. W., Lee, M. H., Kim, K. H., Jung, S. H., & Kang, Y. G. (2014). Time-dependent expression of osteoblast marker genes in human primary cells cultured on microgrooved titanium substrata. *Clin Oral Implants Res, 25*(6), 714-722. doi: 10.1111/clr.12131.

Kruger, T. E., Miller, A. H., & Wang, J. (2013). Collagen scaffolds in bone sialoprotein-mediated bone regeneration. *ScientificWorldJournal, 2013*, 812718. doi: 10.1155/2013/812718.

Kuo, C. K., & Ma, P. X. (2001). Ionically crosslinked alginate hydrogels as scaffolds for tissue engineering: Part 1. Structure, gelation rate and mechanical properties. *Biomaterials, 22*(6), 511-521. doi: 10.1016/s0142-9612(00)00201-5.

Langer, R., & Vacanti, J. (1993). Tissue engineering. *Science, 260*(5110), 920-926. doi: 10.1126/science.8493529.

Lavertu, M., Filion, D., & Buschmann, M. D. (2008). Heat-induced transfer of protons from chitosan to glycerol phosphate produces chitosan precipitation and gelation. *Biomacromolecules, 9*(2), 640-650. doi: 10.1021/bm700745d.

Lawrence, B. J., & Madihally, S. V. (2008). Cell colonization in degradable 3D porous matrices. *Cell Adhesion & Migration, 2*(1), 9-16.

Lee, H. H., Chang, C. C., Shieh, M. J., Wang, J. P., Chen, Y. T., Young, T. H., & Hung, S. C. (2013). Hypoxia enhances chondrogenesis and prevents terminal differentiation through PI3K/Akt/FoxO dependent anti-apoptotic effect. *Sci Rep, 3*, 2683. doi: 10.1038/srep02683.

Lee, H. J., Yu, C., Chansakul, T., Varghese, S., Hwang, N. S., & Elisseeff, J. H. (2008). Enhanced chondrogenic differentiation of embryonic stem cells by coculture with hepatic cells. *Stem Cells Dev, 17*(3), 555-563. doi: 10.1089/scd.2007.0177.

Lee, K. Y., & Mooney, D. J. (2001). Hydrogels for Tissue Engineering. *Chemical Reviews, 101*(7), 1869-1880. doi: 10.1021/cr000108x.

Lee, N. K., Sowa, H., Hinoi, E., Ferron, M., Ahn, J. D., Confavreux, C., . . . Karsenty, G. (2007). Endocrine regulation of energy metabolism by the skeleton. *Cell, 130*(3), 456-469. doi: 10.1016/j.cell.2007.05.047.

Li, Y., Rodrigues, J., & Tomas, H. (2012). Injectable and biodegradable hydrogels: gelation, biodegradation and biomedical applications. *Chem Soc Rev, 41*(6), 2193-2221. doi: 10.1039/c1cs15203c.

Liu, H., Mao, J., Yao, K., Yang, G., Cui, L., & Cao, Y. (2004). A study on a chitosan-gelatin-hyaluronic acid scaffold as artificial skin in vitro and its tissue engineering applications. *Journal of Biomaterials Science, Polymer Edition, 15*(1), 25-40. doi: 10.1163/156856204322752219.

Lohmann, C. H., Schwartz Z Fau - Liu, Y., Liu Y Fau - Guerkov, H., Guerkov H Fau - Dean, D. D., Dean Dd Fau - Simon, B., Simon B Fau - Boyan, B. D., & Boyan, B. D. (2000). Pulsed electromagnetic field stimulation of MG63 osteoblast-like cells affects differentiation and local factor production. (0736-0266 (Print)).

Lowry, W. E., Richter, L., Yachechko, R., Pyle, A. D., Tchieu, J., Sridharan, R., . . . Plath, K. (2008). Generation of human induced pluripotent stem cells from dermal fibroblasts. *Proceedings of the National Academy of Sciences, 105*(8), 2883-2888. doi: 10.1073/pnas.0711983105.

Lozito, T. P., & Tuan, R. S. (2011). Mesenchymal stem cells inhibit both endogenous and exogenous MMPs via secreted TIMPs. *Journal of Cellular Physiology, 226*(2), 385-396. doi: 10.1002/jcp.22344.

Ma, P. L., Lavertu, M., Winnik, F. M., & Buschmann, M. D. (2009). New insights into chitosan-DNA interactions using isothermal titration microcalorimetry. *Biomacromolecules, 10*(6), 1490-1499. doi: 10.1021/bm900097s.

Mahmoudifar, N., & Doran, P. M. (2012). Chondrogenesis and cartilage tissue engineering: the longer road to technology development. *Trends Biotechnol, 30*(3), 166-176. doi: 10.1016/j.tibtech.2011.09.002.

Majumdar, M. K., Wang, E. and Morris, E. A. (2001). BMP-2 and BMP-9 promotes chondrogenic differentiation of human multipotential mesenchymal cells and overcomes the inhibitory effect of IL-1. *J. Cell. Physiol., 189*(3), 275-284. doi: 10.1002/jcp.10025.

Makowski, G. S., & Ramsby, M. L. (1998). Identification and partial characterization of three calcium- and zinc-independent gelatinases constitutively present in human circulation. *IUBMB Life, 46*(5), 1043-1053. doi: 10.1080/15216549800204592.

Mann, B. K., Gobin, A. S., Tsai, A. T., Schmedlen, R. H., & West, J. L. (2001). Smooth muscle cell growth in photopolymerized hydrogels with cell adhesive and proteolytically degradable domains: synthetic ECM analogs for tissue engineering. *Biomaterials, 22*(22), 3045-3051. doi: 10.1016/s0142-9612(01)00051-5.

Matsubara, T., Kida, K., Yamaguchi, A., Hata, K., Ichida, F., Meguro, H., . . . Yoneda, T. (2008). BMP2 regulates Osterix through Msx2 and Runx2 during osteoblast differentiation. *J Biol Chem, 283*(43), 29119-29125. doi: 10.1074/jbc.M801774200.

Mauney, J. R., Sjostorm S Fau - Blumberg, J., Blumberg J Fau - Horan, R., Horan R Fau - O'Leary, J. P., O'Leary Jp Fau - Vunjak-Novakovic, G., Vunjak-Novakovic G Fau - Volloch, V., . . . Kaplan, D. L. (2004). Mechanical stimulation promotes osteogenic differentiation of human bone marrow stromal cells on 3-D partially demineralized bone scaffolds in vitro. (0171-967X (Print)).

Mayr, H. O., Klehm, J., Schwan, S., Hube, R., Südkamp, N. P., Niemeyer, P., . . . Bernstein, A. (2013). Microporous calcium phosphate ceramics as tissue engineering scaffolds for the repair of osteochondral defects: Biomechanical results. *Acta Biomaterialia, 9*(1), 4845-4855. doi: http://dx.doi.org/10.1016/j.actbio.2012.07.040.

Meissner, A., Wernig, M., & Jaenisch, R. (2007). Direct reprogramming of genetically unmodified fibroblasts into pluripotent stem cells. *Nat Biotech, 25*(10), 1177-1181. doi: http://www.nature.com/nbt/journal/v25/n10/suppinfo/nbt1335_S1.html.

Monfort, J., Garcia-Giralt, N., Lopez-Armada, M. J., Monllau, J. C., Bonilla, A., Benito, P., & Blanco, F. J. (2006). Decreased metalloproteinase production as a response to mechanical pressure in human cartilage: a mechanism for homeostatic regulation. *Arthritis Res Ther, 8*(5), R149. doi: 10.1186/ar2042.

Mostafa, N. Z., Uludag, H., Varkey, M., Dederich, D. N., Doschak, M. R., & El-Bialy, T. H. (2011). In vitro osteogenic induction of human gingival fibroblasts for bone regeneration. *Open Dent J, 5*, 139-145. doi: 10.2174/1874210601105010139.

Mow, V. C., Wang, C. C., & Hung, C. T. (1999). The extracellular matrix, interstitial fluid and ions as a mechanical signal transducer in articular cartilage. *Osteoarthritis and Cartilage, 7*(1), 41-58. doi: 10.1053/joca.1998.0161.

Murphy, L., & Helmick, C. G. (2012). The impact of osteoarthritis in the United States: a population-health perspective. *Am J Nurs, 112*(3 Suppl 1), S13-19. doi: 10.1097/01.NAJ.0000412646.80054.21.

Nagase, H., & Kashiwagi, M. (2003). Aggrecanases and cartilage matrix degradation. *Arthritis Res Ther, 5*(2), 94 - 103.

Ng, K. W., Ateshian, G. A., & Hung, C. T. (2009). Zonal Chondrocytes Seeded in a Layered Agarose Hydrogel Create Engineered Cartilage with Depth-Dependent Cellular and Mechanical Inhomogeneity. *Tissue Engineering Part A, 15*(9), 2315-2324. doi: 10.1089/ten.tea.2008.0391.

Ngoenkam, J., Faikrua, A., Yasothornsrikul, S., & Viyoch, J. (2010). Potential of an injectable chitosan/starch/β-glycerol phosphate hydrogel for sustaining normal chondrocyte function. *International Journal of Pharmaceutics, 391*(1–2), 115-124. doi: 10.1016/j.ijpharm.2010.02.028.

Nguyen, L. H., Kudva, A. K., Saxena, N. S., & Roy, K. (2011). Engineering articular cartilage with spatially-varying matrix composition and mechanical properties from a single stem cell population using a multi-layered hydrogel. *Biomaterials, 32*(29), 6946-6952. doi: 10.1016/j.biomaterials.2011.06.014.

Nishimura, R., Wakabayashi, M., Hata, K., Matsubara, T., Honma, S., Wakisaka, S., . . . Yoneda, T. (2012). Osterix regulates calcification and degradation of chondrogenic matrices through matrix metalloproteinase 13 (MMP13) expression in association with transcription factor Runx2 during endochondral ossification. *J Biol Chem, 287*(40), 33179-33190. doi: 10.1074/jbc.M111.337063.

Ogata, Y. (2008). Bone sialoprotein and its transcriptional regulatory mechanism. *J Periodontal Res, 43*(2), 127-135. doi: 10.1111/j.1600-0765.2007.01014.

Okamura, Y., Nomura, A., Minami, S., & Okamoto, Y. (2005). Effects of chitin/chitosan and their oligomers/monomers on release of type I collagenase from fibroblasts. *Biomacromolecules, 6*(5), 2382-2384. doi: 10.1021/bm050092q.

Okita, K., Ichisaka, T., & Yamanaka, S. (2007). Generation of germline-competent induced pluripotent stem cells. *Nature, 448*(7151), 313-317. doi: http://www.nature.com/nature/journal/v448/n7151/suppinfo/nature05934_S1.html.

Okita, K., Ichisaka, T., & Yamanaka, S. (2007). Generation of germline-competent induced pluripotent stem cells. *Nature, 448*(7151), 313-317. doi: nature05934 [pii].

Okita, K., Nakagawa, M., Hyenjong, H., Ichisaka, T., & Yamanaka, S. (2008). Generation of mouse induced pluripotent stem cells without viral vectors. *Science, 322*(5903), 949-953. doi: 1164270 [pii].

Okita, K., & Yamanaka, S. (2010). Induction of pluripotency by defined factors. *Exp Cell Res, 316*(16), 2565-2570. doi: 10.1016/j.yexcr.2010.04.023.

Patois, E., Osorio-da Cruz S Fau - Tille, J.-C., Tille Jc Fau - Walpoth, B., Walpoth B Fau - Gurny, R., Gurny R Fau - Jordan, O., & Jordan, O. (2009). Novel thermosensitive chitosan hydrogels: in vivo evaluation. (1552-4965 (Electronic)).

Patti, A., Gennari, L., Merlotti, D., Dotta, F., & Nuti, R. (2013). Endocrine actions of osteocalcin. *Int J Endocrinol, 2013*, 846480. doi: 10.1155/2013/846480.

Pei, Y., Harvey, A., Yu, X. P., Chandrasekhar, S., & Thirunavukkarasu, K. (2006). Differential regulation of cytokine-induced MMP-1 and MMP-13 expression by p38 kinase inhibitors in human chondrosarcoma cells: potential role of Runx2 in mediating p38 effects. *Osteoarthritis Cartilage, 14*(8), 749-758. doi: 10.1016/j.joca.2006.01.017.

Peter, S. J., Lu, L., Kim, D. J., & Mikos, A. G. (2000). Marrow stromal osteoblast function on a poly(propylene fumarate)/beta-tricalcium phosphate biodegradable orthopaedic composite. *Biomaterials, 21*(12), 1207-1213.

Petersen, A., Joly, P., Bergmann, C., Korus, G., & Duda, G. N. (2012). The impact of substrate stiffness and mechanical loading on fibroblast-induced scaffold remodeling. *Tissue Eng Part A, 18*(17-18), 1804-1817. doi: 10.1089/ten.TEA.2011.0514.

PhosphoSitePlus. AML3 (human). Retrieved December 2014, 2014, from http://www.phosphosite.org/proteinAction.do?id=13408&showAllSites=true.

PhosphoSitePlus. Osterix (human). Retrieved December 2014, 2014, from http://www.phosphosite.org/proteinAction.do?id=3619200&showAllSites=true.

Piraino, F., Camci-Unal, G., Hancock, M. J., Rasponi, M., & Khademhosseini, A. (2012). Multi-gradient hydrogels produced layer by layer with capillary flow and crosslinking in open microchannels. *Lab Chip, 12*(3), 659-661. doi: 10.1039/c2lc20515g.

Piramal Healthcare Ltd, B.-O. D. The advanced biopolymer technology for cartilage regeneration. Retrieved October 2014, 2014, from http://bst-cargel.piramal.com/content/technology.

Podichetty, J. T., Dhane, D. V., & Madihally, S. V. (2012). Dynamics of diffusivity and pressure drop in flow-through and parallel-flow bioreactors during tissue regeneration. *Biotechnol Prog, 28*(4), 1045-1054. doi: 10.1002/btpr.1547.

Podichetty, J. T., & Madihally, S. V. (2014). Modeling of porous scaffold deformation induced by medium perfusion. *J Biomed Mater Res B Appl Biomater, 102*(4), 737-748. doi: 10.1002/jbm.b.33054.

Prevention, C. f. D. C. a. (2007). National and State Medical Expenditures and Lost Earnings Attributable to Arthritis and Other Rheumatic Conditions-United States, 2003. Retrieved December 2014, 2014, from http://www.cdc.gov/mmwr/preview/mmwrhtml/mm5601a2.htm?s_cid=mm5601a2_e.

Prevention, C. f. D. C. a. (2011). Prevalence of Coronary Heart Disease-United States, 2006-2010. Retrieved December 2014, 2014, from http://www.cdc.gov/mmwr/preview/mmwrhtml/mm6040a1.htm.

PromoCell. (2008). Osteogenic Differentiation and Analysis of MSC.

Qi, H., Aguiar, D. J., Williams, S. M., La Pean, A., Pan, W., & Verfaillie, C. M. (2003). Identification of genes responsible for osteoblast differentiation from human mesodermal progenitor cells. *Proc Natl Acad Sci U S A, 100*(6), 3305-3310. doi: 10.1073/pnas.0532693100.

Qiu, X., Yang, Y., Wang, L., Lu, S., Shao, Z., & Chen, X. (2011). Synergistic interactions during thermosensitive chitosan-[small beta]-glycerophosphate hydrogel formation. *RSC Advances, 1*(2), 282-289. doi: 10.1039/C1RA00149C.

Ratakonda, S., Sridhar, U. M., Rhinehart, R. R., & Madihally, S. V. (2012). Assessing viscoelastic properties of chitosan scaffolds and validation with cyclical tests. *Acta Biomaterialia, 8*(4), 1566-1575. doi: http://dx.doi.org/10.1016/j.actbio.2011.12.013.

Ravanti, L., Heino, J., Lopez-Otin, C., & Kahari, V.-M. (1999). Induction of Collagenase-3 (MMP-13) Expression in Human Skin Fibroblasts by Three-dimensional Collagen Is Mediated by p38 Mitogen-activated Protein Kinase. *J. Biol. Chem., 274*(4), 2446-2455. doi: 10.1074/jbc.274.4.2446.

Richardson, S. M., Hoyland, J. A., Mobasheri, R., Csaki, C., Shakibaei, M., & Mobasheri, A. (2010). Mesenchymal stem cells in regenerative medicine: opportunities and challenges for articular cartilage and intervertebral disc tissue engineering. *J Cell Physiol, 222*(1), 23-32. doi: 10.1002/jcp.21915.

Robubi, A., Berger, C., Schmid, M., Huber, K. R., Engel, A., & Krugluger, W. (2014). Gene expression profiles induced by growth factors in in vitro cultured osteoblasts. *Bone Joint Res, 3*(7), 236-240. doi: 10.1302/2046-3758.37.2000231.

Romberg, R. W., Werness, P. G., Riggs, B. L., & Mann, K. G. (1986). Inhibition of hydroxyapatite crystal growth by bone-specific and other calcium-binding proteins. *Biochemistry, 25*(5), 1176-1180.

Ruel-Gariepy, E., Chenite A Fau - Chaput, C., Chaput C Fau - Guirguis, S., Guirguis S Fau - Leroux, J., & Leroux, J. (2000). Characterization of thermosensitive chitosan gels for the sustained delivery of drugs. (0378-5173 (Print)).

Sakiyama, E. (2008). Combining stem cells and biomaterial scaffolds for constructing tissues and cell delivery. *StemBook*. doi: 10.3824/stembook.1.1.1.

Sanz-Herrera, J. A., Garcia-Aznar, J. M., & Doblare, M. (2009). A mathematical approach to bone tissue engineering. *Philos Trans A Math Phys Eng Sci, 367*(1895), 2055-2078. doi: 10.1098/rsta.2009.0055.

Sasson, A., Patchornik, S., Eliasy, R., Robinson, D., & Haj-Ali, R. (2012). Hyperelastic mechanical behavior of chitosan hydrogels for nucleus pulposus replacement-experimental testing and constitutive modeling. *J Mech Behav Biomed Mater, 8*, 143-153. doi: 10.1016/j.jmbbm.2011.12.008.

Schuetz, Y. B., Gurny R Fau - Jordan, O., & Jordan, O. (2007). A novel thermoresponsive hydrogel based on chitosan. (0939-6411 (Print)).

Sharma, B., Williams, C. G., Kim, T. K., Sun, D., Malik, A., Khan, M., . . . H., E. J. (2007). Designing Zonal Organization into Tissue-Engineered Cartilage. *Tissue Engineering, 13*(2), 405-414. doi: 10.1089/ten.2006.0068.

Sila-Asna, M., Bunyaratvej, A., Maeda, S., Kitaguchi, H., & Bunyaratavej, N. (2007). Osteoblast differentiation and bone formation gene expression in strontium-inducing bone marrow mesenchymal stem cell. *Kobe J Med Sci, 53*(1-2), 25-35.

Simion, L., Botez, P., Murphy, M., Eloae, F. Z., & Barry, F. (2010, 15-19 July 2010). *Cell Sources for Cartilage Regeneration - From Basic Science to Clinical Reality.* Paper presented at the Advanced Technologies for Enhancing Quality of Life (AT-EQUAL), 2010.

Slaughter, B. V., Khurshid Ss Fau - Fisher, O. Z., Fisher Oz Fau - Khademhosseini, A., Khademhosseini A Fau - Peppas, N. A., & Peppas, N. A. (2010). Hydrogels in regenerative medicine. (1521-4095 (Electronic)).

Song, K., Qiao, M., Liu, T., Jiang, B., Macedo, H., Ma, X., & Cui, Z. (2010). Preparation, fabrication and biocompatibility of novel injectable temperature-sensitive chitosan/glycerophosphate/collagen hydrogels. *Journal of Materials Science: Materials in Medicine, 21*(10), 2835-2842. doi: 10.1007/s10856-010-4131-4.

Spine-health. Osteoarthritis Increases U.S. Annual Health Care Costs by $186 Billion. Retrieved November 2014, 2014, from http://www.spine-health.com/news/20091203/osteoarthritis-increases-us-annual-health-care-costs-186-billion.

Stevens, M. M., & George, J. H. (2005). Exploring and Engineering the Cell Surface Interface. *Science, 310*(5751), 1135-1138. doi: 10.1126/science.1106587.

Stratford, E. W., Daffinrud, J., Munthe, E., Castro, R., Waaler, J., Krauss, S., & Myklebost, O. (2014). The tankyrase-specific inhibitor JW74 affects cell cycle progression and induces apoptosis and differentiation in osteosarcoma cell lines. *Cancer Med, 3*(1), 36-46. doi: 10.1002/cam4.170.

Stuart, M. (2009). Cartilage Repair: What's the right Combination? *Start-Up, 14*(8), 1-8.

Supper, S., Anton, N., Seidel, N., Riemenschnitter, M., Schoch, C., & Vandamme, T. (2013). Rheological study of chitosan/polyol-phosphate systems: influence of the polyol part on the thermo-induced gelation mechanism. *Langmuir, 29*(32), 10229-10237. doi: 10.1021/la401993q.

Surgeons, A. A. o. O. (2010). Unicompartmental Knee Replacement. Retrieved December 2014, 2014, from http://orthoinfo.aaos.org/topic.cfm?topic=A00585.

Surgeons, A. A. o. O. (2011). Total Knee Replacement. Retrieved September 2012, 2012, from http://orthoinfo.aaos.org/topic.cfm?topic=a00389.

Surgeons, A. A. o. O. (2013). Beyond Surgery Day: The Full Impact of Knee Replacement. Retrieved December 2014, 2014, from http://www.anationinmotion.org/value/knee/.

Szabo, E., Rampalli, S., Risueno, R. M., Schnerch, A., Mitchell, R., Fiebig-Comyn, A., . . . Bhatia, M. (2010). Direct conversion of human fibroblasts to multilineage blood progenitors. *Nature, 468*(7323), 521-526. doi: 10.1038/nature09591.

Takahashi, K., Tanabe, K., Ohnuki, M., Narita, M., Ichisaka, T., Tomoda, K., & Yamanaka, S. (2007). Induction of Pluripotent Stem Cells from Adult Human Fibroblasts by Defined Factors. *Cell, 131*(5), 861-872.

Tew, S. R., Murdoch, A. D., Rauchenberg, R. P., & Hardingham, T. E. (2008). Cellular methods in cartilage research: Primary human chondrocytes in culture and chondrogenesis in human bone marrow stem cells. *Methods, 45*(1), 2-9. doi: 10.1016/j.ymeth.2008.01.006.

Therapeutics, A. (2012). HYALOGRAFT C AUTOGRAFT. Retrieved October 2011, 2011, from www.anikatherapeutics.com/products/jointhealth/hyalograft.html.

Tıglı, R. S., Ghosh, S., Laha, M. M., Shevde, N. K., Daheron, L., Gimble, J., . . . Kaplan, D. L. (2009). Comparative chondrogenesis of human cell sources in 3D scaffolds. *Journal of Tissue Engineering and Regenerative Medicine, 3*(5), 348-360. doi: 10.1002/term.169.

Tillman, J., Ullm A Fau - Madihally, S. V., & Madihally, S. V. (2006). Three-dimensional cell colonization in a sulfate rich environment. (0142-9612 (Print)).

Toh, W. S., Lee Eh Fau - Cao, T., & Cao, T. (2011). Potential of human embryonic stem cells in cartilage tissue engineering and regenerative medicine. (1558-6804 (Electronic)).

Toh, W. S., Lee, E. H., Guo, X.-M., Chan, J. K. Y., Yeow, C. H., Choo, A. B., & Cao, T. (2010). Cartilage repair using hyaluronan hydrogel-encapsulated human embryonic stem cell-derived chondrogenic cells. *Biomaterials, 31*(27), 6968-6980. doi: 10.1016/j.biomaterials.2010.05.064.

Tomasek, J. J., Halliday, N. L., Updike, D. L., Ahern-Moore, J. S., Vu, T. K., Liu, R. W., & Howard, E. W. (1997). Gelatinase A activation is regulated by the organization of the polymerized actin cytoskeleton. *The Journal of biological chemistry, 272*(11), 7482-7487.

Toole, B. P. (2004). Hyaluronan: from extracellular glue to pericellular cue. *Nat Rev Cancer, 4*(7), 528-539.

Treppo, S., Koepp, H., Quan, E. C., Cole, A. A., Kuettner, K. E., & Grodzinsky, A. J. (2000). Comparison of biomechanical and biochemical properties of cartilage from human knee and ankle pairs. *Journal of Orthopaedic Research, 18*(5), 739-748. doi: 10.1002/jor.1100180510.

Truskey, G. A., Yuan, F., & Katz, D. F. (2009). *Transport phenomena in biological systems* (2nd ed.). Upper Saddle River, N.J.: Pearson Prentice Hall.

Tsai, M. T., Li, W. J., Tuan, R. S., & Chang, W. H. (2009). Modulation of osteogenesis in human mesenchymal stem cells by specific pulsed electromagnetic field stimulation. *J Orthop Res, 27*(9), 1169-1174. doi: 10.1002/jor.20862.

Tuan, R. S., Boland, G., & Tuli, R. (2003). Adult mesenchymal stem cells and cell-based tissue engineering. *Arthritis Research & Therapy, 5*(1), 32. doi: 10.1186/ar614.

Vasconcelos, D. P., Fonseca, A. C., Costa, M., Amaral, I. F., Barbosa, M. A., Águas, A. P., & Barbosa, J. N. (2013). Macrophage polarization following chitosan implantation. *Biomaterials, 34*(38), 9952-9959. doi: http://dx.doi.org/10.1016/j.biomaterials.2013.09.012.

Villarreal, X. C., Mann, K. G., & Long, G. L. (1989). Structure of human osteonectin based upon analysis of cDNA and genomic sequences. *Biochemistry, 28*(15), 6483-6491. doi: 10.1021/bi00441a049.

Vincenti, M. P., & Brinckerhoff, C. E. (2002). Transcriptional regulation of collagenase (MMP-1, MMP-13) genes in arthritis: integration of complex signaling pathways for the recruitment of gene-specific transcription factors. *Arthritis Res, 4*(3), 157-164.

Walker, K. J., & Madihally, S. V. (2015). Anisotropic temperature sensitive chitosan-based injectable hydrogels mimicking cartilage matrix. LID - 10.1002/jbm.b.33293 [doi]. (1552-4981 (Electronic)).

Wang, C. C., Yang, K. C., Lin, K. H., Wu, C. C., Liu, Y. L., Lin, F. H., & Chen, I. H. (2014). A biomimetic honeycomb-like scaffold prepared by flow-focusing technology for cartilage regeneration. *Biotechnol Bioeng, 111*(11), 2338-2348. doi: 10.1002/bit.25295.

Wang, L., & Stegemann, J. P. (2010). Thermogelling chitosan and collagen composite hydrogels initiated with β-glycerophosphate for bone tissue engineering. *Biomaterials, 31*(14), 3976-3985. doi: 10.1016/j.biomaterials.2010.01.131.

Wang, L., Verbruggen, G., Almqvist, K. F., Elewaut, D., Broddelez, C., & Veys, E. M. (2001). Flow cytometric analysis of the human articular chondrocyte phenotype in vitro. *Osteoarthritis Cartilage, 9*(1), 73-84. doi: 10.1053/joca.2000.0352

Wasi, S., Otsuka, K., Yao, K. L., Tung, P. S., Aubin, J. E., Sodek, J., & Termine, J. D. (1984). An osteonectinlike protein in porcine periodontal ligament and its synthesis by periodontal ligament fibroblasts. *Can J Biochem Cell Biol, 62*(6), 470-478.

Wells, R. G. (2008). The role of matrix stiffness in regulating cell behavior. *Hepatology, 47*(4), 1394-1400. doi: 10.1002/hep.22193.

Werkmeister, J. A., Adhikari, R., White, J. F., Tebb, T. A., Le, T. P. T., Taing, H. C., . . . Ramshaw, J. A. M. (2010). Biodegradable and injectable cure-on-demand polyurethane scaffolds for regeneration of articular cartilage. *Acta Biomaterialia, 6*(9), 3471-3481. doi: 10.1016/j.actbio.2010.02.040.

Wheeless, I., Clifford R. . (2012, 6/1/2012). Articular Cartilage. 2012, from http://www.wheelessonline.com/ortho/articular_cartilage.

Wilson, R., Whitelock, J. M., & Bateman, J. F. (2009). Proteomics makes progress in cartilage and arthritis research. *Matrix Biol, 28*(3), 121-128. doi: 10.1016/j.matbio.2009.01.004.

Witek, L., Smay, J., Silva, N. F. A., Guda, T., Ong, J., & Coelho, P. (2013). Sintering effects on chemical and physical properties of bioactive ceramics. *Journal of Advanced Ceramics, 2*(3), 274-284. doi: 10.1007/s40145-013-0072-y.

Wu, J., Su Zg Fau - Ma, G.-H., & Ma, G. H. (2006). A thermo- and pH-sensitive hydrogel composed of quaternized chitosan/glycerophosphate. (0378-5173 (Print)).

Xu, J., Wang, W., Ludeman, M., Cheng, K., Hayami, T., Lotz, J. C., & Kapila, S. (2008). Chondrogenic Differentiation of Human Mesenchymal Stem Cells in Three-Dimensional Alginate Gels. *Tissue Engineering Part A, 14*(5), 667-680. doi: 10.1089/tea.2007.0272.

Yamanaka, S. (2008). Induction of pluripotent stem cells from mouse fibroblasts by four transcription factors. *Cell Proliferation, 41*, 51-56. doi: 10.1111/j.1365-2184.2008.00493.

Yamanaka, S. (2009). A fresh look at iPS cells. *Cell, 137*(1), 13-17. doi: 10.1016/j.cell.2009.03.034.

Yamane, S., Iwasaki, N., Majima, T., Funakoshi, T., Masuko, T., Harada, K., . . . Nishimura, S. (2005). Feasibility of chitosan-based hyaluronic acid hybrid biomaterial for a novel scaffold in cartilage tissue engineering. *Biomaterials, 26*(6), 611-619. doi: 10.1016/j.biomaterials.2004.03.013.

Yeung, T., Georges, P. C., Flanagan, L. A., Marg, B., Ortiz, M., Funaki, M., . . . Janmey, P. A. (2005). Effects of substrate stiffness on cell morphology, cytoskeletal structure, and adhesion. *Cell Motility and the Cytoskeleton, 60*(1), 24-34. doi: 10.1002/cm.20041.

Young, M. F., Kerr, J. M., Ibaraki, K., Heegaard, A. M., & Robey, P. G. (1992). Structure, expression, and regulation of the major noncollagenous matrix proteins of bone. *Clin Orthop Relat Res*(281), 275-294.

Yu, C., Young, S., Russo, V., Amsden, B. G., & Flynn, L. E. (2013). Techniques for the isolation of high-quality RNA from cells encapsulated in chitosan hydrogels. *Tissue Eng Part C Methods, 19*(11), 829-838. doi: 10.1089/ten.TEC.2012.0693.

Zanjani, E. D., Ascensao, J. L., & Tavassoli, M. (1993). Liver-derived fetal hematopoietic stem cells selectively and preferentially home to the fetal bone marrow. *Blood, 81*(2), 399-404.

Zhang, Y., & Zhang, M. (2001). Synthesis and characterization of macroporous chitosan/calcium phosphate composite scaffolds for tissue engineering. *J Biomed Mater Res, 55*(3), 304-312.

Zhao, T., Zhang, Z.-N., Rong, Z., & Xu, Y. (2011). Immunogenicity of induced pluripotent stem cells. *Nature, 474*(7350), 212-215. doi: http://www.nature.com/nature/journal/v474/n7350/abs/10.1038-nature10135-unlocked.html#supplementary-information.

Zhou, S., Cui, Z., & Urban, J. P. (2004). Factors influencing the oxygen concentration gradient from the synovial surface of articular cartilage to the cartilage-bone interface: a modeling study. *Arthritis Rheum, 50*(12), 3915-3924. doi: 10.1002/art.20675.

Zhu, F., Friedman, M. S., Luo, W., Woolf, P., & Hankenson, K. D. (2012). The transcription factor osterix (SP7) regulates BMP6-induced human osteoblast differentiation. *J Cell Physiol, 227*(6), 2677-2685. doi: 10.1002/jcp.23010.

APPENDIX A

SUPPLEMENTARY OSTEOGENIC GENE INFORMATION

RUNX2 is a 56 kD transcriptional factor involved in chondrogenic maturation and regulating many of the necessary genes in osteogenesis (PhosphoSitePlus). Phosphorylation and activation of *RUNX2* can come from multiple pathways such as *MAPK/ERK* or protein kinase A (*PKA*). A variety of signals or conditions will stimulate the pathways. For example, the *MAPK* pathway can stimulated by ECM, growth factors such as BMPs, transforming growth factor β (TGF-β), and fibroblast growth factor (FGF) 2, mechanical loading, and hormones such as *PTH* (Franceschi & Xiao, 2003). Also, *RUNX2* expression increases without increases in RNA expression or protein production during the early stages of osteogenesis. Once activated, *RUNX2* stimulates the expression of *COLIA1*, *ALPL*, *IBSP*, and *BGLAP* during osteoblast maturation. *RUNX2* then regulates the osteoblast-related genes by binding to the specific promotor regions. For *SPP1*, the signaling pathways, *Notch* and *Vitamin D*, are used by *RUNX2* for regulation (Bae et al., 2007; Dalle Carbonare et al., 2012; Franceschi & Xiao, 2003). Alternatively, regulation of *RUNX2* is activated by binding interactions with *BGLAP* and *SP7* regulators, activator protein 1 and activating transcription factor 4. Interactions between *RUNX2* and histone deacetylase 3 (*HDAC3*) is reported to repress the *BGLAP* promoter by inhibiting *RUNX2* transcriptional activity (Dalle Carbonare et al., 2012).

SPP1 is a 44 kD bone phosphoprotein synthesized in bone and other epithelial tissues. Preosteoblasts, osteoblasts, and osteocytes synthesize osteopontin as a bone matrix protein, and

secrete osteopontin into osteoids prior to incorporation into bone. Osteopontin is also synthesized by certain bone marrow cells, several types of fibroblasts, HepG2 cells, and hypertrophic chondrocytes. *SPP1* is associated with the regulation of osteoclast function during bone formation and is only expressed when transcription factors *RUNX2* and *SP7* are present. *SPP1* stimulates cellular signaling pathways via various receptors found on most cell types as it contains a glycine-arginine-glycine-aspartate-serine (GRGDS or RGD) amino acid sequence, similar to the cell-binding sequence present in fibronectin.

Similar to *SPP1*, *IBSP* is a 33kD phosphoprotein produced in mineralized tissues such as bone and calcified cartilage (Hunter & Goldberg, 1993; Kruger, Miller, & Wang, 2013). *IBSP* and *SPP1* have many consistencies including amino acid compositions, post-transcriptional modifications, and osteoid residency; however, bone sialoprotein is more sialic acid and sulfate rich, only found in mineralized tissues, and expressed earlier at the beginning of bone formation (Hunter & Goldberg, 1993). During endochondral ossification, *IBSP* is upregulated by hypertrophic chondrocytes, osteoblasts, osteoclasts, and osteocytes. *IBSP* also contains a RDG amino acid sequence and is involved with cell binding and signaling. bone sialoprotein also acts as the nucleus during hydroxyapatite nucleation, activates MMP-2, and may be involved in collagen type I binding in bone (Kruger et al., 2013; Ogata, 2008). *IBSP* regulation comes from cytokines, growth factors and hormones through the cyclic adenosine monophosphate (*cAMP*) dependent, mitogen-activated protein (*MAP*) kinase, tyrosine kinase pathways (Ogata, 2008).

SP7 is a 45 kD zinc finger osteoblast-specific transcription factor known to play a role in osteogenesis and inhibit chondrogenesis during endochondral ossification (PhosphoSitePlus). *Smad* signaling is required to induce *SP7,* and *SP7* expression is regulated by *RUNX2*-dependent and –independent pathways through BMP-2 (Matsubara et al., 2008) and insulin growth factor (IGF-1) signaling (Hong et al., 2009) and by *Msx2* in *RUNX2* deficient cells (Zhu et al., 2012). Nishimura et al. reported that *SP7* specifically targets MMP-13 and up-regulation of MMP-13 is

required for a physical functional interaction to exist between *SP7* and *RUNX2* (Nishimura et al., 2012). *SP7* has been observed to function downstream from *RUNX2*, regulating the expression of osteoblastic genes containing GC-rich and Sp-binding sites on their promoters. Further, osteoblast proliferation may be inhibited by SP7 through the Wnt-signaling pathway. *SP7* was reported to induce expression of *BGLAP*, *COLIA1*, *COLXIA2*, and *SPP1* under forced expression conditions. Up-regulation of *SP7* has been observed by ascorbic acid and 1,25 (OH)2 vitamin D3 (Hong et al., 2009). Alternatively, *SP7* expression is down-regulated by parathyroid hormone (*PTH*) by a transcriptional mechanism through *cAMP* signaling. However, the involvement *SP7* has in osteogenesis and mechanisms of its transcriptional activity are still unclear.

SPARC is a 40 kD acidic glycoprotein rich in cysteine that plays a role in mineralization, collagen binding, cell-matrix interactions, wound healing, and MMP production. Similar to *SPP1*, *SPARC* is synthesized by osteoprogenitors, several types of fibroblasts, HepG2 cells, and hypertrophic chondrocytes but is most commonly expressed in mineralized tissues. *SPARC* also promotes but does not support cell adhesion and inhibits cell spreading. *SPARC* has the ability to bind to cytokines and growth factors mediating proliferation regulation in some cell lines (Guweidhi et al., 2005; Villarreal et al., 1989; Wasi et al., 1984; Young, Kerr, Ibaraki, Heegaard, & Robey, 1992).

BGLAP is a 6 kD noncollagenous osteoblast-specific protein originally thought to take part in bone formation and resorption, and metabolic regulation of the body (Ivaska et al., 2004; N. K. Lee et al., 2007). *BGLAP* is vitamin K dependent and known to bind hydroxyapatite via the 3 γ-carboxylated glutamic acid residues (Kapustin & Shanahan, 2011) as well as bone mineralization regulator by inhibiting hydroxyapatite seeded crystal growth (Hoang, Sicheri, Howard, & Yang, 2003; Romberg, Werness, Riggs, & Mann, 1986). Recently, *BGLAP* is thought to be a novel regulator in osteochondrogenic differentiation of vascular smooth muscle cells through hypoxia-inducible factor 1α (Idelevich, Rais, & Monsonego-Ornan, 2011) and play a role in vascular

calcification, activating novel signaling pathways to promote bone formation (Kapustin & Shanahan, 2011). *BGLAP* production is regulated by various growth factors, hormones, and cytokines through signaling pathways or transcription factors acting on the *BGLAP* gene promoter region (Patti, Gennari, Merlotti, Dotta, & Nuti, 2013). However, the precise function of *BGLAP* has not been fully elucidated.

APPENDIX B

SUPPLEMENTARY DETAIL OF CHAPTER 4 MATERIALS AND METHODS

Hydrogel Suspension Cultures

Design of Cultures

The size or volume of the hydrogel culture is designed around the analysis or analyses that were to be performed after the 28 day culture period. The larger cultures allowed for multiple analyzes to be performed from one sample harvesting. For example, the one set of all aggrecan and MMP assays, IHC, and histology analyses were performed from one biological sample. The hydrogel volumes were 0.5mL (small) and 2mL (large) for cultures containing 0.25×106 and 1×106 cells, respectively. The culture plates used for the large and small hydrogel cultures were six and twenty-four well plates, respectively. Further, 1×106 cells were seeded into hydrogels of each group for all analyses except quantitative polymerase chain reaction (qPCR) which was seeded with 0.25×106 cells. The reduced volume and cell quantity of the qPCR cultures was to ensure similar hydrogel volumes and cell quantities were collected during harvesting. Biological triplicates of all conditions were performed to ensure repeatability of the experiments.

Cells were tested in three culture conditions previously mentioned in suspension cultures for the superficial and radial hydrogels. For the chondrogenic culture protocol, incomplete chondrogenic induction medium (ICM) was prepared fresh by supplementing the Chondrogenic Basal Medium with hMSC Chondrogenic SingleQuots Kit. The lyophilized TGF-β3 was reconstituted in 4mM HCl supplemented with 1 mg/mL bovine serum albumin (BSA) to a concentration of 20μg/mL.

The CCM was prepared by adding fresh TGF-β3 to obtain10ng/mL concentration in ICM before each use due to the limited shelf life of 12 hours.

Cells were washed with PBS then detached using trypsin/EDTA solution. Respective cell line medium was used to neutralize the trypsin/EDTA and wash the plate. The cell suspension was centrifuged for 5 minutes at 270×g for hFF-1 cells and 600×g for hMSCs, resuspended in medium (FBM for hFF-1s and MSCBM for hMSCs), and counted using a hemocytometer. Cells were aliquoted at 1,000,000 and 250,000 cells per culture for the large and small cultures, respectively, and centrifuged at 150×g for 5 minutes.

Cell Preparation for Seeding

After the cells were aliquoted, the cells for the negative control group (hFF-1 control) were stored briefly in FBM until seeding. Alternatively, for positive control (hMSC induced) and experimental groups (hFF-1 induced), the medium (MSCBM or FBM) was removed and the cells were washed twice with of ICM, centrifuged at 150×g, and briefly stored in ICM until seeding. The hydrogels were prepared once the cells were washed with the respective medium for the culture conditions.

Large and Small Hydrogel Culture Process

For the large hydrogel cultures, 2mL of the superficial or radial hydrogel/2GP solution was added to a well of a six well plate. To avoid losing cells, the cells were added after the hydrogel was in the well. Further, the cells were added to the hydrogel while in the liquid state to allow for uniform mixing of the cells and hydrogel. The cells were mixed with the hydrogel in a crisscross pattern to ensure uniform distribution. The hydrogel encapsulated with cells was allowed to setup/gel for 2 hours, then 2mL of the respective medium was added atop the hydrogel culture. All hydrogel cultures were incubated at 37°C and 5% CO2 in air atmosphere and medium was changed twice a week. Culture supernatants were collected and preserved at -80°C for detection

of protein and MMP expression analyses. The large hydrogel cultures were harvested after 28 days and analyzed via histology or immunohistochemistry.

The small hydrogel cultures followed an identical process with the following exceptions: culture apparatus was a twenty-four well plate, hydrogel volume used was 0.5mL, medium volume was 0.5mL, supernatants were not collected, hydrogels were harvested for qPCR analysis.

Aggrecan ELISA

Cell culture supernatants from the hydrogel cultures were tested for aggregan content using human ELISA kit from Life Technologies (Grand Island, NY) following vendor's protocol. The six standards for the ELISA were prepared by reconstituting the lyophilized standards with deionized (DI) water to the concentrations specified on the vial label (197, 89, 51, 28.8, 15.7 and 0ng/mL). Similarly, the three assay controls were reconstituted with distilled water to the specified concentrations (108±36, 78±23, and 38±11ng/mL). The vials remained undisturbed until completely dissolved, then were mixed well by gentle inversion. The wash solution was prepared by diluting 2mL of Wash Solution Concentrate in 400mL of DI water. The conjugate solution was extemporaneously prepared based on the number of samples tested by diluting the concentrated Anti-PG-HRP Conjugate with conjugate buffer at a ratio of 5mL: 20mL.

Once the reagents were prepared, the microplate was loaded with 50µL of standard, control, or supernatant sample followed by 100µL of incubation buffer into the each of the previously foreseen wells. The plate was gently tapped on the side to ensure the plate contents are thoroughly mixed and incubated at room temperature (RT) for 2 hours. After 2 hours, the plate was aspirated and washed three times with 400µL/well with the wash solution. The wells were filled and emptied at each wash and the plate was blotted on paper towels to remove any residual fluid. 200µL of the conjugate solution was pipetted into each of the wells, and the plate was gently tapped. The plate was then covered with aluminum foil and incubated for one hour at RT.

The wells were once more aspirated, washed, and blotted, and 100µL of Chromogenic Solution was pipetted into each of the wells. The plate was covered, incubated and protected from light for 15 minutes. The reaction was stopped by adding 200µL of Stop Solution to each well. The side of plate was tapped gently before and after the Stop Solution was added. All plates were read for absorbance at 450 nm using a Molecular Devices EMax Precision Microplate Reader (Molecular Devices, LLC, Sunnyvale, CA).

Histology and Immunohistochemistry

The hydrogel cultures were harvested after 28 days and fixed with 3.7% formaldehyde for 30 minutes at RT. The samples were rinsed thrice with PBS and stored in EtOH. The samples were paraffin-embedded, sectioned, and stained with haematoxylin and eosin (H/E) and Alcian blue stain (pH 1.0) by Oklahoma Animal Disease and Diagnostic Laboratory (OADDL). Additional sections from the same samples were mounted on slides for immunohistochemistry (IHC).

The unstained slides were used in immunohistochemistry to stain for aggrecan and collagen types I, and II. The unstained slides were deparaffinized and hydrated using the following washes: xylene: 2 x 5 minutes, xylene 1:1 with 100% EtOH: 5 minutes, 100% EtOH: 2 x 5 minutes, 95% EtOH: 5 minutes, 70 % EtOH: 5 minutes, 50 % EtOH: 5 minutes, and DI water: 1 minute. The excess liquid was aspirated from slides.

Antigen unmasking was performed because certain antigenic determinants are masked by formalin fixation and paraffin embedding. The slides were incubated for 15 minutes in 0.1% pepsin in 0.01N HCl at RT and washed several times in DI water. The excess liquid was aspirated from slides.

The slides were incubated in 1% BSA in PBS for 1 hour then removed from the slides. Mineral oil was used to create a barrier around the specimen to avoid liquid runoff and waste of the primary and secondary antibodies. The primary antibody was diluted to a concentration of

5.0µg/ml, pipetted atop the specimen, and incubated for 30 minutes at RT or overnight at 4º C. The slides were washed with three changes of PBS for 5 minutes each. The secondary antibody was diluted using 1% BSA in PBS to 1.0µg/ml then pipetted atop the specimen and incubated for 30 minutes at RT or overnight at 4º C. The slides were washed with three changes of PBS for 5 minutes each. The primary and secondary antibodies and substrates used for staining the specimens are mentioned in Chapter 4. After the incubation with the primary and secondary antibodies peroxidase (HRP) detection system, the slides were incubated in a peroxidase substrate for 15 minutes to allow sufficient color to develop. For detection of aggrecan, collagen type I, and collagen type II Peroxidase Substrates used were Vector SG (develops blue-gray color), Vector Nova Red (develops red color), and Vector VIP (develops purple color), respectively. All substrates were purchased from Vector Laboratories, Burlingame, CA. The slides were then washed with water for 5 minutes, and then dehydrated using the process for hydration in reverse order.

Quantitative Polymerase Chain Reaction Analysis

Instruments were cleaned with EtOH before each use and between samples. All pipette tips and micro centrifuge tubes were autoclaved prior to use. 250,000 cells from the expansion cultures (hMSC in MSCBM and hFF-1 in FBM) were pelleted and used as controls against the hydrogel cultures. The small control pellets and hydrogel cultures were harvested at Day 0 and Day 28 of culture. The RNA from the control pellets was isolated using the RNeasy kit (Qiagen), following vendors's protocol. In each sample, the concentration of RNA and the nucleic acid quantitation (260/280) was assessed initially using NanoDrop ND-1000 (NanoDrop Technologies, Inc., Wilmington, DE). The sample was stored at -80°C until DNase treatment.

APPENDIX C

SUPPLEMENTARY DETAIL OF CHAPTER 5 MATERIALS AND METHODS

Hydrogel Suspension Cultures

Hydrogel Culture Analysis Design

The size or volume of the hydrogel culture is designed around the analyses that were to be performed after the 28 day culture period. The larger cultures allowed for multiple analyzes to be performed from one hydrogel harvesting. For example, the one sample of an assay and histology analyses could be performed from one biological sample. The hydrogel volumes were 2mL (large) and 0.5mL (small) for cultures containing 1,000,000 and 250,000 cells, respectively. The culture plates used for the large and small hydrogel cultures were six and twenty-four well plates, respectively. Further, 1,000,000 cells were seeded into hydrogels of each group for all analyses except quantitative polymerase chain reaction (qPCR) which was seeded with 250,000 cells. The reduced volume and cell quantity of the qPCR cultures was to ensure similar hydrogel volumes and cell quantities were collected during harvesting.

Cell Preparation for Seeding

After the cells were aliquoted, the cells for the positive control group were stored briefly in OBM until seeding. Alternatively, for positive control and experimental groups, the medium (MSCBM or FBM) was removed and the cells were washed twice with of ODM, centrifuged at 150×g, and briefly stored in ODM until seeding. The hydrogels were prepared once the cells were washed

with the respective medium for the culture conditions.

Large and Small Hydrogel Culture Process

For the large hydrogel cultures, 2mL of the superficial or radial hydrogel/2GP solution was added to a well of a six well plate. To avoid losing cells, the cells were added after the hydrogel was in the well. Further, the cells were added to the hydrogel while in the liquid state to allow for uniform mixing of the cells and hydrogel. The cells were mixed with the hydrogel in a crisscross pattern to ensure uniform distribution. The cell encapsulated hydrogel was allowed to setup/gel for 2 hours, then 2mL of the respective medium was added atop the hydrogel culture. All hydrogel cultures were incubated at 37°C and 5% CO2 in air atmosphere and media was changed twice a week. Culture supernatants were collected and preserved at -80°C for detection of protein and MMP expression. The large hydrogel cultures were harvested after 28 days and analyzed via histology and IHC. The small hydrogel cultures followed an identical process with the following exceptions: culture apparatus was a twenty-four well plate, hydrogel volume used was 0.5mL, medium volume was 0.5mL, supernatants were not collected, and hydrogels were harvested for qPCR analysis.

Calcified Hydrogel Deterioration Issues

Hydrogels containing cells undergoing osteogenic differentiation had noticeable deterioration beginning at Day 7. The deterioration continued throughout the 28 day period resulting in uncertainty in those samples. A systematic approach was used to unveil the variable that was causing the deterioration that was appearing in the osteogenic differentiation samples. To determine whether the cells or the medium was the influential factor, hydrogel samples without cells were prepared and cultured with OBM without serum as the control and ODM as the experimental. Deterioration in the samples containing ODM had similar results to the samples containing cells.

In an attempt to continue the substrate influenced osteogenic differentiation, the media was altered by removing the β-glycerol phosphate thinking this might be causing a pH imbalance of the chitosan based hydrogel. It was discovered that the altered medium increased the deterioration rate of the hydrogels to begin on or before Day 4. Further examination lead to determination of the deterioration was from the serum contained in the medium. However, we did not want to alter the medium by removing the serum as the increased proliferation may play a role in differentiation.

Therefore, a two-step approach was established for the large hydrogel cultures. The cells would be expanded and tested for differentiation on TCP for 28 days then seeded in the large hydrogel cultures for 7 days in serum-free OBM to determine stability. The small cultures were no longer used as the cells were tested for differentiation on the TCP cultures. In order to understand the changes in the morphology of cells, phase contrast microscopic images of the cells from each condition were digitally captured.

Quantitative Polymerase Chain Reaction Analysis

Instruments were cleaned with EtOH before each use and between samples. All pipette tips and micro centrifuge tubes were autoclaved prior to use. 250,000 cells from the expansion cultures (NHOst in serum-free OBM, hMSC in MSCBM, and hFF-1 in FBM) were pelleted and used as controls against the hydrogel cultures.

Tissue Preparation

The small hydrogel cultures and control pellets were harvested at Day 28 and Day 0 of culture. The process was identical for both conditions. The sample was placed in a 1.5mL micro centrifuge tube. 500µL of Trizol (Life Technologies, Grand Island, NY) was used to wash the twenty-four well plate and added to the tube. The sample was homogenized using a glass stir rod, vortexing, and vigorous shaking combination, and incubated for 5 minutes at RT. 100µL of

chloroform was added to the Trizol/sample solution and vigorously shaken for 15 seconds. The sample was incubated for 3 minutes at RT then centrifuged at 12,000×g for 15 minutes at 2-8°C. During centrifugation, three phases (clear aqueous RNA, white DNa interphase, and red phenol-chloroform phases) were formed. The sample was removed from the centrifuge and the clear aqueous RNA phase was extracted from the tube taking care to not contaminate the RNA sample with DNA. The RNA was placed in a fresh 1.5mL micro centrifuge tube.

RNA Isolation

The RNA was precipitated by adding 250µL of 70% isopropyl alcohol (IPA), incubating at RT for 10 minutes, and centrifuging at 12,000×g for 10 minutes at 2-8°C. The supernatant was removed leaving only the RNA pellet. The pellet was washed with 500µL of 95% EtOH, vortexed, and centrifuged at 7,500×g for 5 minutes at 2-8°C. The alcohol was discarded and the pellet was air dried for 10 minutes ensuring all of the alcohol was removed. The pellet was resuspended in 20µL of RNase-free water (Life Technologies, Grand Island, NY) by passing the solution up and down several times through a pipette tip. The solution was Nanodropped using NanoDrop ND-1000 (NanoDrop Technologies, Inc., Wilmington, DE) to determine the concentration and the nucleic acid quantitation (260/280). The sample was stored at -80°C until DNase treatment.

DNase Treatment

The DNase treatment was performed using DNase I, Amplification Grade kit (Life Technologies, Grand Island, NY). The RNA sample volume was calculated from the nanodrop concentration to reach a mass of 0.8µg. The 0.8µg sample was added to an RNase-free 500µL micro centrifuge tube on ice. The following components were added to the tube: 1µL of 10X DNase I reaction buffer, 1µL of DNase I amplification grade, and DEPC-treated water bringing the volume to 10µL. The mixture was incubated at RT for 15 minutes taking care that time was not exceeded.

DNase I was inactivated by adding 1µL of 25mM EDTA to the mixture and heated at 65°C for 10 minutes. The sample was stored at -80°C until reverse transcriptase cDNA synthesis.

First-strand cDNA Synthesis

The cDNA synthesis was performed using SuperScript™ III First-Strand Synthesis SuperMix for qRT-PCR kit (Life Technologies, Grand Island, NY) and MultiGene™ OptiMax Thermal Cycler (Labnet International, Inc., Edison, NJ). The maximum mass (0.58µg) of the RNA sample after DNase treatment was calculated for reverse transcriptase. The following components were added to the PCR tube on ice then mixed by pipetting up and down: 10µL of 2X reverse transcriptase reaction mix, 2µL of reverse transcriptase enzyme mix, and 0.8 µL RNA (0.58µg). The mixture was kept on ice and transferred to the preprogrammed thermocycler. The tube was added to the thermocycler and the lid was carefully closed to not crush the tube. The program was as follows: incubate at 25°C for 10 minutes, incubate at 50°C for 30 minutes, and reaction termination at 85°C for 5 minutes. The tube was removed, 1µL of E. coli RNase H was added, and the tube was replaced in the thermocycler. The program was completed by incubating at 37°C for 20 minutes. The synthesized cDNA template was stored at -80°C until qPCR detection.

SYBR GreenER qPCR Detection

The qPCR detection was performed using SYBR GreenER™ qPCR SuperMix Universal kit (Life Technologies, Grand Island, NY). Prior to beginning the experiment, all component, master mix, sample, and template control volumes were calculated to minimize time and reduce human error between samples. The template controls (using water in place of cDNA template) were established to be a check against primer dimers. The components and volumes per 200µL tube are as follows: 10µL of SYBR GreenER, 0.4µL of forward primer, 0.4µL of reverse primer, 0.2µL of cDNA template, 9µL of DEPC-treated water to make a 20µL reaction. The forward and reverse primers (Integrated DNA Technologies, Coralville, IA) used are listed in **Table 5.2.**

The three master mixes prepared were (1) SYBR GreenER and cDNA Template, (2) forward primer and DEPC-treated water, and (3) reverse primer and DEPC-treated water and added to the tube in that order. The mixtures were added to a pre-labeled qPCR 96-well plate and sealed with a qPCR adhesive seal film sheet (Phenix Research Products, Candler, NC). The plate was centrifuged to bring all liquid to the bottom of the wells. The Applied Biosystems 7500 Fast real-time PCR thermocycler (Life Technologies, Grand Island, NY) was programmed with the following settings for the reaction: incubate at 50°C for 2 minutes, incubate at 95°C for 10 minutes, and 40 cycles of 95°C for 15 seconds and 60°C for 15 seconds. When multiple plates were prepared, the plate not being run was stored at 2-8°C until the thermocycler was available.

Expression of beta-actin in each condition was used as the internal control. All expressions were subtracted from the internal control and fold expression was obtained using $2^{-\Delta Ct}$ method. Further, upper limit and lower limits were obtained from the standard deviations.

VITA

Kenneth James Walker

Candidate for the Degree of

Doctor of Philosophy

Thesis: PHENOTYPIC AND GENOTYPIC ALTERATIONS OF MATURE CELLS DISPERSED IN INJECTABLE ZONAL HYDROGELS MIMICKING THE CARTILAGE MATRIX COMPOSITION TYPE FULL TITLE HERE IN ALL CAPS

Major Field: Chemical Engineering

Biographical:

Education:

Completed the requirements for the Doctor of Philosophy In Chemical Engineering at Oklahoma State University, Stillwater, Oklahoma in May, 2015.

Completed the requirements for the Master of Science in Chemical Engineering at Oklahoma State University, Stillwater, Oklahoma in December, 2011.

Completed the requirements for the Bachelor of Science in Chemical Engineering at Oklahoma State University, Stillwater, Oklahoma in May, 2010.

Experience:

Research Associate, School of Chemical Engineering and Material Science and Engineering, Oklahoma State University, Stillwater, Oklahoma. 2009-2015.

Teaching Associate, School of Chemical Engineering, Oklahoma State University, Stillwater, Oklahoma . 2010-2015.

Professional Memberships:
Tissue Engineering & Regenerative Medicine International Society (TERMIS)
Society for Biomaterials (SFB)
Biomedical Engineering Society (BMES)
American Institute of Chemical Engineers (AIChE)
Omega Chi Epsilon Honorary Society, Mu Chapter
Chemical Engineering Graduate Student Association (ChEGSA), OSU
Graduate & Professional Student Government Association (GPSGA), OSU